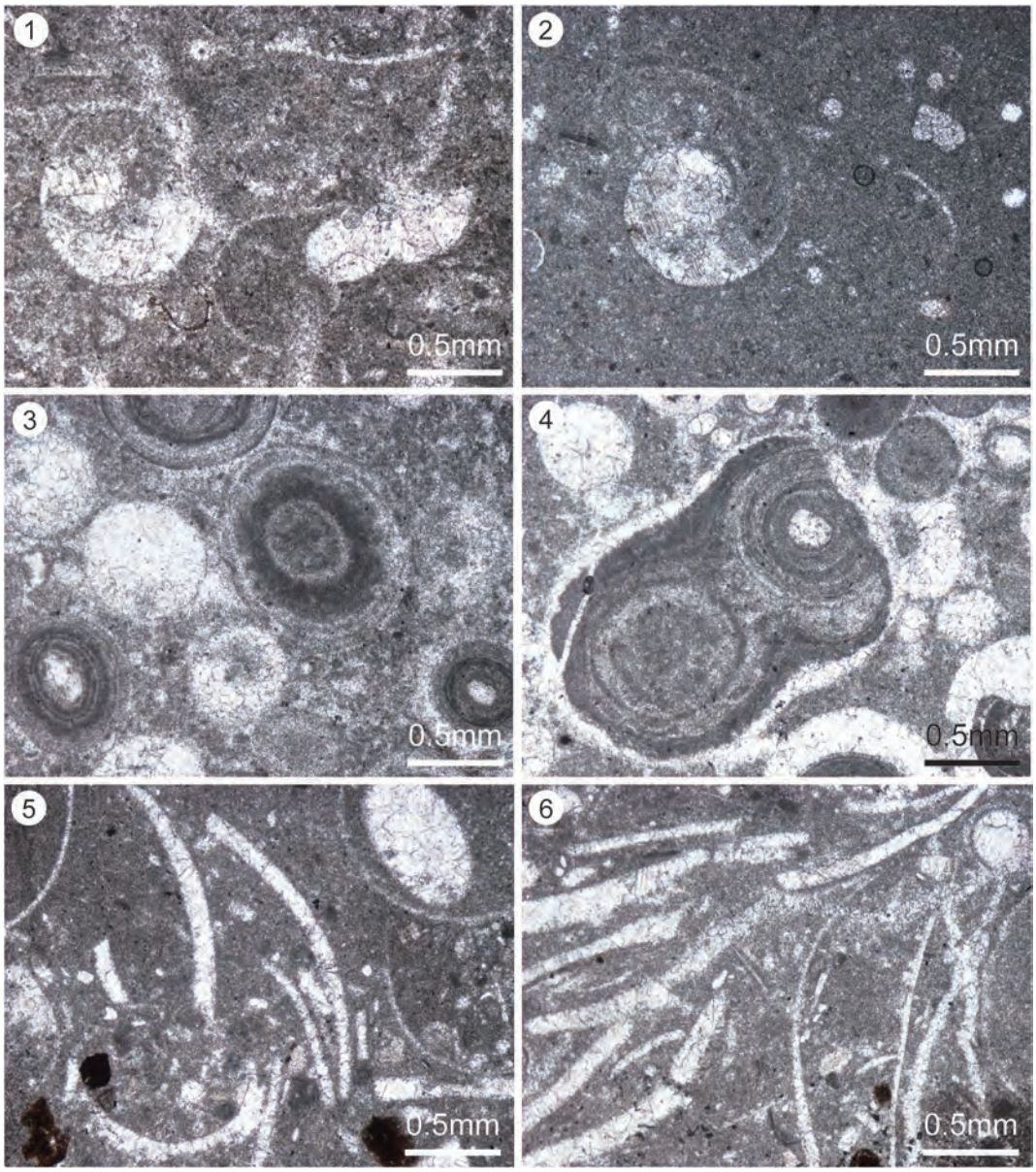


Fig. 30. Photomicrographs of vertical thin sections. 1–2, Bioclastic limestone containing juvenile ammonoids from KC01-03. 3–4, Oolitic limestone from KC01-08. 5–6, Bioclastic limestone containing fragmental and disarticulated thin-shelled bivalves from KC01-08. Thin-shelled bivalves are arranged edgewise and perpendicular to the bedding, which indicates formation by strong wave currents.

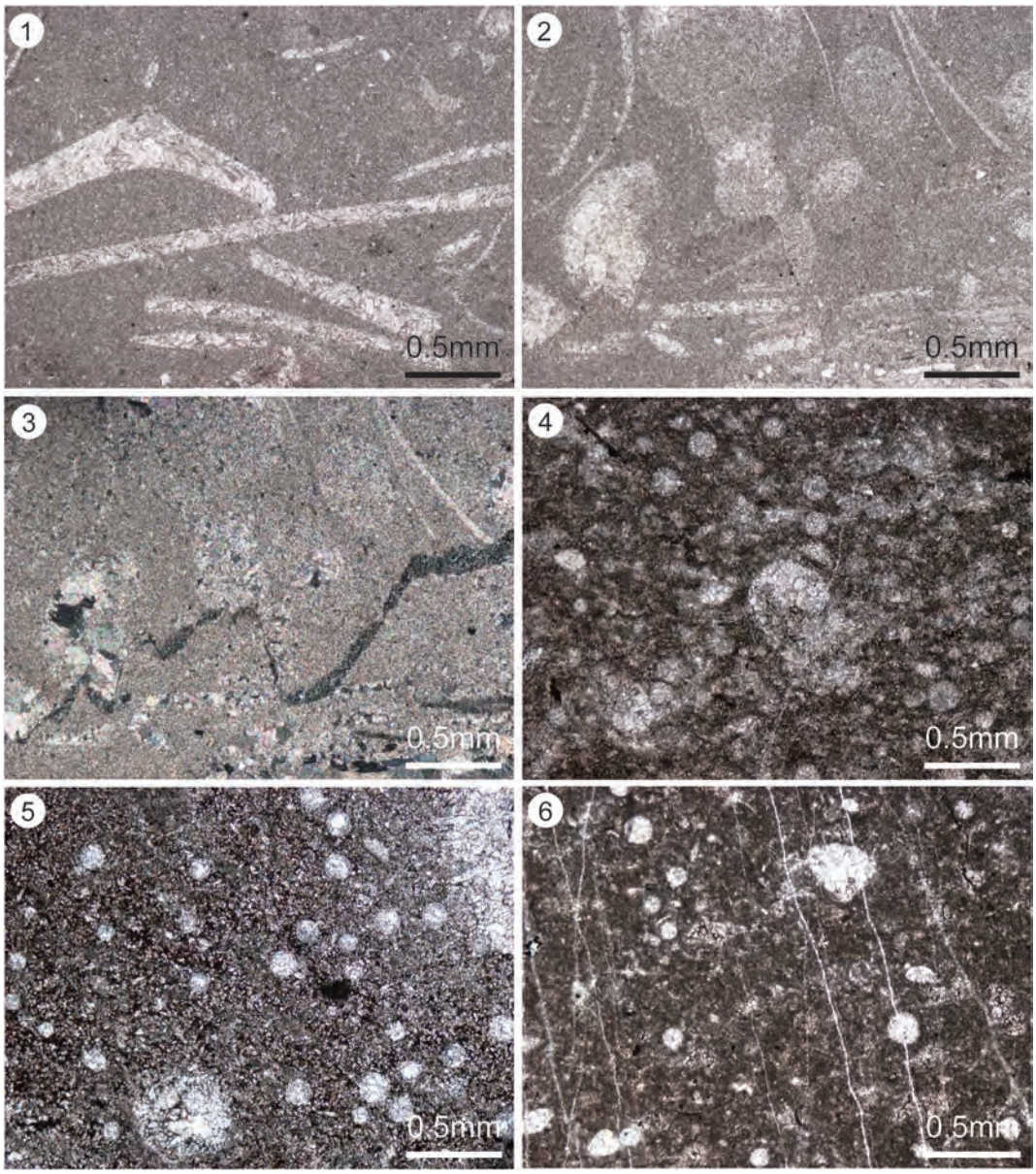


Fig. 31. Photomicrographs of vertical thin sections. 1–2, Bioclastic limestone containing thin-shelled bivalves and juvenile ammonoids from BT01-14. 3, Sutured stylolites commonly found in hemipelagic limestone from KC01-14. 4, Organic-rich dark gray calcareous nodule containing abundant spheroidal radiolarians from NT01-07. 5, Organic-rich dark gray limestone containing abundant spheroidal radiolarians from KC02-10. 6, Organic-rich dark gray calcareous nodule containing abundant spheroidal radiolarians and ostracods from BR01-05.

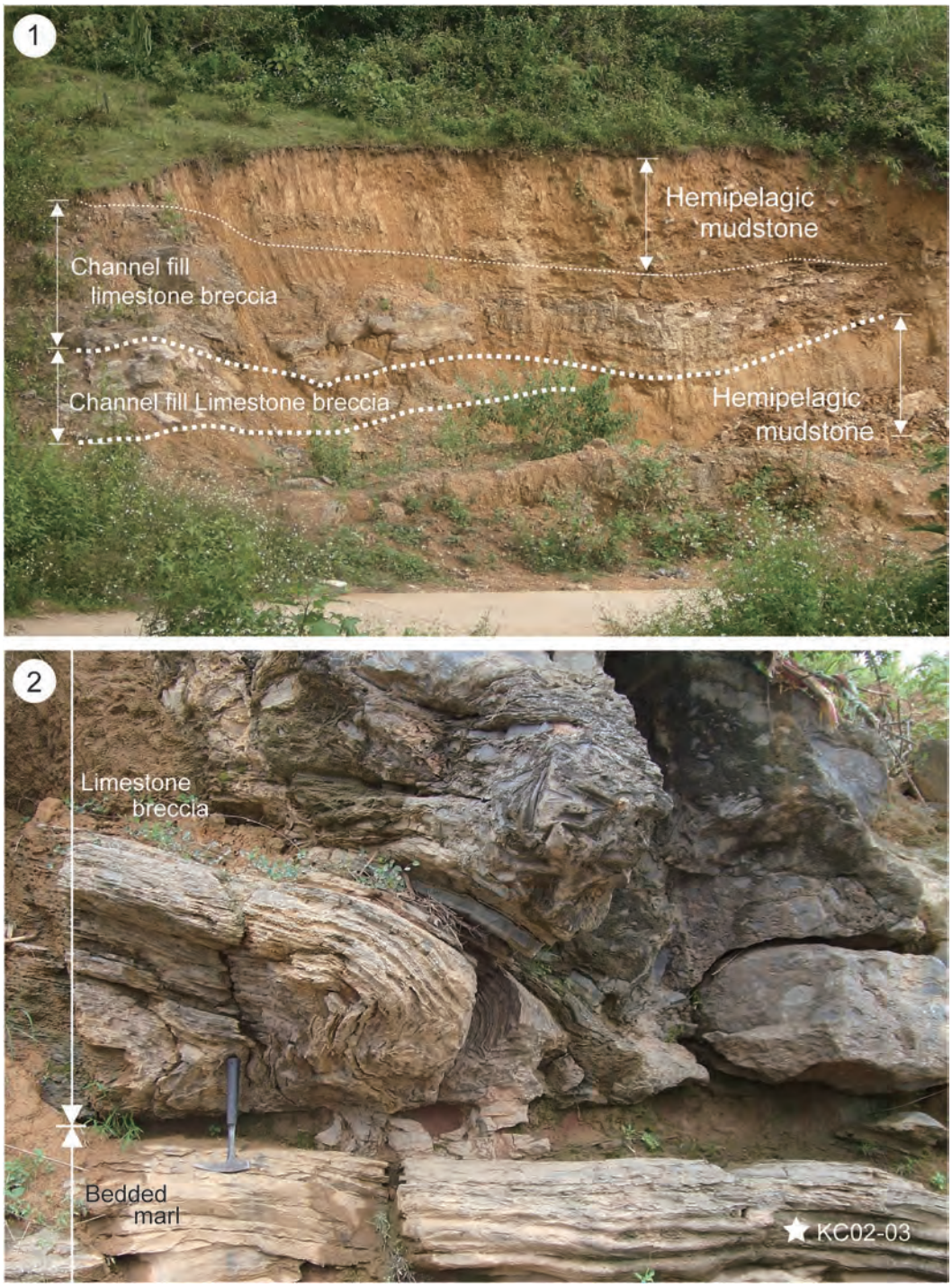


Fig. 32. Lithofacies of slope deposits. 1, Exposures of isolated channel-filling limestone breccias in hemipelagic mudstone in NT02. 2, Limestone breccia containing slump beds and overlying thin-bedded marl at KC02-03.

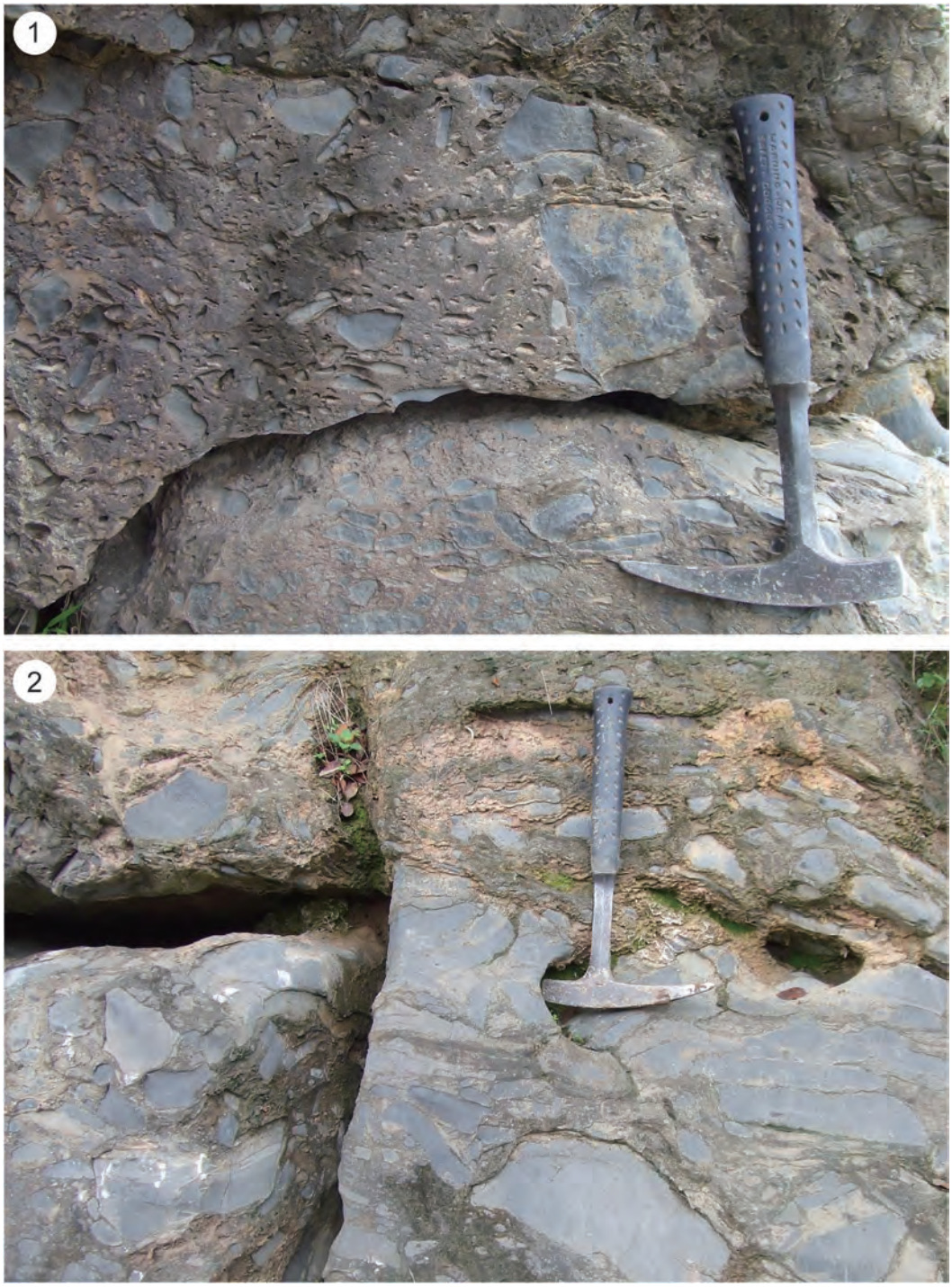


Fig. 33. Lithofacies of slope deposits in KC02. 1, Limestone breccia characterized by matrix- and clast-supports. 2, Clast-supported limestone breccia containing pebble and cobble intraclasts.

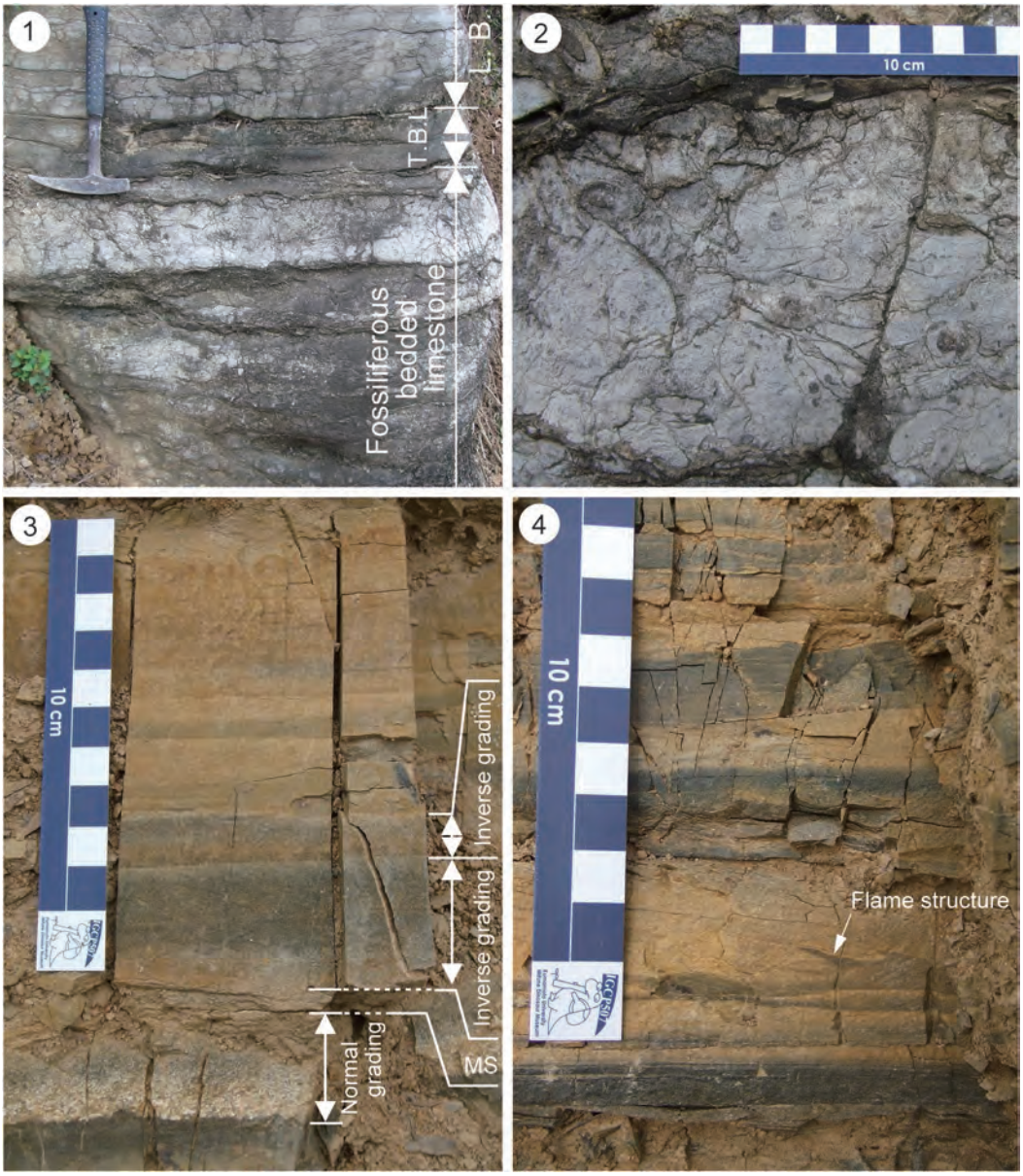


Fig. 34. 1–2, Fossiliferous bedded limestone in PK01. 1, Fossiliferous bedded limestone overlain by thin-bedded limestone (T. B. L) and limestone breccia (L. B.). 2, Fossiliferous bedded limestone containing abundant ammonoids (e.g. *Owenites koeneni*) at PK01-02. 3–4, Exposures of gravity flow deposits in NT01. 3, Gravelly and very coarse calcareous sandstone displaying normal and inverse grading. 4, Convolute- and parallel laminated calcareous sandstone and mudstone. The basal part of the calcareous sandstone occasionally contains flame structures.

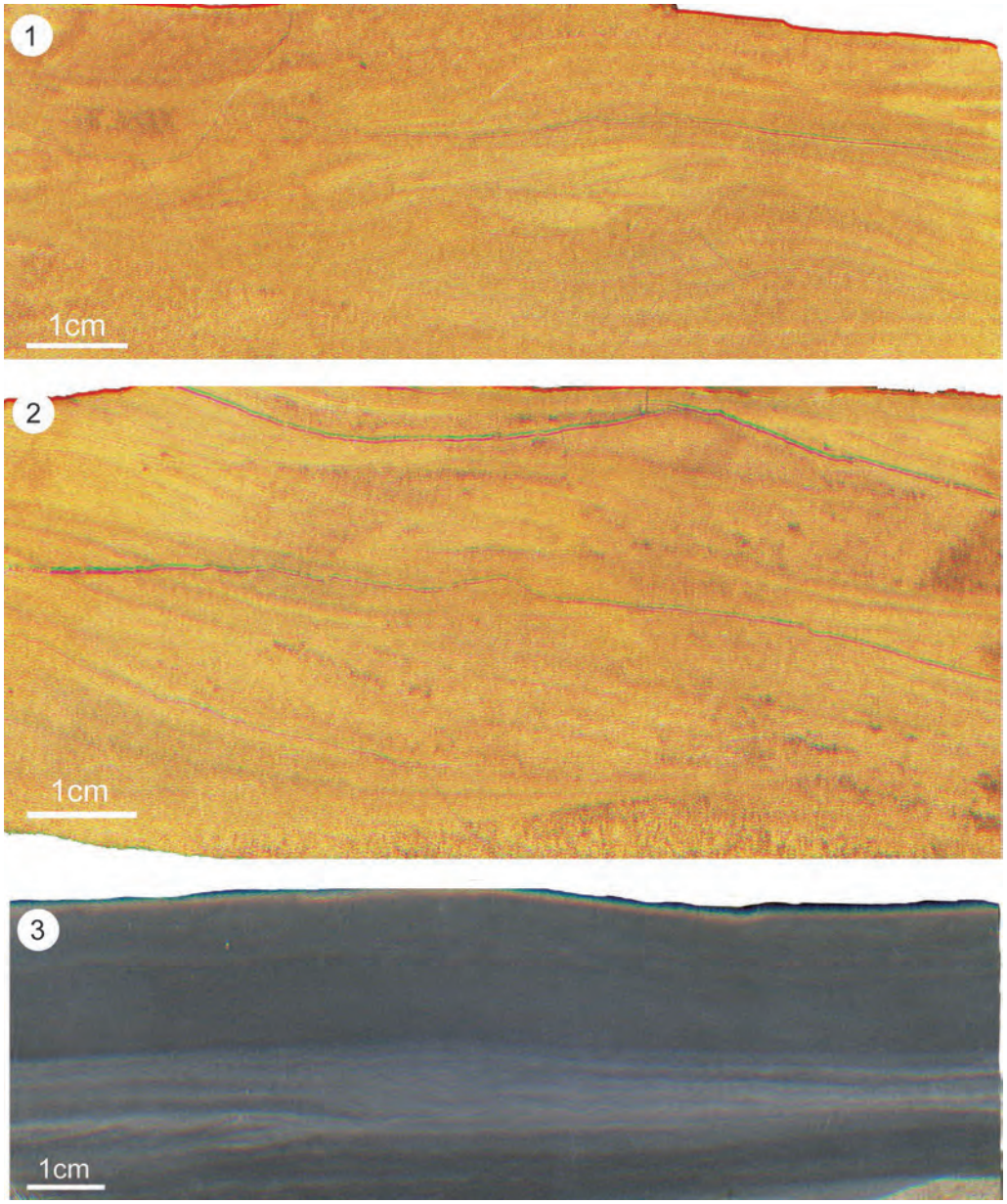


Fig. 35. Vertical cross sections of sandstone in the upper part of the Bac Thuy Formation. 1–2, Very fine siliciclastic sandstone contains climbing-ripple lamination from NT01. 3, Thin calcareous turbidite characterized by Tc and Td divisions is embedded in thick hemipelagic mudstone at KC02-15.

and poorly ornamented ostracods (Fig. 31). Komatsu *et al*. (2011, 2013) reported a monospecific ammonoid assemblage composed of *Xenoceltites variocostatus* and a thin-shelled epifaunal bivalve assemblage consisting mainly of *Crittendenia australasiatica* from this facies. In the Ban Ru area, a low diversity ostracod assemblage from the organic-rich dark gray bedded limestone is composed of several species of *Paracypris* of which *Paracypris vietnamensis* and *Paracypris* sp. A are abundant. A similar low diversity assemblage exists in the same lithologic unit in the Na Trang area, in which only two species of *Bairdia* are common.

## Biostratigraphy

**Ammonoid succession** (by Y. Shigeta)

Based on carefully controlled bed-by-bed sampling, a total of five distinct Olenekian (Smithian and Spathian) ammonoid faunas are recognized in the studied area (Fig. 36). These faunas, ranging in age from the earliest Middle Smithian through the Early Spathian, represent a more or less continuous succession that can be correlated with other Tethyan sequences such as the Salt Range (Pakistan), Spiti (India), Tulong (South Tibet), Oman and South China as well as the eastern Panthalassa. Formal zones are not introduced for these assemblages because fossil occurrences are not stratigraphically continuous and our knowledge of Early Triassic ammonoid faunas in northeastern Vietnam is only in a preliminary stage. Hence, the term "beds" is used to describe each of the local faunal sequences.

Flemingites rursiradiatus *beds*: These beds, of earliest Middle Smithian age (Brayard *et al*., 2013), are well-documented from the lower part of the fossiliferous limestone beds in the basal portion of the Bac Thuy Formation in exposures at Bac Thuy (sections BT01, 02). *Flemingites rursiradiatus* as well as *Pseudaspidites muthianus*, *Submeekoceras hsüyüchieni* and *Jinyaceras* cf. *bellum* all cooccur in these beds. This fauna correlates with that from the *Flemingites rursiradiatus* beds in Guangxi, South China (Brayard and Bucher, 2008) and Oman (Brühwiler *et al*., 2012a), as well as the *Flemingites* beds in Spiti (Brühwiler *et al*., 2012c), *Flemingites flemingianus* beds of the Salt Range (Brühwiler *et al*., 2012b) and *Flemingites* sp. beds of Utah, USA (Brayard *et al.*, 2013).

Urdyceras tulongensis *beds*: This subdivision, which occurs in the middle part of the basal portion of the Bac Thuy Formation in exposures at Bac Thuy (sections BT01, 02), is characterized by the association of *Urdyceras tulongensis*, *Ussuria kwangsiana*, *Galfetites simplicitatis*, *Pseudaspidites muthianus*, *Submeekoceras hsüyüchieni*, *Jinyaceras* cf. *bellum*, *Paranannites sinensis* and *Aspenites acutus*.

Recently, Brühwiler *et al.* (2010) documented the occurrence of *Urdyceras tulongensis* in the *Brayardites compressus* beds (lower Middle Smithian) at Tulong, South Tibet, and since an equivalent fauna is not known from South China, Brühwiler *et al*. (2010, 2012c) pointed out that the *Brayardites compressus* beds can probably be correlated with an interval between the *Flemingites rursiradiatus* beds and the *Owenites koeneni* beds of South China. Although *Brayardites compressus* Brühwiler *et al*., 2010 has not yet been found in northeastern Vietnam, the occurrence of *U. tulongensis* supports the suggestion of Brühwiler *et al*. (2010, 2012c). Therefore, this subdivision is considered to be of early Middle Smithian age.

Owenites koeneni *beds*: This subdivision occurs in the upper part of the basal portion of the Bac Thuy Formation in the Bac Thuy sections (BT01, 02) and the Pac Khanh section (PK01) as well as in limestone breccia and bedded limestone in the lower portion of the Bac Thuy Formation exposed along the Ky Cung River (sections KC01, 02). These beds are mainly characterized by *Owenites koeneni* and *Dieneroceras*? *goudemandi*, but other taxa

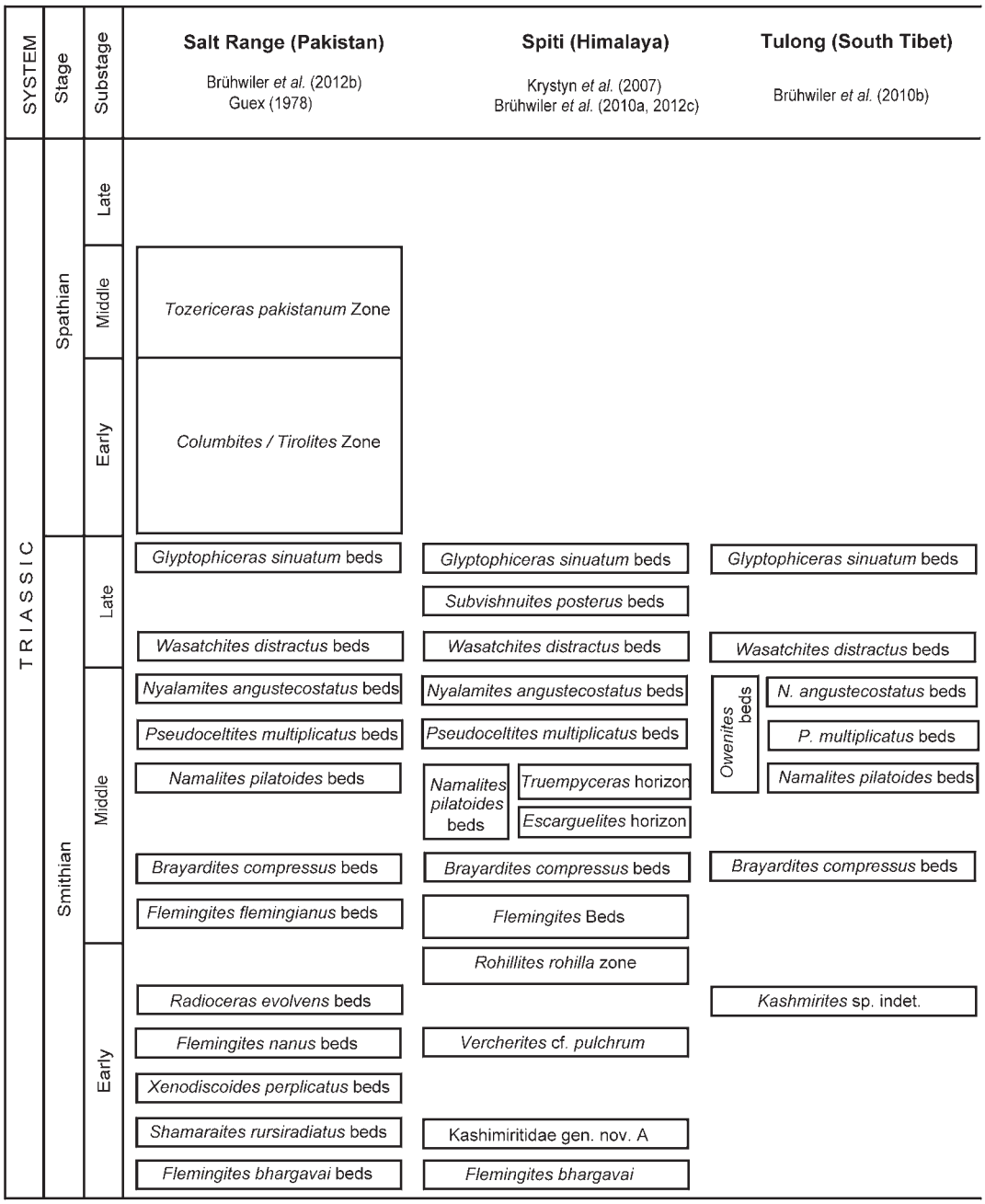


Fig. 36. Ammonoid and conodont biostratigraphic subdivision of the Lower Triassic of northeastern Vietnum and correlation with other regions. *N. p.*: *Novispathodus pingdingshanenesis*, *T. s.*: *Triassospathodus symmetricus*.

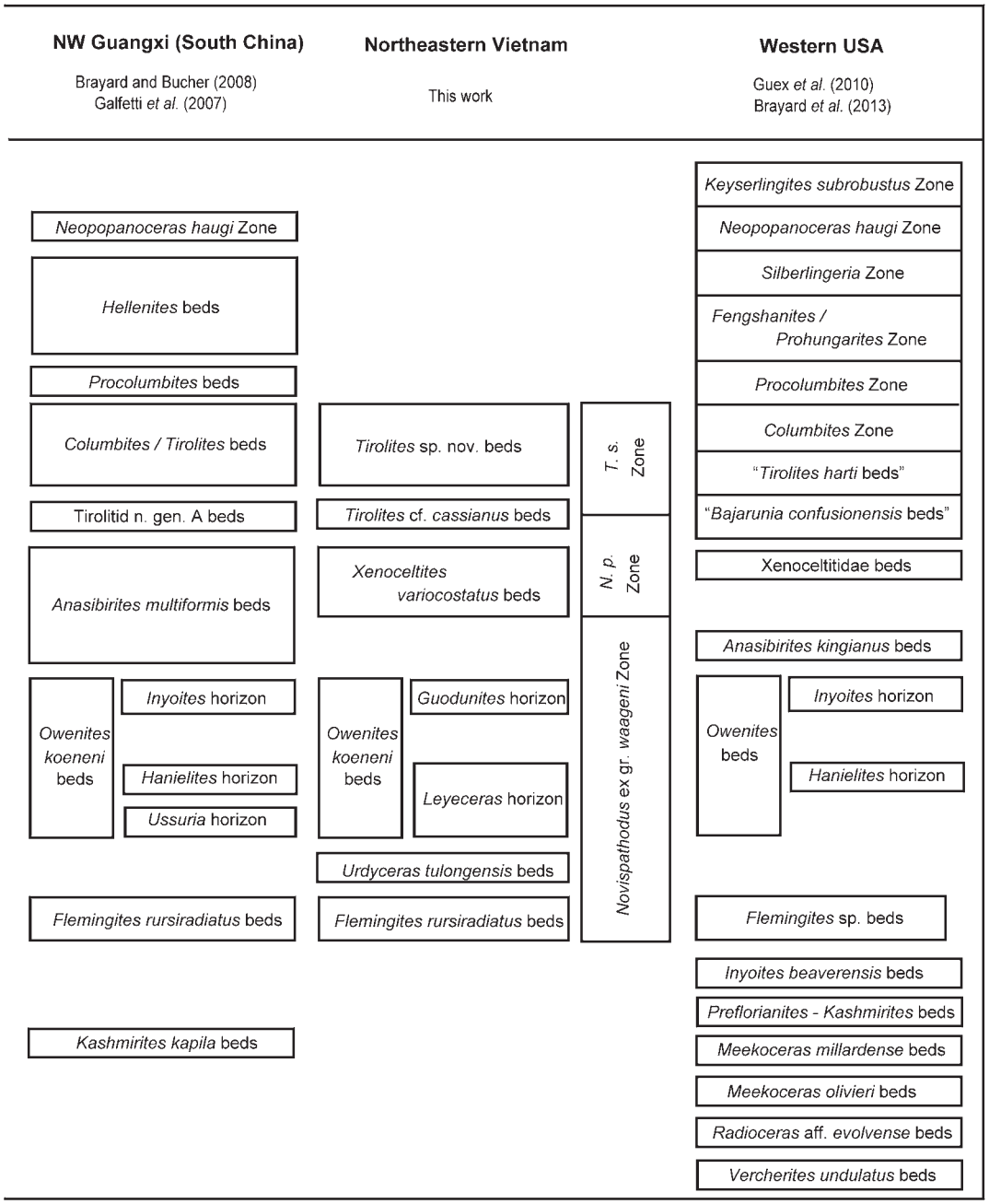
NW Guangxi (South China)
Brayard and Bucher (2008)
Galfetti et al. (2007)
Northeastern Vietnam
This work
Western USA
Guex et al. (2010)
Brayard et al. (2013)
Neopopanoceras haugi Zone
Hellenites beds
Procolumbites beds
Columbites / Tirolites beds
Tirolitid n. gen. A beds
Anasibirites multiformis beds
Owenites koeneni beds
Inyoites horizon
Hanielites horizon
Ussuria horizon
Flemingites rursiradiatus beds
Kashmirites kapila beds
Tirolites sp. nov. beds
Tirolites cf. cassianus beds
Xenoceltites variocostatus beds
Owenites koeneni beds
Guodunites horizon
Leyeceras horizon
Urdyceras tulongensis beds
Flemingites rursiradiatus beds
T. s. Zone
N. p. Zone
Novispathodus ex gr. waageni Zone
Keyserlingites subrobustus Zone
Neopopanoceras haugi Zone
Silberlingeria Zone
Fengshanites / Prohungarites Zone
Procolumbites Zone
Columbites Zone
"Tirolites harti beds"
"Bajarunia confusionensis beds"
Xenoceltitidae beds
Anasibirites kingianus beds
Owenites beds
Inyoites horizon
Hanielites horizon
Flemingites sp. beds
Inyoites beaverensis beds
Preflorianites - Kashmirites beds
Meekoceras millardense beds
Meekoceras olivieri beds
Radioceras aff. evolvense beds
Vercherites undulatus beds

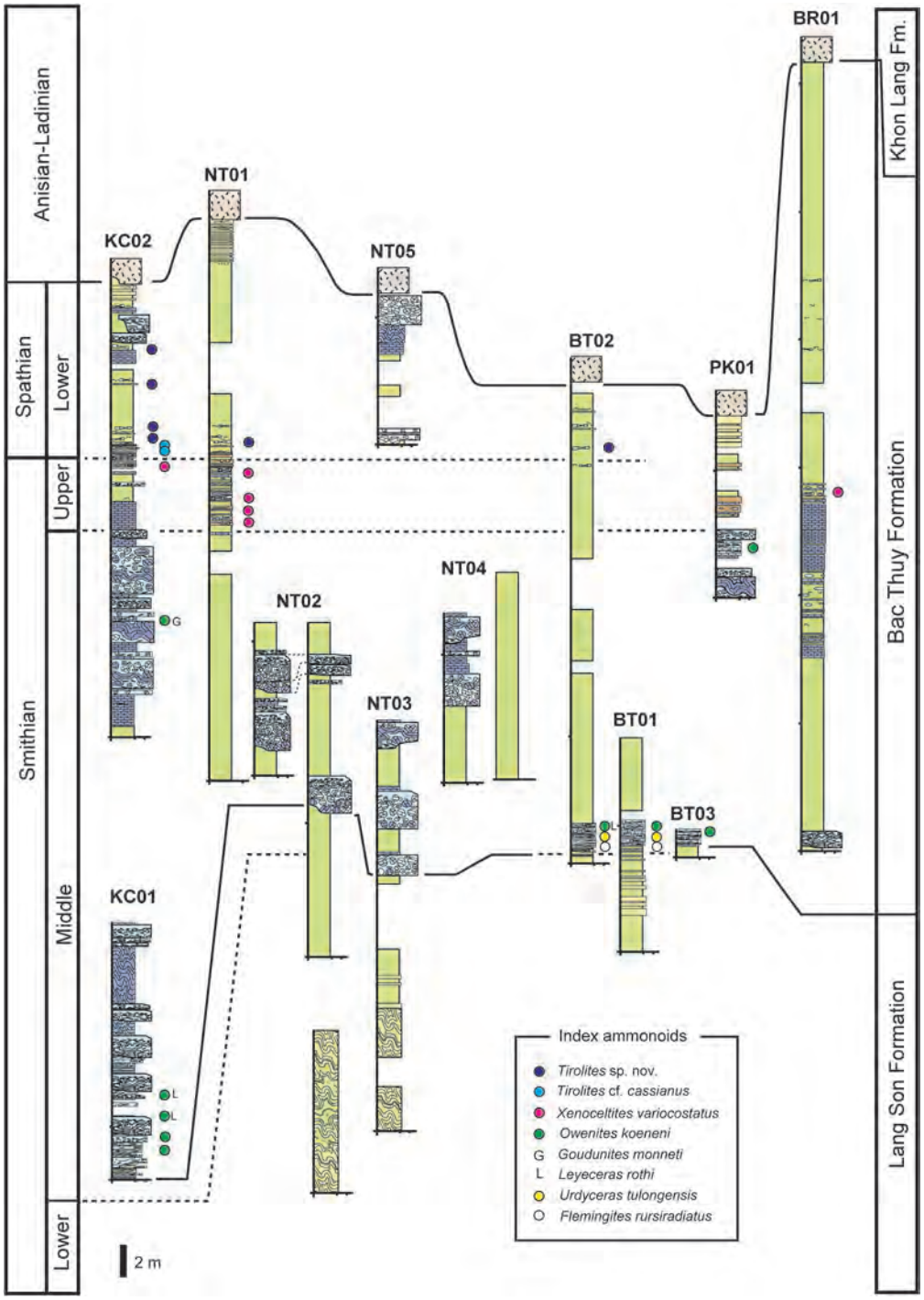


Fig. 37. Distribution of index ammonoid taxa in the Bac Thuy Formation.

are also found at two different horizons as follows: *Preflorianites radians*, *Leyeceras rothi*, *Anaflemingites hochulii*, *Juvenites sinuosus* and *Parussuria compressa* in the lower part (*Leyeceras* horizon), and *Guodunites monneti* in the upper part (*Guodunites* horizon).

In Guangxi, South China, Brayard and Bucher (2008) subdivided the Middle Smithian *Owenites koeneni* beds into three horizons in ascending order as follows: *Ussuria*, *Hanielites* and *Inyoites* horizons. The *Leyeceras* horizon, of middle Middle Smithian age, probably can be correlated with the *Ussuria* and *Hanielites* horizons as well as the *Nammalites pilatoides* beds in the Salt Range (Brühwiler *et al*., 2012b), Spiti (Brühwiler *et al*., 2012c) and Tulong (Brühwiler *et al*., 2010). The *Guodunites* horizon, of late Middle Smithian age, correlates with the *Inyoites* horizon of South China and Utah, USA (Brayard *et al*., 2013), the *Meekoceras gracilitatis* Zone in Nevada, USA (Jenks *et al*., 2010) and the *Nyalamites angustecostatus* beds in the Salt Range (Brühwiler *et al*., 2012b), Spiti (Brühwiler *et al*., 2012c) and South Tibet (Brühwiler *et al*., 2010).

Xenoceltites variocostatus *beds*: These beds, which are well-documented from the middle portion of the Bac Thuy Formation (sections NT01, KC02, BT02, BR01), are characterized by the unique occurrence of *Xenoceltites variocostatus*. This subdivision is middle to late Late Smithian in age, because *X. variocostatus* occurs in the upper part of the *Anasibilites multiformis* beds in Guangxi, South China (Brayard and Bucher, 2008), the *Glyptophiceras sinuatus* beds of South Tibet (Brühwiler *et al*., 2010) and the Salt Range (Brühwiler *et al*., 2012b) and the *Subvishnuites posterus* beds in Spiti (Brühwiler *et al*., 2012c).

Tirolites *cf.* cassianus *beds*: Of earliest Early Spathian age, these beds are well-documented in the upper portion of the Bac Thuy Formation exposed along the Ky Cung River (section KC02). Also found with *Tirolites* cf. *cassianus* are *Pseudosageceras* sp. and *Xenoceltites*? sp. *Tirolites cassianus* has long been recognized as one of the more important age-diagnostic species of the earliest Early Spathian in the Tethys (Krystyn, 1974; Posenato, 1992).

Tirolites *sp. nov. beds*: This subdivision, of Early Spathian age, occurs in the upper portion of the Bac Thuy Formation (sections NT01, KC02, BT02, BR01). Its fauna is characterized by the association of *Tirolites* sp. nov., *Columbites* sp., *Xenoceltites*? sp., *Yvesgalleticeras*? sp., *Procarnites*? sp., *Eodanubites*? sp. and *Goudemandites langsonensis* sp. nov. *Tirolites* and *Columbites* are typical age-diagnostic taxa of the Early Spathian (Kummel, 1969; Guex *et al*., 2010).

**Conodont succession** (by T. Maekawa and T. Komatsu)

The Lower Triassic section in the northeastern Vietnam can be divided into three conodont zones in ascending order as follows: *Novispathodus* ex gr. *waageni* Zone, *Novispathodus pingdingshanensis* Zone, and *Triassospathodus symmetricus* Zone (Fig. 36).

Novispathodus *ex gr.* waageni *Zone*: This zone begins with the first occurrence of *Novispathodus* ex gr. *waageni* and ends with the first occurrence of *Nv. pingdingshanensis*. The following taxa are associated: *Conservatella conservativa*, *C.* sp. indet. A, *Discretella discreta*, *D. robustus*, *D.* sp. indet. A through G, *Guangxidella bransoni*, *G.* sp. indet. A, *G.* sp. indet. B, *Eurygnathodus costatus*, *Neospathodus* aff. *concavus*, *Ns. cristagalli*, *Ns. dieneri*, *Ns. novaehollandiae*, *Ns. pakistanensis*, *Ns. posterolongatus*, *Ns. spitiensis*, *Ns.* sp. indet. A, *Ns.* sp. indet. B, *Ns.* sp. indet. C, *Smithodus longiusculus*, *Novispathodus pingdingshanensis*, *Hadrodontina*? sp. indet. A, and *H.*? sp. indet. B. The Zone encompasses the *Flemingites rursiradiatus*, *Urdyceras tulongensis*, *Owenites koeneni*, and part of the *Xenoceltites variocostatus* ammonoid beds in the Bac Thuy Formation. Conodonts are abundant in the in-

terval between the *Flemingites rursiradiatus* beds and *Owenites koeneni* beds, but are scarce in the *Xenoceltites variocostatus* beds.

*Novispathodus waageni* is a well-known species whose range covers the entire Smithian (Sweet *et al*., 1971; Orchard, 2007a). Sweet (1970b) first reported the species from the Mianwali Formation, West Pakistan and designated it as the guide species of Zone 7, which corresponds to the Smithian part of the formation. Subsequently, *Nv. waageni* has been reported from throughout the Smithian in other parts of the world (McTavish, 1973; Mosher, 1973; Goel, 1977; Buryi, 1979; Solien, 1979; Wang and Cao, 1981; Koike, 1982; Matsuda, 1983; Beyers and Orchard, 1991; Orchard, 2007b; Orchard and Krystyn, 2007; Zhao *et al*., 2007; Orchard, 2008; Beranek *et al*., 2010; Goudemand *et al*., 2012 etc.). Orchard and Krystyn (2007), Zhao *et al*. (2007) and Orchard (2010) reported that the first appearance datum of the species is an indicator of the Induan/Olenekian boundary (IOB). Furthermore, the range of the species extends to the uppermost Smithian (Orchard, 2007a; Zhao *et al*., 2007).

A significant morphological change in *Novispathodus waageni* was pointed out by Matsuda (1983), Orchard and Krystyn (2007), Zhao *et al*. (2007) and Igo (2009). Orchard and Krystyn (2007) divided the species into six morphotypes based on the form of denticles, lateral ribs, and basal cavities of abundant specimens from the Mud section, Spiti, India. According to Orchard and Krystyn (2007), the first appearance data of these morphotypes are different, and Morphotype 1 (M1), which has a prominent lateral rib, is the oldest, with a range limited to the lowermost part of the formation. M1 does not occur in the Bac Thuy Formation, which indicates that lowermost Smithian strata are not included in the formation.

*Discretella discreta* was first described from the Smithian ammonoid beds at Crittenden Springs, Nevada as *Ctenognathus discreta* (Müller, 1956). It has also been reported from Malaysia (Koike, 1982), South China (Duan, 1987), northeastern Vietnam (Bui, 1989), Spiti, India (Krystyn *et al*., 2007), and British Columbia (Orchard, 2008; Beranek *et al*., 2010). In particular, Krystyn *et al*. (2007) and Orchard (2007b) reported the occurrence of *D. discreta* from the *Rohillites rohilla* ammonoid Zone (= Lower Smithian) of Spiti, India, and Orchard (2008) reported that it co-occurs with the Smithian ammonoid *Euflemingites romunderi* Tozer, 1961, which indicates an Early to Middle Smithian age. Thus, *D. discreta* ranges from the Lower to the Middle Smithian, and its occurrence extends from throughout the Tethyan realm to the Panthalassan region. Hence, this world-wide species is an important indicator of Lower to Middle Smithian sediments.

Abundant specimens of *Guangxidella bransoni* occur in the middle part of the Bac Thuy Formation in association with *Conservatella conservativa* and *Discretella discreta*, and its range extends from throughout the *Urdyceras tulongensis* ammonoid beds up through the *Leyeceras* horizon of the *Owenites koeneni* ammonoid beds. *G. bransoni*, characterized by an arched element and cordiform basal cavity, has only been reported from the Panthalassan realm; Nevada (Müller, 1956), Utah (Solien, 1979), northeastern Vietnam (Bui, 1989), and South China (Zhang and Yang, 1991).

*Eurygnathodus costatus* is a well-known species that ranges from the Upper Dienerian to the Lower Smithian in certain parts of the world. This segminiplanate element is characteristic and its distribution is limited mainly to the Tethyan realm. However, the species has been reported from Smithian strata in British Columbia, Canada (Beyers and Orchard, 1991). In the Bac Thuy Formation, the species co-occurrs with *Flemingites rursiradiatus*, and it also coexists with flemingitid ammonoids in Spiti and South China (Orchard and Krystyn, 2007; Zhao *et al*., 2007).

*Smithodus longiusculus*, which has only been reported from a few worldwide locations, co-occurs with the following ammonoids and conodonts: *Arctoceras tuberculatum* (Smith, 1932) and *Furnishius triserratus* (Buryi, 1997, South Primorye); *Euflemingites romunderi* and *Neospathodus waageni* (= *Novispathodus waageni*) (Mosher, 1973, British Columbia). These taxa indicate that *S. longiusculus* ranges from the Lower to the Middle Smithian, and furthermore, its geographical occurrence is limited to the marginal region of Panthalassa.

Novispathodus pingdingshanensis *Zone*: This zone extends from the first occurrence of *Novispathodus pingdingshanenesis* to the first appearance of *Triassospathodus symmetricus*. Other co-occurring taxa include *Nv*. ex gr. *waageni*, *Nv*. sp. nov. A, *Nv*. sp. indet. A, and *Icriospathodus*? *zaksi*. The zone encompasses the *Xenoceltites variocostatus* and *Tirolites* cf. *cassianus* ammonoid beds.

Compared to the other two zones, conodonts in this zone are fewer in number and their size is smaller. Chen *et al*. (2013) reported a size reduction in conodonts around the Smithian/Spathian boundary (SSB) and suggested that the phenomenon is related to the SSB global worming event. In this study, a similar trend is also documented near the SSB in the Bac Thuy Formation.

*Novispathodus pingdingshanenesis* was first described by Zhao *et al*. (2007) from the West Pingdingshan section, Anfui Province, South China. Subsequently, the taxa has been reported from other Chinese localities including Anhui (Liang *et al*., 2011), Guizhou (Ji *et al*., 2011) and Guangxi (Goudemand *et al*., 2012). These authors reported only a lowermost Spathian occurrence for the species. However, in Guangxi (Goudemand *et al*., 2012) and northeastern Vietnam (this study), *Nv*. *pingdingshanensis* co-occurs with *Xenoceltites variocostatus*, which indicates a latest Smithian age. Furthermore, in this study the Spathian part of the Bac Thuy Formation also yields the mentioned species. This evidence revises the range of the species downwards such that it extends from the uppermost Smithian to the Lower Spathian.

*Icriospathodus*? *zaksi*, an important species for recognition of the SSB, was first described by Buryi (1979) from the upper part of the *Anasibirites nevolini* Zone (= Upper Smithian) and the lower part of the *Tirolites cassianus* Zone (= Lower Spathian) in South Primorye, Russia (Buryi, 1979). The taxa has also been reported from the southern Alps (Perri and Andraghetti, 1987, pl. 33, figs. 1–4) where it co-occurs with *Triassospathodus symmetricus* (Perri and Andraghetti, 1987, pl. 33, fig. 5), which indicates a range from the Lower to the Upper Spathian (both species were described as *Neospathodus triangularis*). According to these reports, the range of *I*.? *zaksi* extends from the uppermost Smithian to the Lower Spathian.

The form of the $P_1$ element of *Icriospathodus*? *zaksi* resembles that of *I. collinsoni* except for a single row of denticles. Obviously, the species exhibits a form that is ancestral to *I. collinsoni*, but their rarity in the Bac Thuy Formation makes it difficult to resolve the evolutionary process between them. However, the existence of *I*.? *zaksi* may result in a revision of conodont biostratigraphy around the SSB based on the evolutionary process of *Neospathodus* or *Novispathodus*.

*Novispathodus* sp. nov. A has only been reported from the Guangxi Province, South China (Goudemand *et al*., 2012) where it co-occurs with *Nv*. *pingdingshanensis* and *Nv*. *waageni*. Moreover, according to Goudemand *et al*. (2012), these species were collected from the *Xenoceltites* ammonoid Zone, which contains the latest Smithian aged ammonoid *X*. *variocostatus*.

Triassospathodus symmetricus *Zone*: This zone, consisting of typical Spathian species, is defined by the first appearance of *Triassospathodus symmetricus*. Co-occuring taxa include *Novispathodus pingdingshanensis*, *Nv*. *triangularis*, *T*. *homeri*, *Icriospathodus collin-*

*soni*, and *I.*? *crassatus*. The zone encompasses the *Tirolites* cf. *cassianus* and *Tirolites* sp. nov. ammonoid beds. In this study, relatively few conodonts were collected in the middle to upper parts of the zone, but the occurrence of *Nv. pingdingshanensis* at KC02-17 demonstrates that the zone is continuous.

*Triassospathodus symmetricus*, first reported from Jabal Safra, Oman by Orchard (1995), is described as having a symmetrical segminate element with fused and reclined denticles, and a strongly expanded subtriangular or subquadrate basal cavity, which exhibits several morphological changes (Orchard, 1995). In addition, the larger basal cavity and fewer posterior processes are different from those of *T. homeri*. Furthermore, its range extends from the Lower to the Upper Spathian (Orchard, 1995).

In the Bac Thuy Formation, *Triassospathodus symmetricus* also exhibits morphological variations of the denticulation and basal cavity. In addition, its posterior small processes gradually increase from the lowermost to the lower part of the zone (KC02-12 to KC02-15). *T. homeri* also co-occurs with *T. symmetricus* in KC02-15, which indicates rapid evolution of *Triassospathodus*. *T. symmetricus* probably evolved into *T. homeri* during early Spathian time.

*Novispathodus triangularis* and *Triassospathodus homeri* are well-known Spathian species and have been reported from many localities. In addition, the range of these species has been extended to the uppermost Spathian (Orchard, 2010).

The $P_1$ element of *Icriospathouds collinsoni* is characterized by ridge-like denticles and a developed lateral rib. Although its range is of relatively short duration, its distribution covers a wide area, extending from the Tethys to Panthalassa and also to the boreal region (Sweet *et al*., 1971; Solien, 1979; Duan, 1987; Koike, 1992; Orchard, 1995; Lucas and Orchard, 2007; Ji *et al*., 2011). These facts demonstrate that *I. collinsoni* is one of the most important index fossils for the Lower Spathian.

**Correlation** (by Y. Shigeta and T. Maekawa)

Based on Smithian ammonoid and conodont biostratigraphy (Fig. 37), the lowest part of the basal portion of the Bac Thuy Formation, containing the *Flemingites rursiradiatus* beds and the lower part of the *Novispathodus* ex. gr. *waageni* Zone, can be correlated with the lowermost Middle Smithian. The overlying middle and upper parts of the basal portion of the Bac Thuy Formation, characterized by the *Urdyceras tulongensis* beds and the *Leyeceras* horizon of the *Owenites koeneni* beds, are correlatable with the lower to middle Middle Smithian. The *Guodunites* horizon of the *Owenites koeneni* beds indicates that the upper lower portion of the Bac Thuy Formation is correlatable with the upper Middle Smithian.

A change in the ammonoid and conodont assemblages in middle portion of the Bac Thuy Formation, in which the *Xenoceltites variocostatus* beds and the *Novispathodus pingdingshanensis* Zone are recognized, suggests that this part is correlatable with the Upper Smithian (Fig. 37). The upper portion of the Bac Thuy Formation, yielding the Early Spathian ammonoid *Tirolites* and *Columbites* and a typical Spathian conodont *Icriospathodus collinsoni* and *Triassospathodus homeri*, can be correlated with the Lower Spathian (Fig. 37).

## Age of rhyolite from the Khon Lang Formation

(by Y. Tsutsumi and T. Komatsu)

Rhyolite samples from the basal part of the Khon Lang Formation at NT01 were investigated for radiometric age analysis of zircon. Cathodoluminescence imaging reveals (Fig. 38) that the sample includes two types of zircon grains, those exhibiting core-rim structure (core-rim grains) and those having less

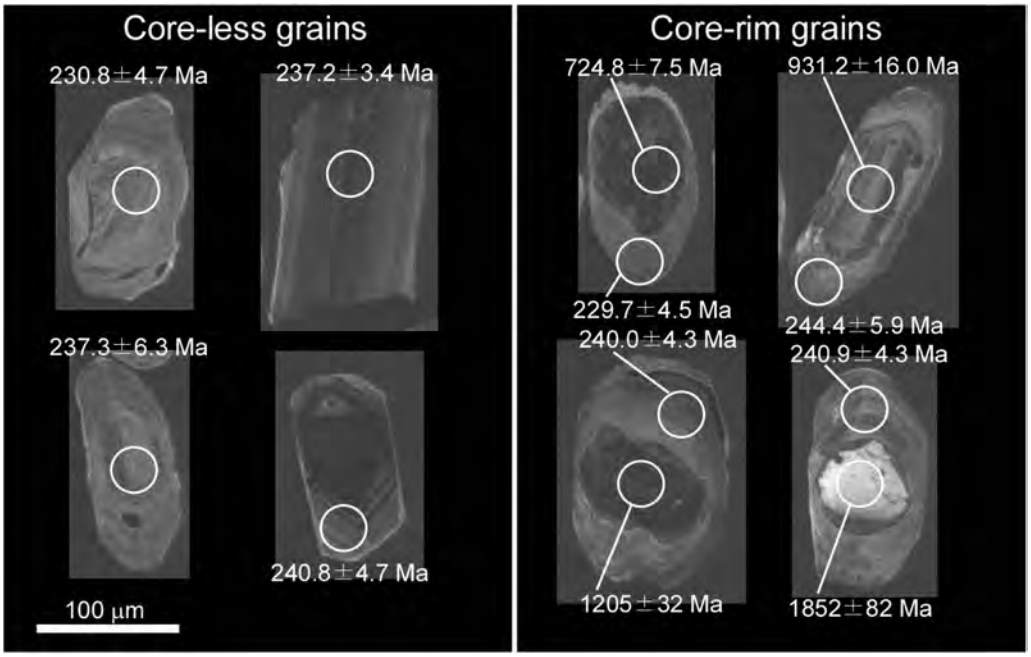


Fig. 38. Cathodoluminescence images of typical zircon grain in the sample. Circles on the images indicate the analyzed spots by LA-ICP-MS.

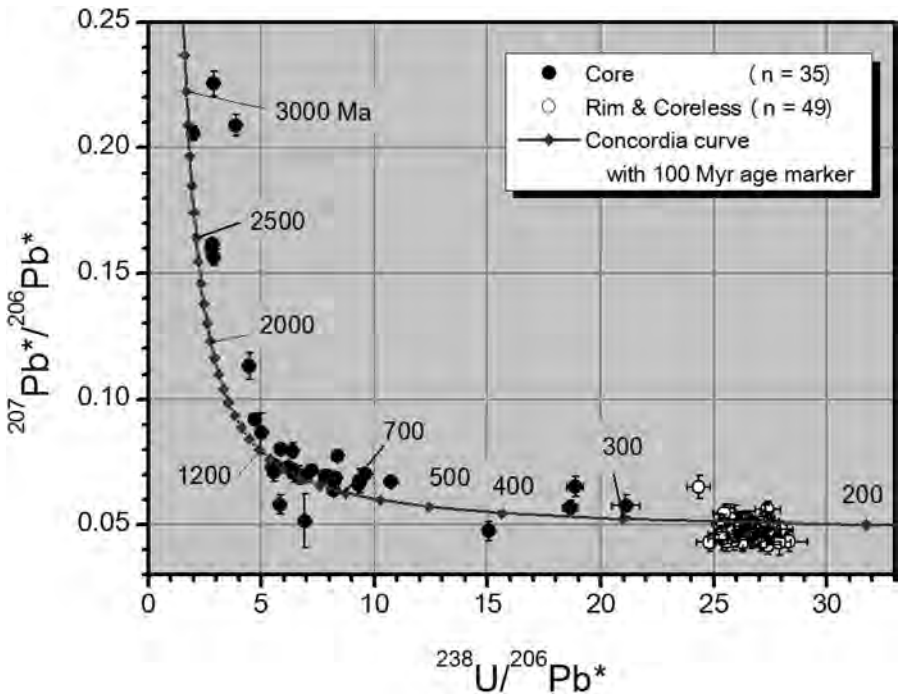


Fig. 39. Tera-Wasserberg U-Pb concordia diagram of all data from the sample. $^{207}$Pb* and $^{206}$Pb* indicate radiometric $^{207}$Pb and $^{206}$Pb, respectively.

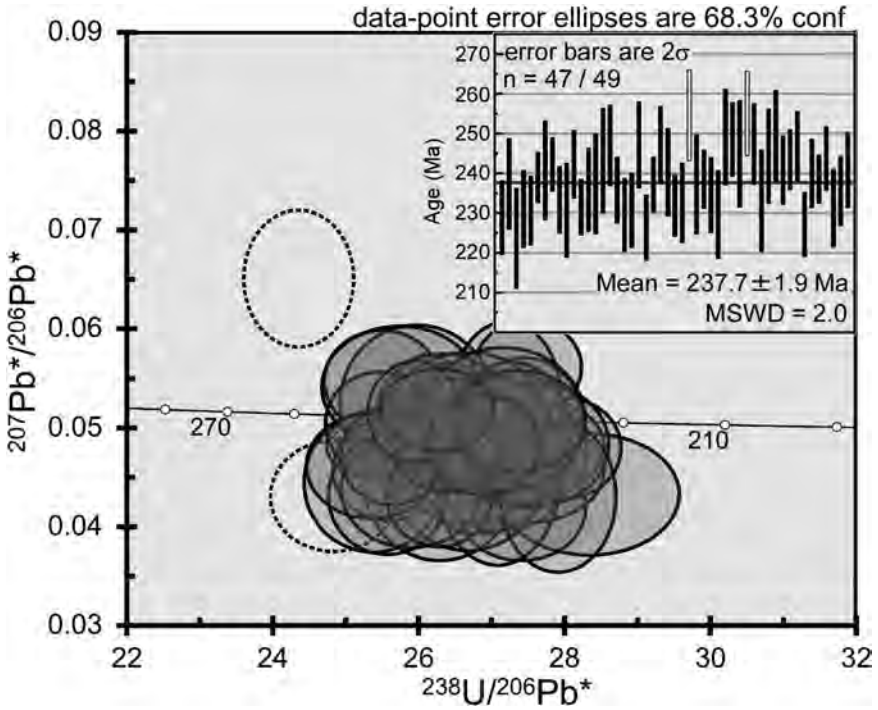


Fig. 40. Tera-Wasserberg U-Pb concordia diagrams and age distribution plot of the zircons from the sample. $^{207}Pb^*$ and $^{206}Pb^*$ indicate radiometric $^{207}Pb$ and $^{206}Pb$, respectively.

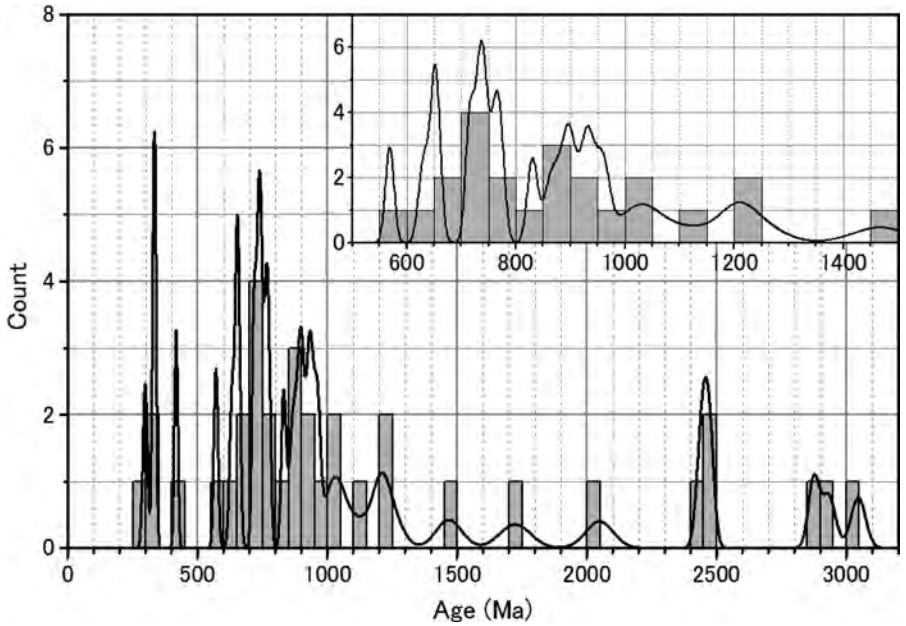


Fig. 41. Probability distribution diagram of the core ages from the grains that show core-rim structure. The $^{207}Pb^*/^{206}Pb^*$ ages for older (>1 Ga) zircons, and $^{206}Pb^*/^{238}U$ ages for younger zircons are used in this diagram. $^{207}Pb^*$ and $^{206}Pb^*$ indicate radiometric $^{207}Pb$ and $^{206}Pb$, respectively.

core (core-less grains). The core-less grains show magmatic oscillatory zoning.

The ages of the core-less grains and rims in the core-rim grains show a concentration of ~240 Ma, but data from the cores in the core-rim grains yield older and variable ages (Fig. 39). The weighted mean age of the core-less grains and rims in the core-rim grains indicate 237.7±1.9 Ma (95% conf.; Fig. 40), which is thought to be the magmatism (eruption) age of the rhyolite. On the other hand, the cores in the core-rim grains indicate multiple ages (Fig. 41); ca. >500 Ma, 600–800 Ma, 800–1100 Ma, ~2500 Ma and ~3000 Ma. This age-distribution is analogous to the detrital zircon from the South China Craton (e.g. Xu. *et al*., 2007; Jia *et al*., 2010). In consideration of the above data, the zircon cores are thought to have originated from rocks of sedimentary-origin associated with the South China Craton, and the cores thought to be xenocrysts were captured by the rhyolitic magma from the wall and/or cap rocks when the magma rose in the surrounding rocks.

## Discussion

**Aspects of Smithian ammonoid fauna** (by Y. Shigeta)

Because of the difficulty encountered in collecting macrofossils from the very hard limestones in the Bac Thuy Formation, a complete faunal list of Smithian ammonoids is not yet possible. However, ammonoids collected thus far and described herein clearly suggest that the Smithian ammonoid fauna in northeastern Vietnam is nearly identical to that of South China (Chao, 1959; Brayard and Bucher, 2008).

These ammonoid taxa exhibit six different geographical distribution patterns (Fig. 42). The first pattern, characterized by endemic distribution restricted to South China and northeastern Vietnam, is represented by *Ussuria kwangsiana* (Fig. 42.1), *Jinyaceras* cf. *bellum*, *Paranannites sinensis* and *Paranannites involutus* (Chao, 1959). The second pattern, consisting of numerous taxa, exhibits a relatively wide distribution in the Tethys (e.g. South China, Timor, South Tibet, Spiti, the Salt Range, Oman), and includes the following species: *Preflorianites radians* (Fig. 42.2), *Xenoceltites variocostatus*, *Pseudaspidites muthianus*, *Leyeceras rothi*, *Guodunites monneti*, *Dieneroceras*? *goudemandi*, *Flemingites rursiradiatus*, *Anaflemingites hochulii*, *Galfettites simplicitatis*, *Urdyceras tulongensis* and *Submeekoceras hsüyüchieni*. *Aspenites acutus*, the only taxon of third pattern (Fig. 42.3) is distributed in the Tethys and the eastern equatorial side of the Panthalassa (e.g. California, Nevada, Utah, Idaho). In contrast, the fourth pattern, consisting of *Juvenites sinuosus* (Fig. 42.4) also exhibits a Tethyan distribution, but its Panthalassan distribution is limited to the western middle latitude (South Promorye). *Parussuria compressa* and *Owenites koeneni* (Fig. 42.5), which are widely distributed in the low- to middle-paleolatitudinal regions in the Tethys and both sides of the Panthalassa, are members of the fifth pattern. The sixth pattern is represented by the pandemic distribution of *Pseudosageceras multilobatum* (Fig. 42.6), which occurs in the Tethys, both sides of the Panthalassa and the Boreal Realm (e.g. Arctic Canada, Spitsbergen).

Most species belonging to the first, second, and fourth distribution patterns also have related species belonging to the same genus in other low- to middle-paleolatitudinal regions. For example, *Preflorianites toulai* (Smith, 1932), *Xenoceltites youngi* Kummel and Steele, 1962, *Pseudaspidites silberlingi* Jenks *et al.*, 2010, *Galfettites lucasi* Jenks *et al.*, 2010, *Anaflemingites silberlingi* Kummel and Steele, 1962, *A. russelli* (Hyatt and Smith, 1905), *Guodunites hooveri* (Hyatt and Smith, 1905), *Submeekoceras mushbachanum* (White, 1879) and *Juvenites septentrionalis* Smith, 1932 all occur on the eastern equatorial side of the Panthalassa (western USA). Brayard *et al*. (2006, 2009) discussed the paleobiogeography

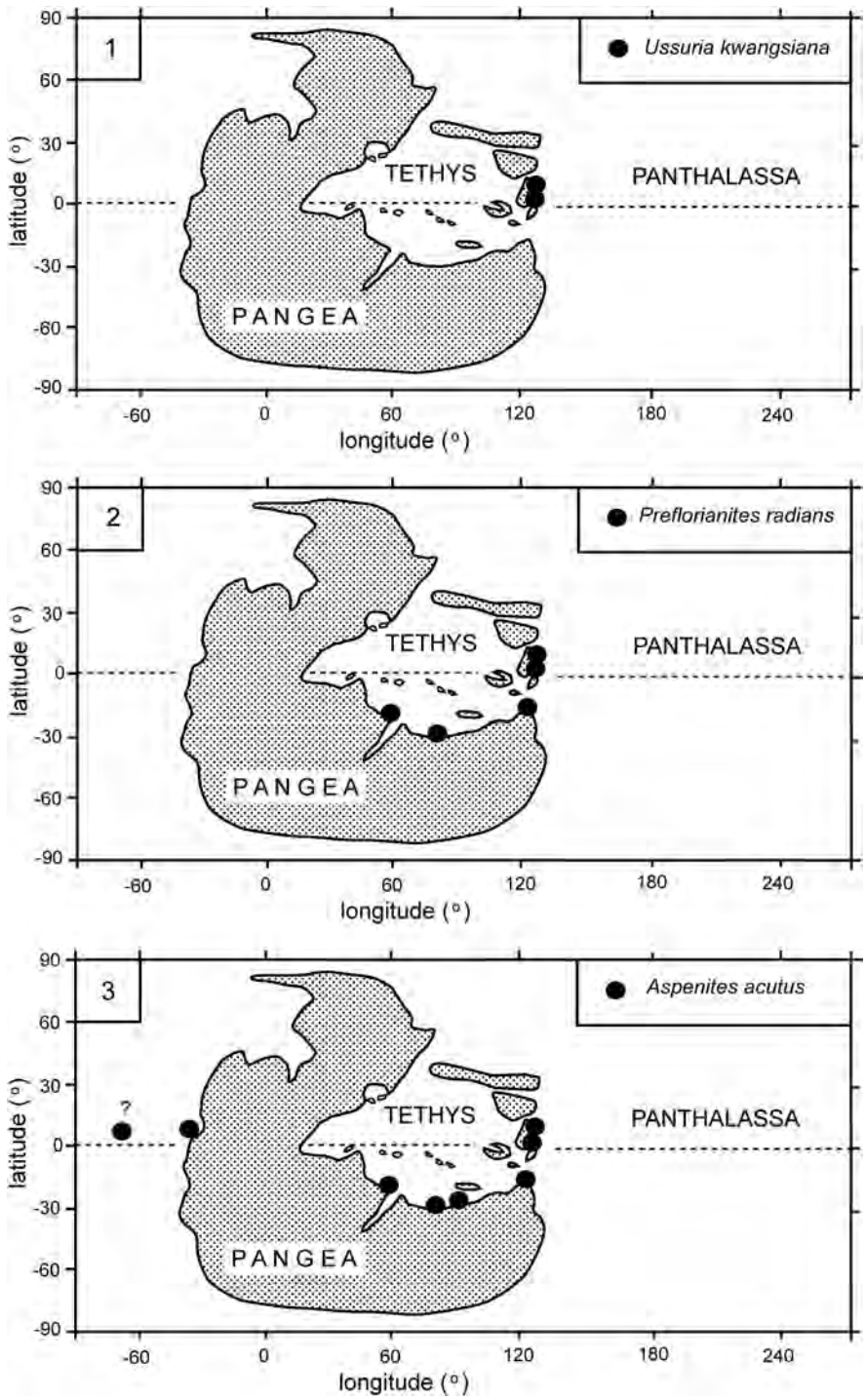


Fig. 42. Paleogeographical distribution of selected Smithian ammonoids. Paleomaps modified after Péron *et al*., 2005, Brayard *et al*., 2006 and Brayard *et al*., 2009. 1, *Ussuria kwangsiana*. 2, *Preflorianites radians.* 3, *Aspenites acutus*. 4, *Juvenites sinuosus*. 5, *Owenites koeneni*. 6, *Paseudosageceras multilobatum*.

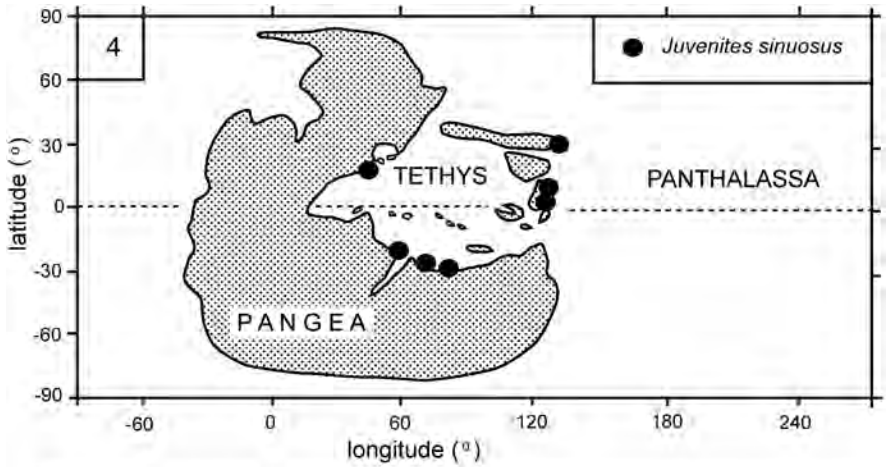
4
Juvenites sinuosus
TETHYS
PANTHALASSA
PANGEA
latitude (°)
longitude (°)
90
60
30
0
-30
-60
-90
-60
0
60
120
180
240

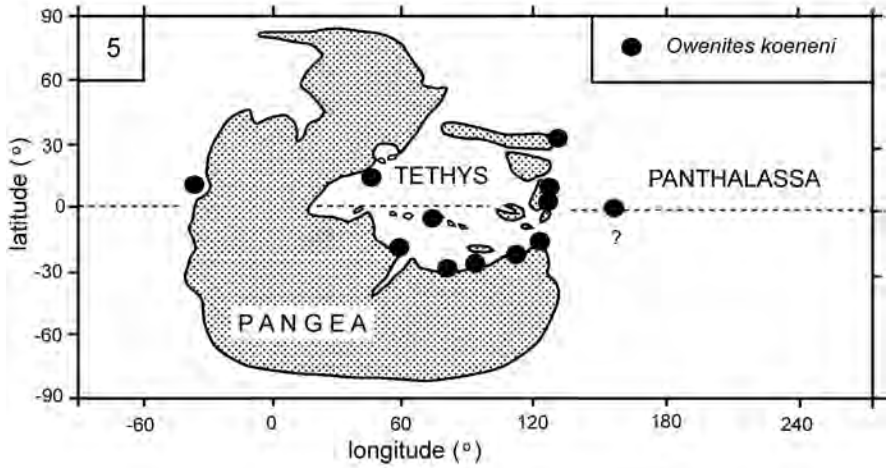
5
Owenites koeneni
TETHYS
PANTHALASSA
?
PANGEA
latitude (°)
longitude (°)
90
60
30
0
-30
-60
-90
-60
0
60
120
180
240

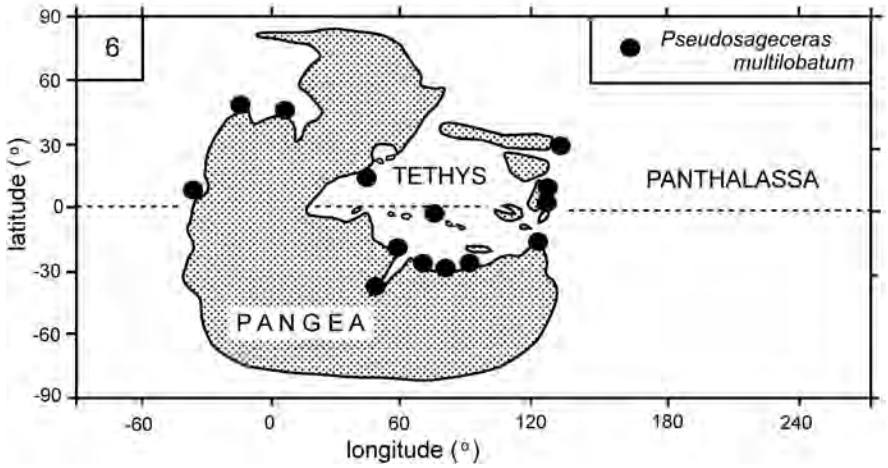
6
Pseudosageceras multilobatum
TETHYS
PANTHALASSA
PANGEA
latitude (°)
longitude (°)
90
60
30
0
-30
-60
-90
-60
0
60
120
180
240

of Smithian ammonoids from South China and concluded that the fauna exhibits strong affinities at the generic level with the low-paleolatitudinal regions (Tethys and eastern Panthalassa) and South Primorye. However, Shigeta *et al.* (2009) pointed out that the Smithian ammonoid fauna in South Primorye contains many endemic species and it actually shares very few common species with South China. Thus, faunal affinity at the generic level does not coincide with that at the specific level for Smithian ammonoids. Smithian ammonoid occurrences in the Bac Thuy Formation suggest that the fauna exhibits a very strong relationship with other Tethyan faunas, but relatively weak relationships with faunas on both sides of the Panthalassa.

**Internal features in the early whorls of ammonoids** (by Y. Shigeta and T. Maekawa)

Following the treatment of limestone samples from the Bac Thuy Formation with acetic acid, many well-preserved micro-ammonoid specimens free of obscuring matrix were found in the residue together with abundant conodonts. The sparry calcite filling of the phragmocones had been completely dissolved as had all of the shell material, thus leaving only insoluble thin layers (probably of organic origin) that originally covered the shell surfaces. This phenomenon permitted observation of the unique three-dimensional geometry of the internal features of the early whorls.

These early whorls consist of the initial chamber, caecum, flange, siphuncle, and septa (Fig. 43). Shaped somewhat like a rugby football, the initial chamber is separated from the succeeding whorls by the first septum (=prosseptum), which is slightly convex adapically. The bulb-like beginning of the siphuncle, termed the caecum, is attached to the inside surface of the initial chamber and is located in the ventral position at the first septum. A granular structure is also visible on the inside surface of the initial chamber near the inner lip of initial chamber (=flange).

Since the mid-nineteenth century, many workers have studied the internal shell features of the early whorls of ammonoids, and it has been determined that these embryonic shells all share a number of common morphological features (Landman *et al*., 1996). The relative shape of these features as well as their size and position with respect to each other appear to be stable at higher taxonomic levels (Druschits and Khiami, 1970; Druschits and Doguzhaeva, 1974, 1981; Tanabe *et al*., 1979, 2003; Tanabe and Ohtsuka, 1985; Ohtsuka, 1986; Tanabe *et al*., 1994; Landman *et al*., 1996; Shigeta *et al*., 2001). This fact suggests that these internal shell features are strongly constrained phylogenetically, and therefore, it is possible to investigate the higher-level systematics and evolution of the ammonoids on the basis of subtle changes in these features. Shigeta *et al*. (2001) studied these early internal shell features in 40 species of the Goniatitida, Prolecanitida and Ceratitida, and discussed the origin of the Ceratitida. Shigeta and Weitschat (2004) also discussed the origin of the Ammonitina inferred from the internal shell features of some latest Triassic and Jurassic ammonoids.

Compared to Carboniferous, Permian, Jurassic and Cretaceous ammonoids, the internal shell features of Triassic ammonoids have received relatively little attention. Most previous studies, excluding that of Weitschat (1986), are based on the observation of sections polished parallel to the median section plane of matrix-filled specimens (Arkadiev and Vavilov, 1984; Vavilov, 1992; Zakharov, 1978; Shigeta and Weitschat, 2004). After dissolving the sparry calcite filling of the phragmocones with acetic acid, Weitschat (1986) then described the three-dimensional inner structures that included complex networks of cameral membranes in Middle Anisian ammonoids from Central Spitsbergen.

It is quite rare to find specimens whose phragmocones are free of interior matrix, but this preservational feature has been noted in

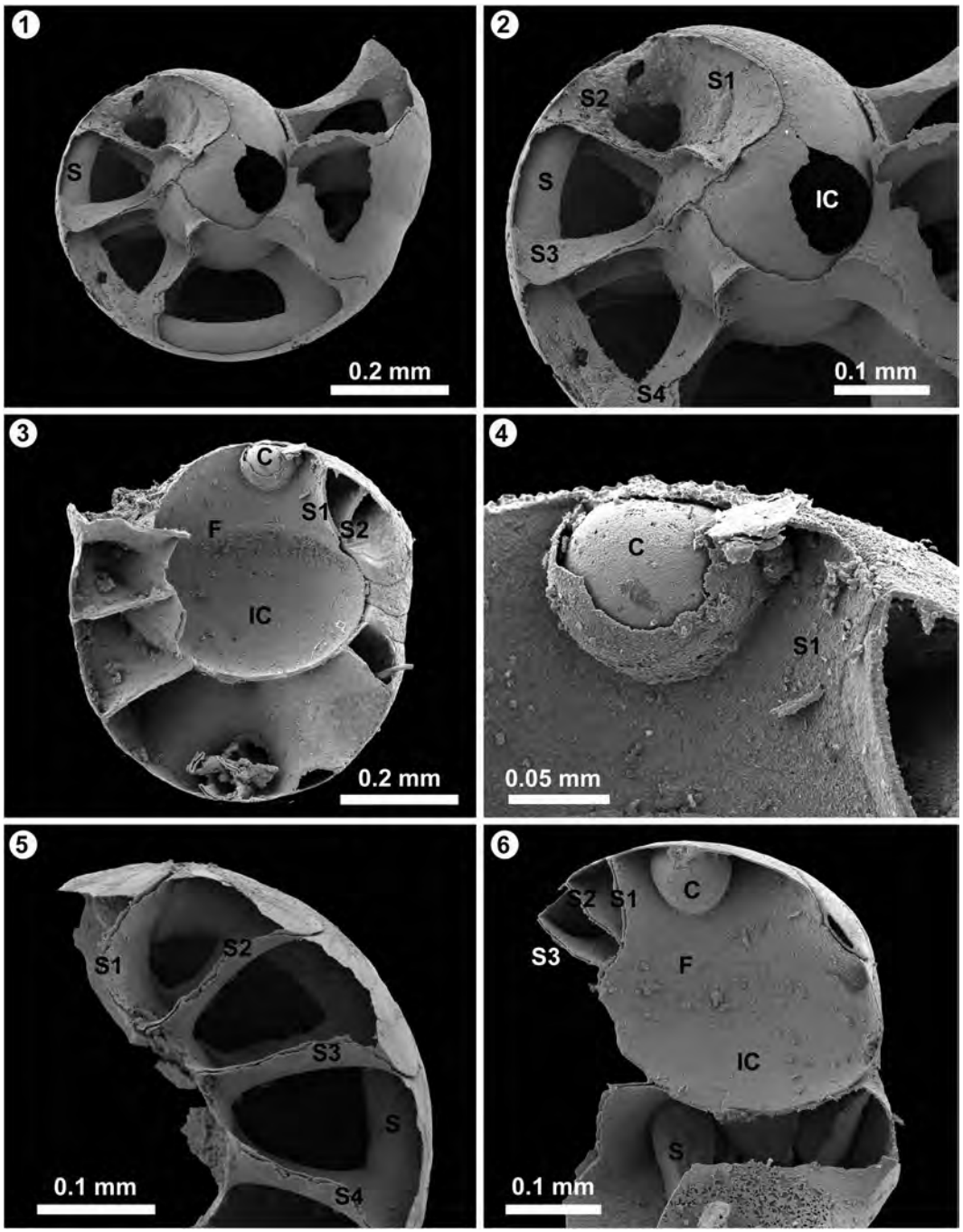


Fig. 43. Internal features in the early whorls of the Lower Triassic ammonoids from the Bac Thuy Formation in northeastern Vietnam. 1–2, NMNS PM23855, from BR01-06. 3–4, NMNS PM23856, from PK01-01. 5, NMNS PM23857, from BT02-01. 6, NMNS PM23858, from KC01-10. C: caecum, F: flange, IC: initial chamber, S: siphuncle, S1: first septum (proseptum), S2: second septum, S3: third septum, S4: fourth septum.

some Jurassic and Cretaceous ammonoids. This phenomenon permits detailed observations regarding the shape and spacing of the first few septa and associated structures in the early whorls (Landman and Bandel, 1985), and it has contributed significantly to the understanding of the sequence of embryonic development (Bandel, 1982). Furthermore, Maeda and Seilacher (1996) reported the existence of fungal "pseudomorphs" preserved in the hollow phragmocone of a Cretaceous ammonoid from Hokkaido and discussed early decay processes. Recently, Hoffmann's (2010) study of a hollow Cretaceous ammonoid from northern Kamchatka with a three-dimensional visualization method that utilized a computer tomography (CT-scan) showed a clear image of internal shell features.

Acid treatment of limestone samples from various horizons of the Bac Thuy Formation yields numerous well-preserved micro-ammonoids whose phragmocones are free of obscuring matrix. Continued studies of the internal shell features of these specimens may provide an important key for understanding the detailed microstructural relationships of their morphological features, as well help establish a clearer understanding of the higher taxonomy and evolution of Early Triassic ammonoids.

**Ammonoid mode of occurrence** (by Y. Shigeta and T. Komatsu)

Ammonoids are not preserved in the portion of the lower part of the Bac Thuy Formation consisting of wavy, lenticular thin flat-bedded carbonates and intraclastic limestones containing angular flat carbonate pebbles and cobbles that were deposited in a tidal flat environment, between the supratidal and intertidal zones (Komatsu *et al*., 2014). However, the cross-stratified limestones presumably deposited in an intertidal to subtidal calcareous sand-flat environment do yield rare, poorly preserved ammonoids. Various types of ammonoids occur abundantly in the alternating beds of bioclastic, oolitic, and intraclastic limestone characterized by wave ripples and low-angle cross-stratification that were deposited in a subtidal flat to storm-wave-influenced shallow marine environment. Ammonoids are also abundant in the alternating beds of bioclastic and intraclastic limestone formed by concentrated density flows as well as the marls of hemipelagic calcareous deposits. Poorly preserved ammonoids occur only rarely in the structureless intraclastic limestones that probably represent transgressive lag deposits. Ammonoids are not found in the limestone breccias formed by debris flows.

In the middle part of the Bac Thuy Formation, only *Xenoceltites variocostatus* occurs in the organic-rich dark gray bioclastic limestone and mudstone. The limestone is interpreted as a turbidity flow deposit (calciturbidite), whereas the mudstone is considered to be a hemipelagic siliciclastic deposit formed in an anoxic to dysoxic environment in a slope to marginal basin plain (Komatsu *et al*., 2014). Ammonoid shells were probably transported by turbidity flows.

In the upper part of the Bac Thuy Formation, ammonoids are preserved mainly in fine- to very-fine grained calcareous sandstone embedded in a thick and weakly laminated mudstone. The sandstone beds are typical of distal turbidites, and the mudstone accumulated from suspension under calm conditions (Komatsu *et al*., 2014). As with the middle part of the Bac Thuy Formation, ammonoid shells were probably transported by turbidity flows. The scarcity of ammonoids in the surrounding mudstone suggests that the slope to marginal basin plane was not a suitable environment in which to live. A similar mode of occurrence of ammonoids has been reported for the gravity flow deposits of the Lower Triassic Abrek section in South Primorye, Russia (Shigeta *et al*., 2009).

In summary, the ammonoid mode of occurrence in the Bac Thuy Formation suggests that while the supratidal to intertidal environ-

ment was uninhabitable, the majority of ammonoids probably lived in the subtidal flat to storm-wave-influenced shallow marine environment typical of a carbonate platform. After death their shells were transported from their biotope to the slope to marginal basin plane by gravity flow.

**Smithian gastropod assemblages of the Bac Thuy Formation** (by A. Kaim, A. Nützel and T. Maekawa)

All gastropods described and illustrated in this paper were removed from the limestone samples by applying acetic acid. The specimens are silicified larval and/or juvenile shells or their moulds. The preservation of the shells vary from well preserved shells with external ornamentation preserved (e.g., Figs. 125.1–125.3, 132.4–132.6, 135.4–135.6), shells where the external layer peeled off (e.g., Figs.125.7–125.12, 132.7–132.9) and specimens where only internal mould is preserved (Figs. 123.1–123.3, 130.6, 132.1–132.3, 133.4–133.9). Both the preservation and the larval/juvenile nature of the specimens cause that the detailed taxonomy (i.e., species level) is impossible.

The gastropods come from the fossiliferous limestone beds in the basal portion of the Bac Thuy Formation (BTF) exposed at Bac Thuy (sections BT01, 02), bedded limestone in the lower to middle portions of the BTF exposed along the Ky Cung River (sections KC01, 02), and the upper middle portion of the BTF (section KC02). Gastropod shells have been found in following stratigraphic levels of the Smithian though they significantly differ in number and preservation (Table 1).

*Lowest Middle Smithian gastropods*: Only two poorly preserved gastropods were collected from the *Flemingites rursiradiatus* beds. Specimen NMNS PM23849 from BT01-04 (Fig. 123.1–123.3) is moderately high-spired juvenile shell with deeply incised suture. The shell is poorly preserved with no external ornamentation preserved. The shell may have belonged to a caenogastropod juvenile (see e.g., *Atorcula*-type and *Ampezzopleura*-type juvenile shells it this paper). Another single poorly preserved specimen NMNS PM23848 from BT02-01 (Fig. 123.4–123.6) may belong to *Atorcula* though the preservation does not allow any precise identification.

Table 1. The number of gastropod taxa and the number of specimens in the recognized ammonoid biostratigraphic units. F: *Flemingites rursiradiatus* beds, O: *Owenites koeneni* beds, X: *Xenoceltites variocostatus* beds, F/O: beds between the *Flemingites rursiradiatus* and the *Owenites koeneni* beds.

| Species | F | F/O | O | X |
|---|---|---|---|---|
| *Worthenia* sp. indet. | | 2 | | |
| *Anomphalus* sp. indet. | | | 8 | 1 |
| *Abrekopsis* sp. indet. | | | 1 | |
| *Naticopsis* sp. indet. A | | 2 | 7 | 1 |
| *Naticopsis* sp. indet. B | | | 9 | |
| *Strobeus* sp. indet. | | | 1 | |
| *Ampezzopleura* sp. indet. | | | 2 | |
| *Atorcula* sp. indet. | 1 | 10 | 4 | |
| Others | 1 | 1 | 4 | |
| Total specimens | 2 | 15 | 36 | 2 |
| Total taxa | 2 | 4 | 8 | 2 |

*Lower Middle Smithian gastropods*: Fifteen juvenile gastropod shells representing four taxa were obtained from beds between the *Flemingites rursiradiatus* beds and the *Owenites koeneni* beds. They are dominated by *Atorcula* sp. indet. (10 specimens) associated by *Worthenia* sp. indet. (2 specimens), *Naticopsis* sp. indet. A (2 specimens) and single poorly preserved gastropod (Fig. 127.10–127.12) that could not be matched to any other species recognized in the samples from Vietnam.

*Middle to upper Middle Smithian gastropods*: The *Owenites koeneni* beds provided not only the richest by number but also most diversified assemblage of gastropods: thirty-six shells are classifies in eight taxa. Most common are neritoids represented by sixteen specimens of *Naticopsis* (sp. indet. A + sp. indet. B) and single specimen of *Abrekopsis*? sp. indet. *Anomphalus*? sp. indet. (8 specimens) is also common. *Atorcula* sp. indet. (4 specimens),

*Ampezzopleura* sp. indet. (2 specimens), and *Strobeus* sp. indet. (1 specimen). Additional four specimens are too poorly preserved for generic identification (Figs. 130.6, 133.4–133.12).

*Upper Smithian gastropods*: Single specimen of *Anomphalus*? sp. and *Naticopsis* sp. indet. A were collected from the *Xenoceltites variocostatus* beds.

The shells found in the Smithian of northeasternVietnam are only larval conchs or early juveniles of taxa displaying mostly planktotrophic type of development. This is indicated by the small size of the specimens (smaller 1 mm) and the fact that the initial whorl is present in most specimens showing that the apical portions of gastropods are present. Gastropod larval fall assemblages have been reported from several Palaeozoic formations (Bockelie and Yochelson, 1979; Herholz, 1992; Nützel and Mapes, 2001; Nützel *et al*., 2007; Mapes and Nützel, 2009). Nützel and Mapes (2001) and Mapes and Nützel (2009) reported a larval fall assemblage from the Mississippian of the United States and showed that metamorphosis and growth to larger adult sizes of the larvae was impossible due to anoxic condition in bottom waters. The same is probably the case in the studied assemblages from the Early Triassic of Vietnam. The gastropods either failed to survive metamorphosis or died soon thereafter. Most likely the bottom water was dysoxic or periodically anoxic.

Most of the taxa present in the investigated samples have also been reported from other associations of Smithian or more generally Early Triassic age (see e.g. Batten and Stokes, 1986; Nützel, 2005; Nützel and Schubert, 2005; Wheeley and Twitchett, 2005; Kaim, 2009; Kaim *et al*., 2010, 2013). The only taxa not recorded before in the Early Triassic are *Anomphalus* and *Atorcula* though known from Permian and Late Triassic and therefore not surprising in the Early Triassic.

**Bivalve assemblages and mode of occurrence**
(by T. Komatsu, H. T. Dang and T. C. Dinh)

Bivalves are found in uppermost Smithian to lowermost Spathian marginal basin deposits consisting of thin-bedded turbidite limestone (= calciturbidite), marl and hemipelagic mudstone containing calcareous nodules. The calciturbidites are composed mainly of Tb (parallel laminated limestone), Tc (cross-laminated limestone) and Td (week parallel laminated limestone and marl) divisions. Well-preserved shells are commonly found in the calciturbidites, marls and calcareous nodules, but nearly all specimens in the hemipelagic mudstone are poorly preserved and completely flattened.

Bivalve preservation exhibits two different types in the modes of occurrence. The first type is a shell- and matrix-supported thin (1–3 cm) lenticular shell-concentration within the thin calciturbidite beds and marl layers consisting of ammonoids and bivalves such as *Crittendenia australasiatica*, *C. langsonensis*, *Leptochondria bittneri*, *Bositra limbata* and "*Pseudomonotis*" *himaica*. In Facies 8, which consists of organic-rich dark gray wackestone and hemipelagic mudstone containing marl layers (Komatsu *et al*., 2014), *C. australasiatica* is the dominant species, accounting for +80% of the bivalve assemblage from the basal parts of Tb, Tc and Td divisions of the organic-rich dark gray calciturbidites. In Facies 10, which consists of thick hemipelagic mudstone intercalated with sandstone and wackestone layers (Komatsu *et al.*, 2014), *C. australasiatica* and "*Pseudomonotis*" *himaica* are abundant in the Tc and Td divisions of the turbidite wackestone layers, respectively (Fig. 17). Furthermore, in both Facies 8 and 10 *B. limbata*, *Bositra* sp. indet. and juveniles of *Crittendenia* form small lenticular shell-concentrations 3–10 cm thick in the Td divisions of the thin turbidite layers and hemipelagic mudstone. These bivalves are commonly disarticulated and/or fragmentary, which is indicative of gravity flow transport and typical allochthonous occurrence.

The second mode of occurrence consists of shell-scattered beds in the hemipelagic mudstone overlying the calciturbidite and marl. Both articulated and disarticulated shells of *B. limbata* and *Bositra* sp. indet. are found in the hemipelagic mudstone. Some of the articulated shells are preserved in a butterfly position, and disarticulated right and left valves of the same individual are seen to occasionally overlap. Both articulated and disarticulated shells of *C. australasiatica* are also commonly found in the hemipelagic mudstones of Facies 8. These species may represent a parautochthonous assemblage.

**Brief note on the radiolarian faunas of the Upper Smithian (Lower Triassic)** (by O. Takahashi)

Very little has been published on the distributions and relative abundances of radiolarians in the Lower Triassic, particularly in the Induan and lower Olenekian (Smithian), as radiolarian occurrences from these times are apparently restricted and scarce, and the diversity is very low. Induan and lower Olenekian radiolarians have been recovered from the following five sections: the Dienerian (upper Induan) to lower Smithian (lower Olenekian) marly limestone beds of northwestern Turkey (Kozur *et al*., 1996a), the Induan to Olenekian chert beds of northern New Zealand (Kamata *et al*., 2007; Takemura *et al*., 2007; Hori *et al*., 2011), the Dienerian limestone beds of southern Thailand (Sashida *et al*., 1998), the Smithian chert beds of central Oregon (Blome and Reed, 1992), and the Olenekian limestone beds of southern Italy (Marsella *et al*., 1993). In addition, Sugiyama (1997) described well-preserved Early Triassic radiolarian faunas from central Japan; his *Follicucullus-Parentactinia* Assemblage Zone (TR0), which correlates with the lower part of the *Parentactinia nakatsugawaensis* assemblage of Sugiyama (1992) and the lower part of the *Stylosphaera fragilis* Zone of Bragin (1991), may be early Spathian or older in age.

The Upper Smithian radiolarian fauna from the Bac Thuy Formation presented in this study has a unique species composition and a relatively high diversity for this stratigraphic level. The fauna includes a mixture of Paleozoic- and Triassic-type radiolarians. The Paleozoic-type radiolarians are dominated by entactinarians with several species of the following genera: *Multisphaera*, *Plenoentactinia*, *Retentactinia*, and *Spongentactinia*. These genera have been reported from the Devonian and Carboniferous of western Australia (Aitchison, 1993; Won, 1997) and western Germany (Won, 1990), and from the Permian of Urals (Afanasieva, 2000; Dumitrica, 2011), but none of them have been previously reported from Mesozoic strata. Interestingly, the same type of faunas, dominated by entactinarians, have been reported in other faunas from the Lower Triassic limestone beds such as: the Dienerian to lower Smithian of Turkey (Kozur *et al*., 1996a), the Dienerian of Thailand (Sashida *et al*., 1998), and the latest Spathian to earliest Anisian of Thailand (Sashida and Igo, 1992). Moreover, all of these Early Triassic occurrences have been restricted to limestone beds in low-latitude regions along the western margin of Panthalassa (Scotese, 2002). Therefore, the radiolarian fauna described here has the biostratigraphic potential to be of Early Triassic age, and may also have paleogeographic and paleoceanographic affinities to Early Triassic low-latitude faunas along the western margin of Panthalassa.

## Systematic Paleontology

**Cephalopods** (by Y. Shigeta and H. D. Nguyen)

Systematic descriptions basically follow the classification established by Sweet (1964) for orthocerids and Tozer (1981, 1994) for ceratitids and phylloceratids. Morphological terms are those used in the Treatise on Invertebrate Paleontology (Moore, 1957, 1964). Quantifiers used to describe the size and shape of ammonoid shell replicate those proposed by

Matsumoto (1954, p. 246) and modified by Haggart (1989, table 8.1).

*Abbreviations for shell dimensions*: D = shell diameter; U = umbilical diameter; H = whorl height; W = whorl width.

*Institution abbreviations*: CGM = Central Research Geological Prospecting Museum (CNIGR Museum), St. Petersburg; GPIBo = Goldfuss Museum (Steinmann Institute), Bonn University; GSI = Geological Survey of India, Kolkata; IPUW = Department of Palaeontology, University of Vienna, Vienna; NIGP = Nanjing Institute of Geology and Palaeontology, Chinese Academy of Sciences, Nanjing; NMNS = National Museum of Nature and Science, Tsukuba; PIMUZ = Institute and Museum of Paleontology, University of Zurich, Zurich; USNM = Smithonian National Museum of Natural History, Washington, D. C.

Class Cephalopoda Cuvier, 1795
Order Orthocerida Kuhn, 1940
Superfamily Orthoceratoidea McCoy, 1844
Family Orthoceratidae McCoy, 1844
Genus ***Trematoceras*** Eichwald, 1851

*Type species*: *Orthoceras elegans* Münster, 1841.

### ***Trematoceras*** sp. indet.

Figs. 44, 45

*Material examined*: Five specimens, NMNS PM23459–23463, from NT01-04.

*Description*: Moderately expanding orthoconic shell with 4–5 degree adoral angle of expansion and circular whorl cross-section. Juvenile shell ornamented with fine transverse lirae, while adult body chamber exhibits very weak ribs as well as fine transverse lirae. Siphuncle located at center, with cylindrical connecting ring and short, orthochoanitic septal neck. Suture simple and straight. Cameral deposits not observed.

*Discussion*: Although the described specimens are very close to *Trematoceras subcampanile* (Kiparisova, 1954), they are easily distinguished by the fine transverse lirae on the juvenile shell, which contrasts with network lirae on the juvenile shell of *T. subcampanile* (Shigeta and Zakharov, 2009, Fig. 27). They differ from *T. mangishlakense* Schastlivtceva (1981) and *T. insperatum* Schastlivtceva (1988) by the smaller angle of shell expansison. The described specimens are morphologically very similar to *T. campanile* (Mojsisovics, 1882), *T. vulgare* Schastlivtceva (1981), *T. ciarum* Schastlivtceva (1986), and *T. boreale* Schastlivtceva (1986), but a definitive species assignment cannot be made due to an insufficient number of well-preserved specimens.

*Occurrence*: Described specimens from NT01-04 within the portion of the *Novispathodus pingdingshanensis* Zone represented by the *Xenoceltites variocostatus* beds (Upper Smithian = upper Lower Olenekian) in the Bac Thuy Formation, northeastern Vietnam.

Order Ceratitida Hyatt, 1884
Superfamily Xenodiscoidea Frech, 1902
Family Kashmiritidae Spath, 1934
Genus ***Preflorianites*** Spath, 1930

*Type species*: *Danubites strongi* Hyatt and Smith, 1905.

### ***Preflorianites radians*** Chao, 1959

Figs. 46, 47

*Xenodiscus bittneri* Hyatt and Smith, 1905. Welter, 1922, p. 106, pl. 158, figs. 8–9.

*Preflorianites radians* Chao, 1959, p. 196, pl. 3, figs. 6–8; Brühwiler *et al*., 2012a, p. 15, pl. 1, figs. 8–9, pl. 2, figs. 1–7.

? *Glyptophiceras langsonense* Vu Khuc, 1984, p. 31, pl. 1, figs. 2–3, pl. 2, fig. 1; Vu Khuc, 1991, p. 121, pl. 45, figs. 1–3, pl. 50, fig. 3.

*Pseudoceltites*? *angustecostatus* (Welter, 1922). Brayard and Bucher, 2008, p. 18, pl. 3, figs. 1–7, text-fig. 19.

*Preflorianites* cf. *radians* Chao, 1959. Brühwiler *et al*., 2012c, p. 132, fig. 13A–E.

*Holotype*: NIGP 12564, figured by Chao (1959, p. 196, pl. 3, figs. 7–8), from the Owenitian (Middle Smithian) of the Tientung district (Tsoteng), western Guangxi, South

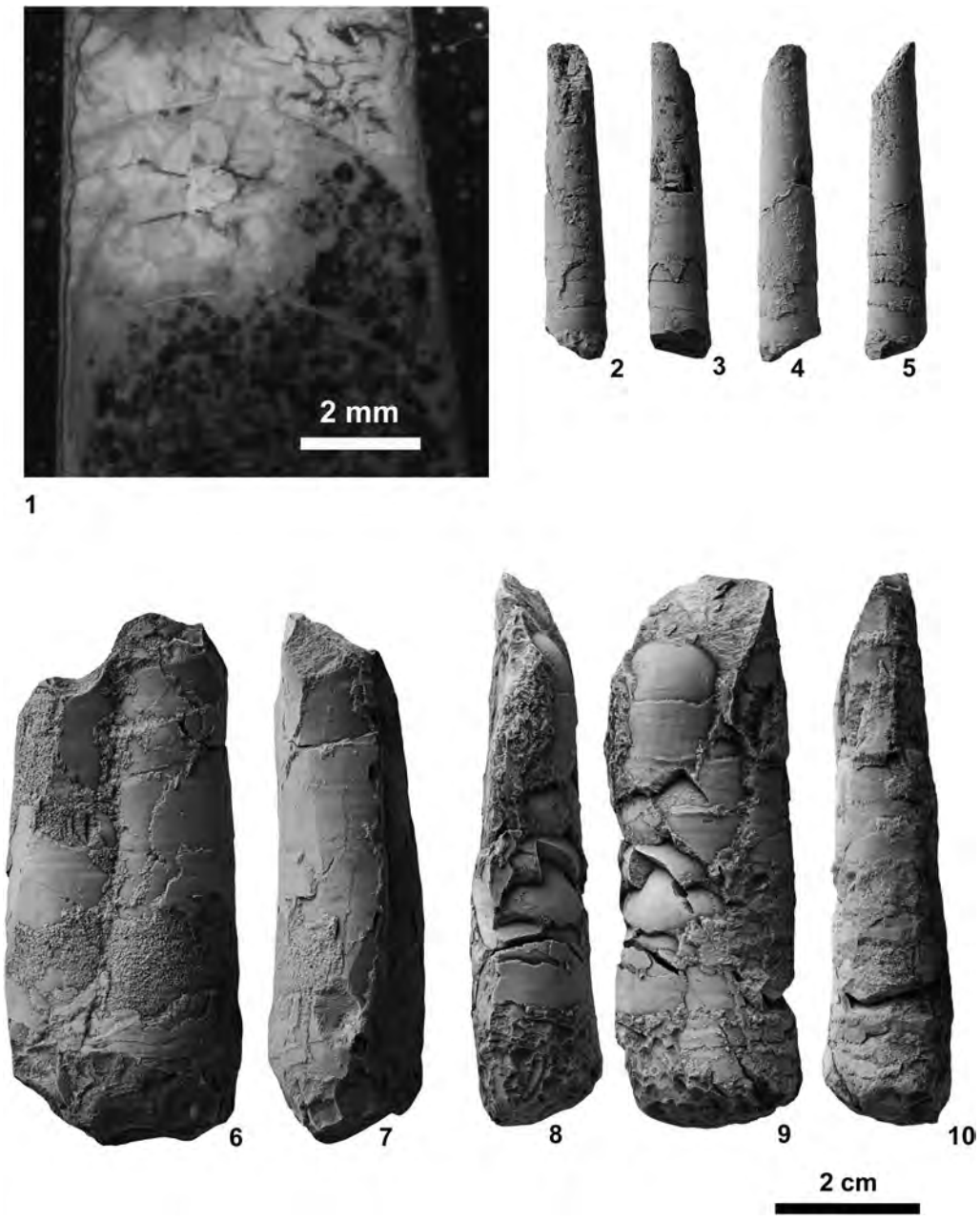


Fig. 44. *Trematoceras* sp. indet. from NT01-04. 1, NMNS PM23459. 2–5, NMNS PM23460. 6–7, NMNS PM23461. 8–10, NMNS PM23462.

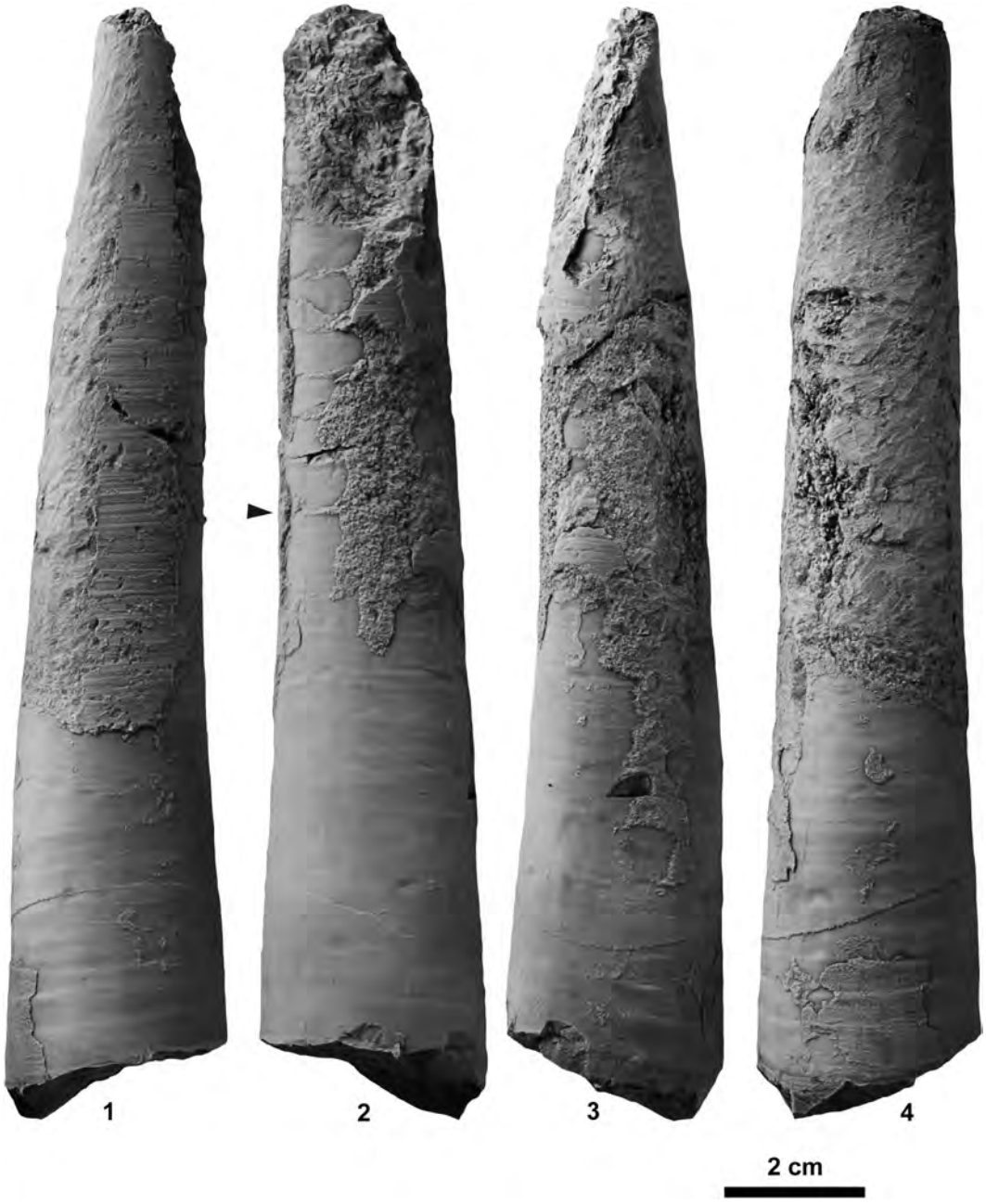


Fig. 45. *Trematoceras* sp. indet., NMNS PM23463, from NT01-04. Arrow indicates position of last septum.

China.

*Material examined*: Five specimens, NMNS PM23464–23468, from BT01-14, one specimen, NMNS PM23469, from BT02-03, one specimen, NMNS PM23470, from a float limestone block at BT03, one specimen, NMNS PM23471, from KC01-10, and three specimens, NMNS PM23472–23474, from KC01-13.

*Description*: Evolute, fairly compressed shell with elliptical whorl section, arched venter, indistinct ventral shoulders and slightly convex flanks with maximum whorl width slightly below mid-flank. Umbilicus fairly wide with moderately high, nearly vertical wall and rounded shoulders. Ornamentation consists of regularly spaced, strong, radial or slightly rursiradiate rounded ribs arising on umbilical shoulder and fading away on ventral shoulder. Suture ceratitic. First lateral saddle higher than second saddle, and third saddle lower than second saddle. First lateral lobe deep, wide with many denticulations at base, and second lateral lobe one-half depth of first lobe.

*Measurements (mm)*:

| Specimen no. | D | U | H | W | U/D | W/H |
|---|---|---|---|---|---|---|
| NMNS PM23466 | 32.0 | 13.0 | — | — | 0.41 | — |
| NMNS PM23467 | 33.5 | 15.0 | — | — | 0.45 | — |
| NMNS PM23472 | 39.5 | 17.8 | 12.4 | 10.0 | 0.45 | 0.81 |
| NMNS PM23464 | 57.0 | 25.0 | 17.0 | 13.3 | 0.44 | 0.78 |
| NMNS PM23465 | 59.2 | 28.5 | 17.0 | 14.0 | 0.48 | 0.82 |
| NMNS PM23470 | 77.0 | 38.0 | 22.0 | 17.2 | 0.49 | 0.78 |
| NMNS PM23468 | 79.0 | 42.3 | — | — | 0.54 | — |
| NMNS PM23474 | 79.0 | 40.0 | 20.0 | 16.0 | 0.51 | 0.80 |

*Discussion*: The shell features of the specimens described herein match well with specimens from South China described as *Pseudoceltites*? cf. *angustecostatus* by Brayard and Bucher (2008). However, as Brühwiler *et al*. (2012a, p. 15) later indicated, these Chinaese specimens actually belong to *Preflorianites radians.*

Brühwiler *et al*. (2012a) recently described *Preflorianites radians* from exotic blocks in Oman, and illustrated the intraspecific variation in shell form and ornamentation of this species. One of their specimens, PIMUZ 27316 (Pl. 2, fig. 7), has a slightly narrower umbilicus and weaker ribs than the typical shell of this species (e.g. PIMUZ 27311, Pl. 2, fig. 1). This particular specimen is very similar to a specimen from Timor described as *Xenodiscus bittneri* by Welter (1922, pl. 158, figs. 8–9). Welter's specimen probably should be assigned to *P. radians.*

The specimen described as *Preflorianites* cf. *radians* by Brühwiler *et al*. (2012c, PIMUZ 28201) from Spiti exhibits a slightly more involute coiling than *P. radians*, but this specimen is slightly flattened. Had its shell not been deformed, its coiling would be more evolute, which would fit well within the range of variation of *P. radians*.

Specimens attributed to *Preflorianites* cf. *radians* by Brayard and Bucher (2008) from the *Flemingites rursiradiatus* beds (lowest Middle Smithian) of South China have weaker ornamentation and thicker whorls than *P. radians*. This taxon probably represents the ancestor of *P. radians* because it is otherwise very similar.

*Occurrence*: Described specimens from BT01-14, BT02-03, BT03, KC01-10 and KC01-13 within the portion of the *Novispathodus* ex gr. *waageni* Zone that includes the *Leyeceras* horizon of the *Owenites koeneni* beds (middle Middle Smithian = middle Lower Olenekian) in the Bac Thuy Formation, northeastern Vietnam. This species also occurs in the Middle Smithian of South China (*Owenites koeneni* beds, Brayard and Bucher, 2008), Timor (Welter, 1922), Spiti (*Truempyceras compressum* horizon, Brühwiler *et al*., 2012c), and Oman (*Owenites koeneni* fauna, Brühwiler *et al*., 2012a).

## Family Xenoceltidae Spath, 1930

## Genus ***Xenoceltites*** Spath, 1930

*Type species*: *Xenoceltites subevolutus*

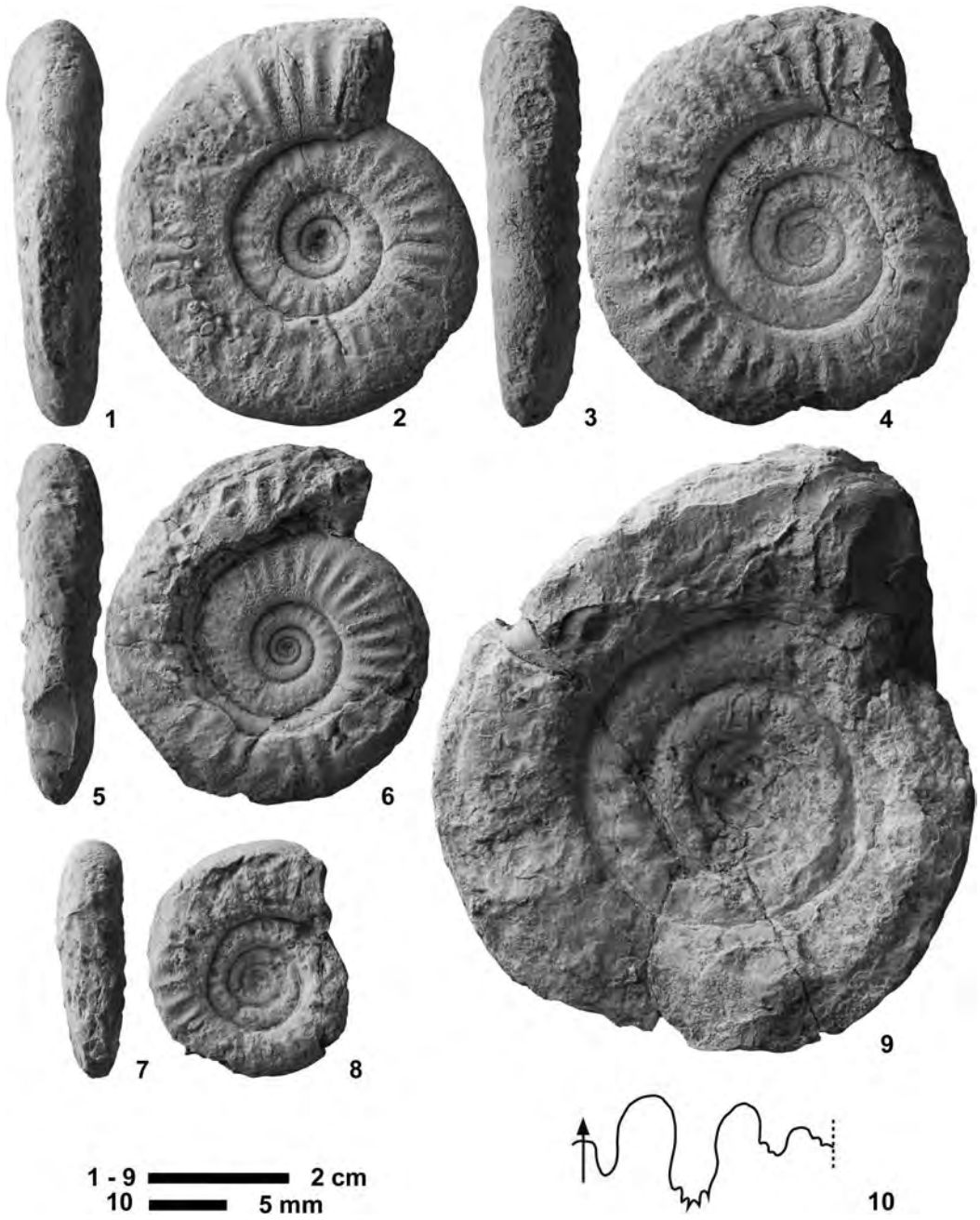


Fig. 46. *Preflorianites radians* Chao, 1959 from BT01-14. 1–2, 10, NMNS PM23464. 3–4, NMNS PM23465. 5–6, NMNS PM23466. 7–8, NMNS PM23467. 9, NMNS PM23468.

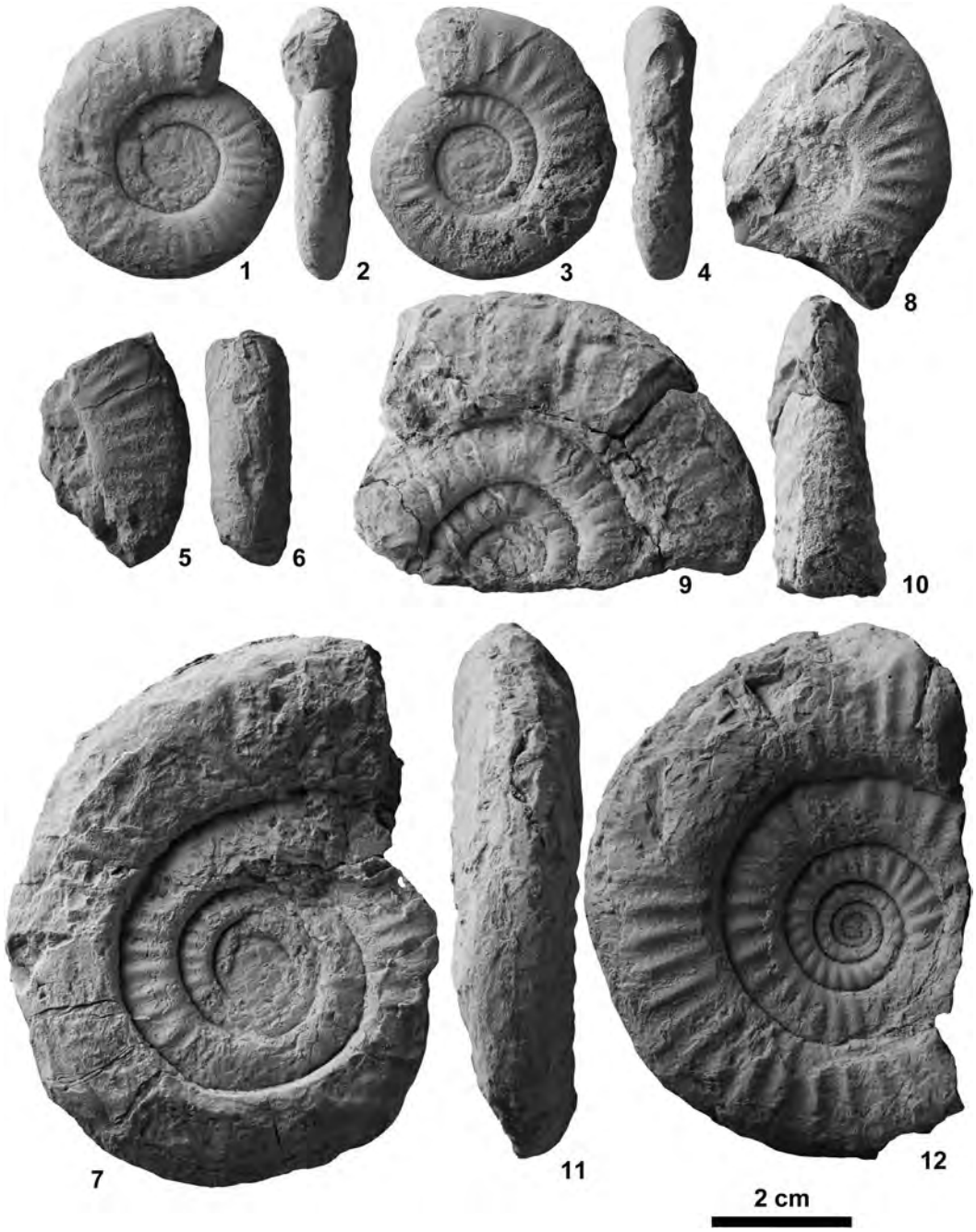


Fig. 47. *Preflorianites radians* Chao, 1959. 1–4, NMNS PM23472, from KC01-13. 5–6, NMNS PM23473, from KC01-13. 7, NMNS PM23474, from KC01-13. 8, NMNS PM23471, from KC01-10. 9–10, NMNS PM23469, from BT02-03. 11–12, NMNS PM23470, from BT03.

Spath, 1930.

### ***Xenoceltites variocostatus*** Brayard and Bucher, 2008

Figs. 48–51

*Xenoceltites variocostatus* Brayard and Bucher, 2008, p. 21, pl. 5, figs, 1–14, pl. 6, figs. 1–6, text-fig. 21.

*Xenoceltites* cf. *variocostatus* Brayard and Bucher, 2008. Brühwiler *et al*., 2010, p. 411, fig. 7.1–7.2; Brühwiler *et al*., 2012b, p. 31, fig. 24A–AG; Brühwiler *et al*., 2012c, p. 134, fig. 14A–G.

*Holotype*: PIMUZ 25838, figured by Brayard and Bucher (2008, p. 21, pl. 5, fig. 1), from the *Anasibirites multiformis* beds in Waili, northwestern Guangxi, South China.

*Material examined*: One specimen, NMNS PM23483, from NT01-04, one specimen, NMNS PM23484, from NT01-05, one specimen, NMNS PM23485, from NT01-06, fourteen specimens, NMNS PM23475–23482, 23492–23497, from NT01-07, one specimen, NMNS PM23498, from NT01-09, three specimens, NMNS PM23486–23488, from KC02-10, and one specimen, NMNS PM23489, from BR01-05.

*Description*: Early whorls (up to 10 mm in diameter): Fairly evolute, fairly compressed to very compressed shell with elliptical whorl section, arched venter, indistinct ventral shoulders and slightly convex flanks with maximum whorl width at mid-flank. Umbilicus moderately wide with low, nearly vertical wall and rounded shoulders. Ornamentation consists of conspicuous, sinuous, prorsiradiate ribs arising at umbilical shoulder, becoming strongly projected at ventral shoulders, and crossing venter in an acute convex arch.

Middle whorls (10–50 mm in diameter): As size increase, elliptical whorl section tends to become more compressed, with narrow rounded to sub-acute venter and slightly convex flanks with maximum whorl width near mid-flank. Umbilicus varies from fairly narrow to fairly wide with low, oblique wall and rounded shoulders. Distinctive ribs gradually lose strength and become low, weak, fold-type ribs. Shell surface covered by numerous growth lines, which arise at umbilical seam, curve backwards on umbilical shoulder, become sinuous, prorsiradiate, and cross venter in broad convex arch. Suture ceratitic. First lateral saddle nearly equal to second saddle, and third saddle lower than second saddle. First lateral lobe deep, wide with many denticulations at base, and second lateral lobe nearly equal to first lobe.

Later whorls (over 50 mm in diameter): As shell grows larger, whorl section becomes even more compressed and umbilicus becomes narrower. Shell surface ornamented by growth lines as well as low, weak, fold-type ribs.

*Measurements (mm)*:

| Specimen no. | D | U | H | W | U/D | W/H |
|---|---|---|---|---|---|---|
| NMNS PM23489 | 11.7 | 3.4 | 5.0 | 4.0 | 0.29 | 0.80 |
| NMNS PM23497 | 12.1 | 4.1 | 4.4 | 3.3 | 0.34 | 0.75 |
| NMNS PM23495 | 12.7 | 5.0 | 4.8 | 4.2 | 0.39 | 0.88 |
| NMNS PM23496 | 14.1 | 5.3 | 4.9 | 3.6 | 0.38 | 0.73 |
| NMNS PM23485 | 15.3 | 4.8 | 6.2 | 4.0 | 0.31 | 0.65 |
| NMNS PM23498 | 16.5 | 5.0 | 7.2 | 4.2 | 0.30 | 0.58 |
| NMNS PM23475 | 22.2 | 9.4 | 7.0 | 5.3 | 0.42 | 0.76 |
| NMNS PM23478 | 23.0 | 7.6 | 9.0 | 5.6 | 0.33 | 0.62 |
| NMNS PM23483 | 26.0 | 8.0 | 10.3 | 5.4 | 0.31 | 0.52 |
| NMNS PM23484 | 31.5 | 10.2 | 12.8 | 7.2 | 0.32 | 0.56 |
| NMNS PM23488 | 37.0 | 10.2 | 15.0 | 6.8 | 0.28 | 0.45 |
| NMNS PM23477 | 40.0 | 12.5 | 15.0 | 8.5 | 0.31 | 0.56 |
| NMNS PM23482 | 46.0 | 15.4 | 17.8 | 10.0 | 0.33 | 0.56 |
| NMNS PM23479 | 49.0 | 15.7 | 19.0 | 11.0 | 0.32 | 0.58 |
| NMNS PM23481 | 49.3 | 15.2 | 19.0 | 11.2 | 0.31 | 0.59 |
| NMNS PM23480 | 50.0 | 17.0 | 17.5 | 10.5 | 0.34 | 0.60 |
| NMNS PM23487 | 59.0 | 14.3 | 25.4 | 12.3 | 0.24 | 0.48 |
| NMNS PM23486 | 68.0 | 20.6 | 28.0 | 14.3 | 0.30 | 0.51 |

*Discussion*: NMNS PM23475 has a very similar shell morphology to the type specimens of *Xenoceltites variocostatus*, but most specimens described herein exhibit a slightly narrower umbilicus at comparable shell sizes. Because the other shell features are very similar to those of the types, our specimens are considered to be assignable to *X. variocostatus*. Close scrutiny of the type specimens together with the Vietnam specimens reveals that this species displays a wide range of intra-

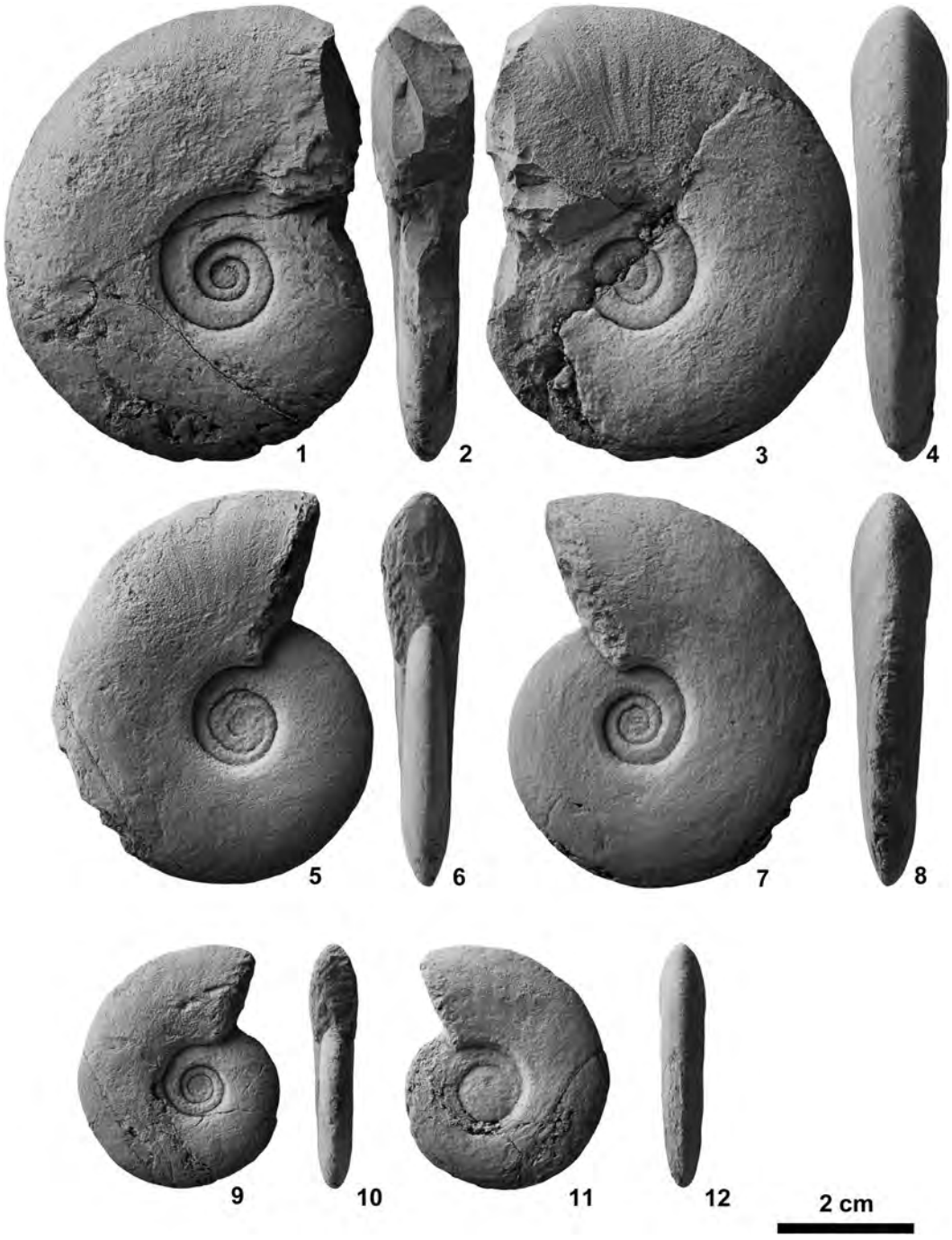


Fig. 48. *Xenoceltites variocostatus* Brayard and Bucher, 2008 from KC02-10. 1–4, NMNS PM23486. 5–8, NMNS PM23487. 9–12, NMNS PM23488.

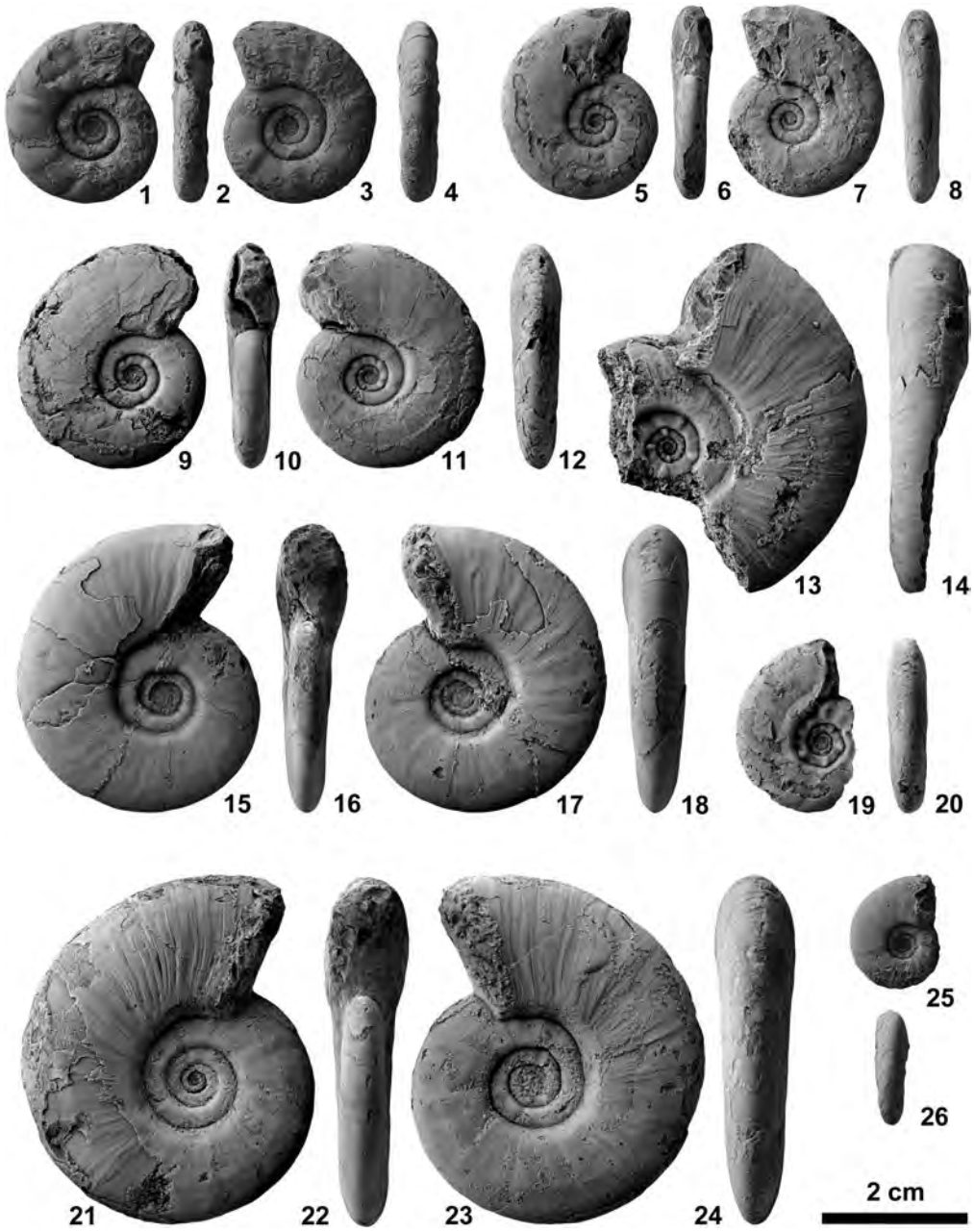


Fig. 49. *Xenoceltites variocostatus* Brayard and Bucher, 2008. 1–4, NMNS PM23475, from NT01-07. 5–8, NMNS PM23483, from NT01-04. 9–12, NMNS PM23484, from NT01-05. 13–14, NMNS PM23476, from NT01-07. 15–18, NMNS PM23477, from NT01-07. 19–20, NMNS PM23478, from NT01-07. 21–24, NMNS PM23479, from NT01-07. 25–26, NMNS PM23485, from NT01-06.

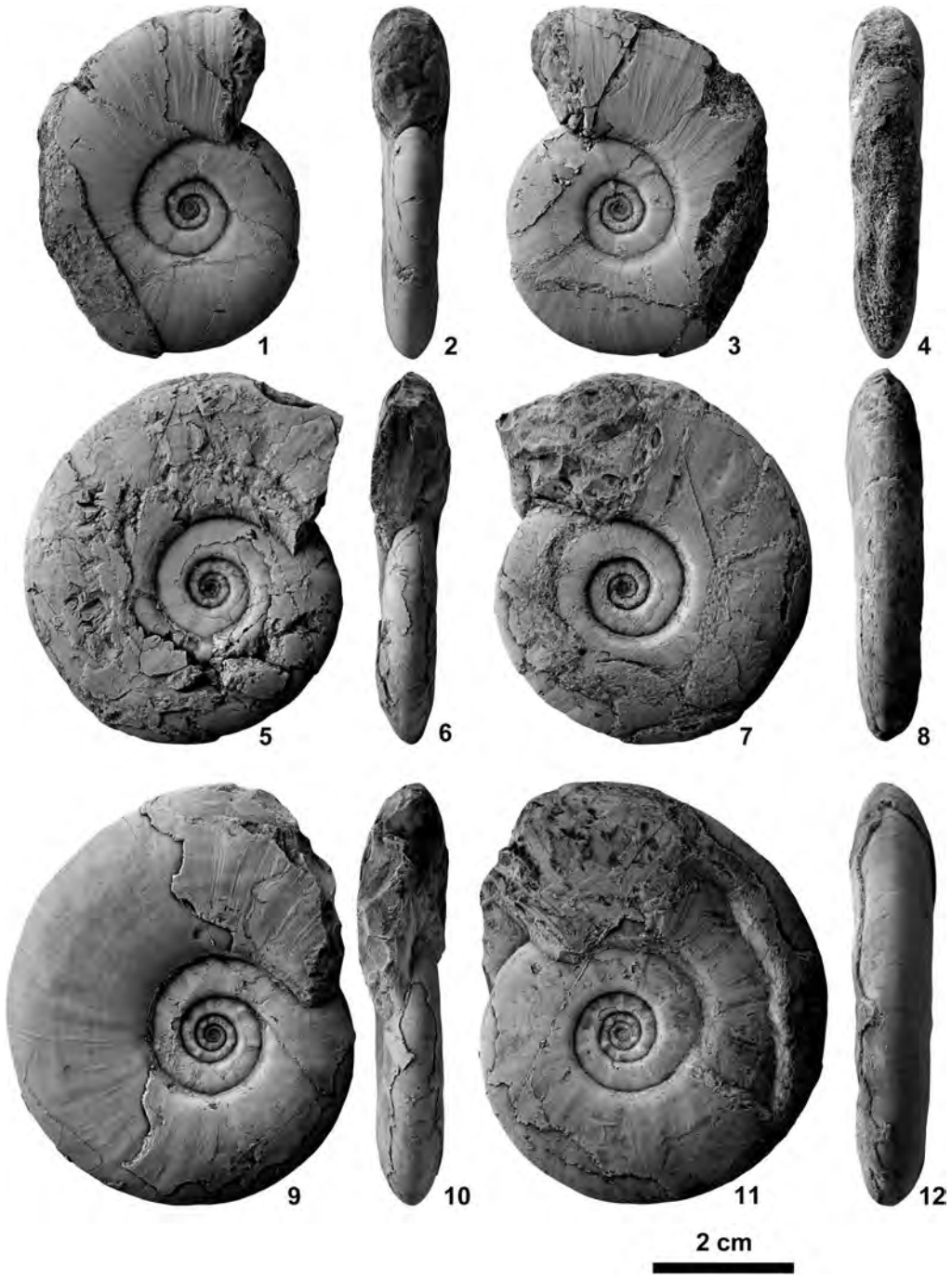


Fig. 50. *Xenoceltites variocostatus* Brayard and Bucher, 2008 from NT01-07. 1–4, NMNS PM23480. 5–8, NMNS PM23481. 9–12, NMNS PM23482.

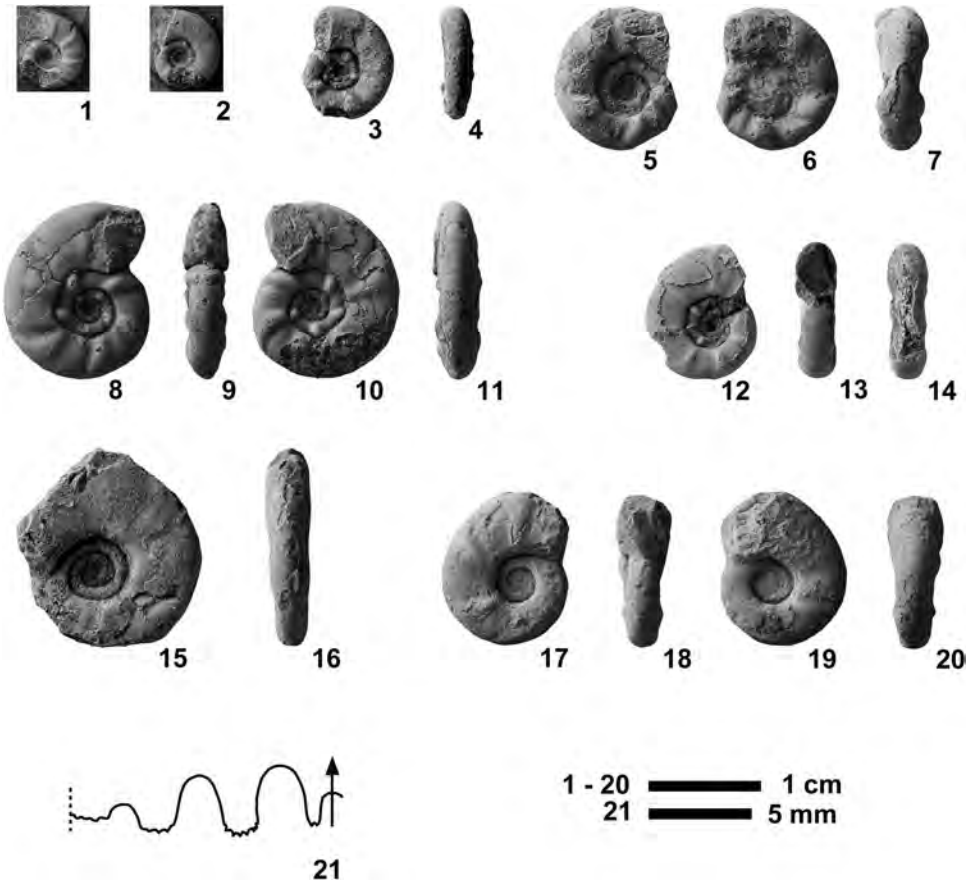


Fig. 51. *Xenoceltites variocostatus* Brayard and Bucher, 2008. 1, NMNS PM23492, from NT01-07. 2, NMNS PM23493, from NT01-07. 3–4, NMNS PM23494, from NT01-07. 5–7, NMNS PM23495, from NT01-07. 8–11, NMNS PM23496, from NT01-07. 12–14, NMNS PM2497, from NT01-07. 15–16, NMNS PM23498, from NT01-09. 17–20, NMNS PM23489, from BR01-05. 21, NMNS PM23484, from NT01-05.

specific variation with respect to umbilical diameter.

Specimens described as *Xenoceltites* cf. *variocostatus* by Brühwiler *et al*. (2010) from South Tibet, Brühwiler *et al*. (2012b) from the Salt Range and Brühwiler *et al*. (2012c) from Spiti all have slightly thinner whorls than the types, but otherwise are very similar. This variation almost certainly should be included within the intraspecific variation of *X. variocostatus.*

*Xenoceltites compressus* Chao, 1959 from the Middle Smithian of South China is very close to *X. variocostatus*, but differs by its slightly phylloid saddles. It possibly should be assigned to *Subflemingites* Spath, 1934.

*Occurrence*: Described specimens from NT01-04 to NT01-07, NT01-09, KC02-10 and BR01-05 within the portion of the *Novispathodus pingdingshanensis* Zone represented by the *Xenoceltites variocostatus* beds (Upper Smithian = upper Lower Olenekian) in the Bac Thuy Formation, northeastern Vietnam. This species also occurs in the Upper Smithian in South China (*Anasibirites multiformis* beds, Brayard and Bucher, 2008), South Tibet (*Glyptophiceras sinuatum* beds, Brühwiler *et al*., 2010), Spiti (*Subvishnuites posterus* beds, Brühwiler *et al*., 2012c) and the Salt Range (*Glyptophiceras sinuatum* beds, Brühwiler *et*

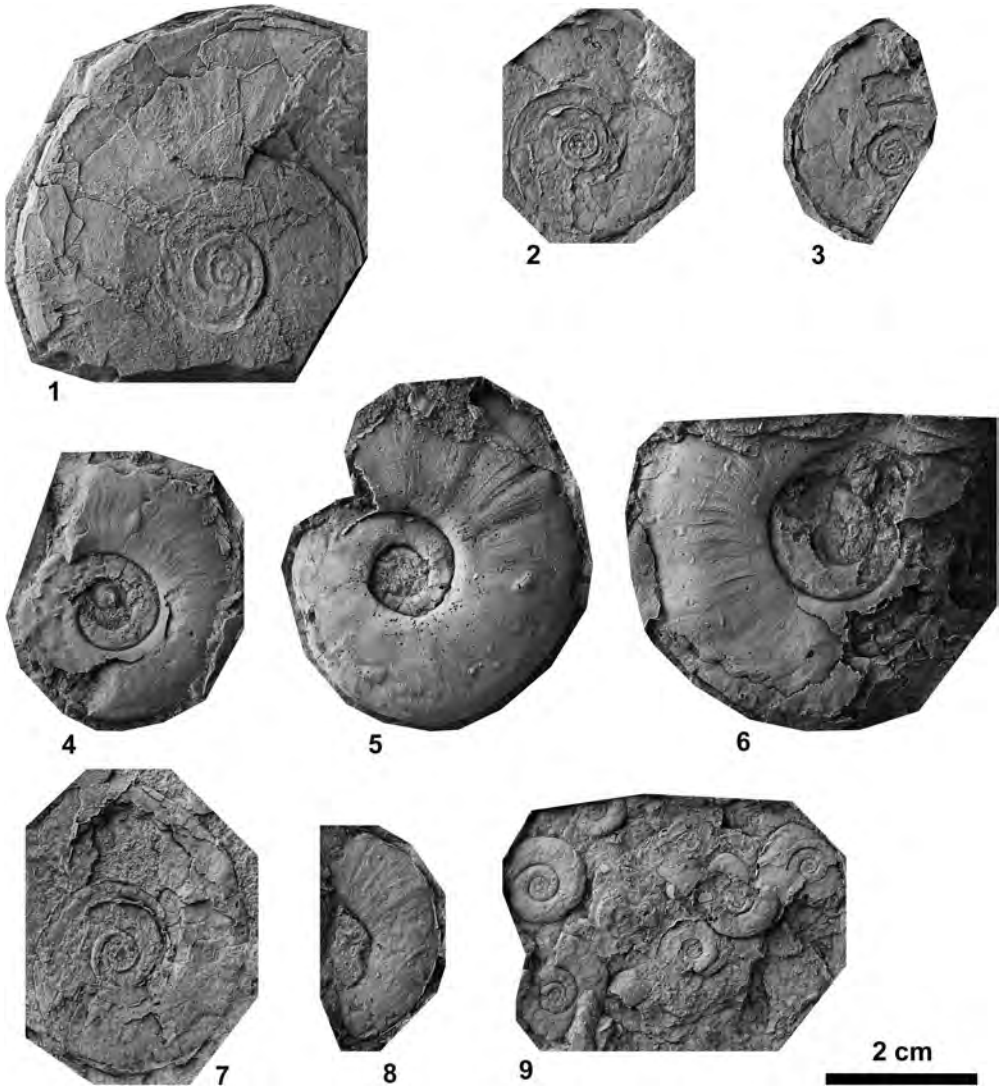


Fig. 52. *Xenoceltites*? sp. indet. 1, NMNS PM23640, from KC02-11. 2, NMNS PM23641, from KC02-11. 3, NMNS PM23642, from KC02-11. 4–8, rubber casts of outer molds. 4, NMNS PM23643, from KC02-15. 5, NMNS PM23644, from KC02-15. 6, NMNS PM23645, from KC02-14. 7, NMNS PM23761, from KC02-12. 8, NMNS PM23490, from BT02-05. 9, NMNS PM23491, from BT02-05.

*al*., 2012b).

### ***Xenoceltites***? sp. indet.

Fig. 52

*Material examined*: Two specimens, NMNS PM23490–23491, from BT02-05, three specimens, NMNS PM23640–23642, from KC02-11, one specimen, NMNS PM23761, from KC02-12, and three specimens, NMNS PM23643–23645, from KC02-15.

*Description*: Fairly evolute, very compressed shell with elliptical whorl section, rounded to subacute venter, indistinct ventral shoulders, and slightly convex flanks with maximum whorl width at mid-flank. Umbilicus moderately wide with low, nearly vertical wall and rounded shoulders. Ornamentation consists of low, weak, fold-type ribs. Suture not visible.

*Discussion*: Assignment of these specimens to *Xenoceltites* is uncertain because of their poor preservation and is based only on the similarity of their morphology with *Xenoceltites*.

*Occurrence*: Described specimens from KC02-11 within the portion of the *Novispathodus pingdingshanensis* Zone that includes the *Tirolites* cf. *cassianus* beds (lowest Lower Spathian = lowest Upper Olenekian), and those form KC02-12 and KC02-15 within the portion of the *Triasssospathodus symmetricus* Zone that includes the *Tirolites* cf. *cassianus* beds (lowest Lower Spathian = lowest Upper Olenekian) and *Tirolites* sp. nov. beds (Lower Spathian = lower Upper Olenekian) and from BT02-05, whose horizon probably lies within the the *Tirolites* cf. *cassianus* beds in the Bac Thuy Formation, northeastern Vietnam.

## Superfamily Meekoceratoidea Waagen, 1895
## Family Proptychitidae Waagen, 1895
## Genus ***Pseudaspidites*** Spath, 1934

*Type species*: *Aspidites muthianus* Kraft and Diener, 1909.

### ***Pseudaspidites muthianus*** (Krafft and Diener, 1909)

Figs. 53–56

*Aspidites muthianus* Krafft and Diener, 1909, p. 59, pl. 6, fig. 5, pl. 15, figs. 1–2.
*Clypeoceras lenticulare* Chao, 1959, p. 225, pl. 12, figs. 3–5, text-fig. 19b.
*Clypeoceras kwangiense* Chao, 1959, p. 226, pl. 17, figs. 1–2, text-fig. 19a.
*Pseudaspidites lolouensis* Chao, 1959, p. 229, pl. 13, figs. 17–21, text-figs. 20a, 21a.
*Pseudaspidites kwangsianus* Chao, 1959, p. 230, pl. 12, figs. 6–8, text-fig. 21d.
*Pseudaspidites simplex* Chao, 1959, p. 231, pl. 13, figs. 6–13, pl. 45, figs. 5–7, text-figs. 20b, 21b.
*Pseudaspidites stenosellatus* Chao, 1959, p. 231, pl. 13, figs. 4–5, pl. 45, fig. 8, text-fig. 21c.
*Pseudaspidites aberrans* Chao, 1959, p. 232, pl. 13, figs. 14–15, text-fig. 20d.
*Pseudaspidites longisellatus* Chao, 1959, p. 232, pl. 13, figs. 1–3, text-fig. 20c.
*Proptychites hemialis* var. *involutus* Chao, 1959, p. 237, pl. 15, figs. 13–16, text-fig. 24d.
*Proptychites markhami* Chao, 1959, p. 239, pl. 15, figs. 3–5, text-fig. 23c.
*Proptychites sinensis* Chao, 1959, p. 240, pl. 16, figs. 5–6, pl. 17, figs. 14–16, text-fig. 22c.
*Proptychites angusellatus* Chao, 1959, p. 240, pl. 15, figs. 1–2.
*Proptychites* aff. *trilobatus* Waagen, 1895. Chao, 1959, p. 241, pl. 16, figs. 11–12, text-fig. 24c.
*Proptychites latilobatus* Chao, 1959, p. 243, pl. 16, figs. 1–2, pl. 19, figs. 4–5.
*Proptychites abnormalis* Chao, 1959, p. 243, pl. 16, figs. 3–4.
*Proptychites* sp. A. Chao, 1959, p. 243, pl. 15, figs. 9–12.
*Ussuriceras* sp. Chao, 1959, p. 247, pl. 19, fig. 1.
*Pseudohedenstroemia magna* Chao, 1959, p. 265, pl. 41, figs. 13–16, pl. 45, figs. 1–2, text-fig. 32b.
*Pseudaspidites muthianus* (Krafft and Diener, 1909). Brayard and Bucher, 2008, p. 33, pl. 10, figs. 1–10, pl.

→

Fig. 53. *Pseudaspidites muthianus* (Krafft and Diener, 1909). 1–2, NMNS PM23505, from BT01-11. 3–4, NMNS PM23503, from BT01-05.

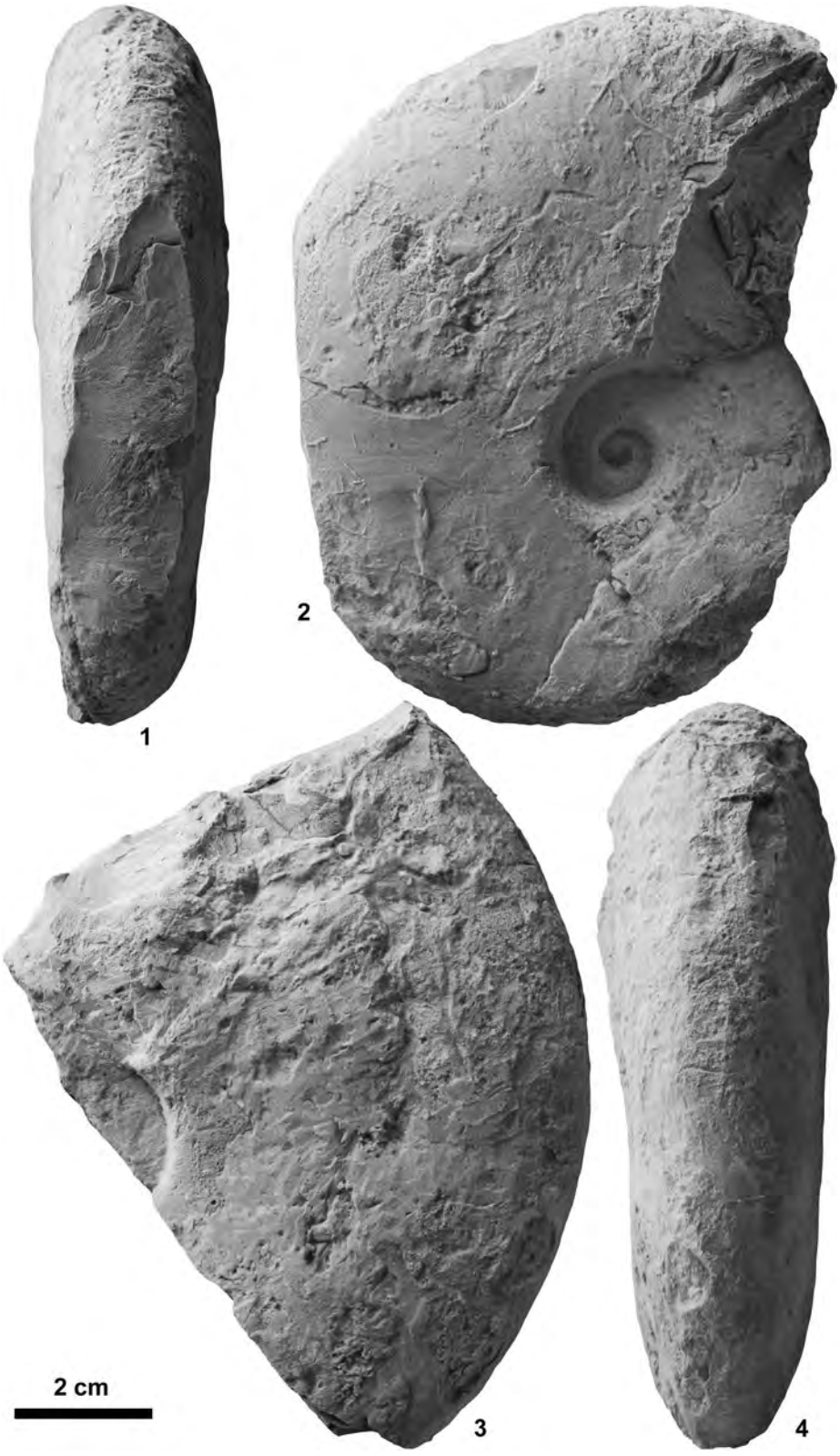
1
2
3
4
2 cm

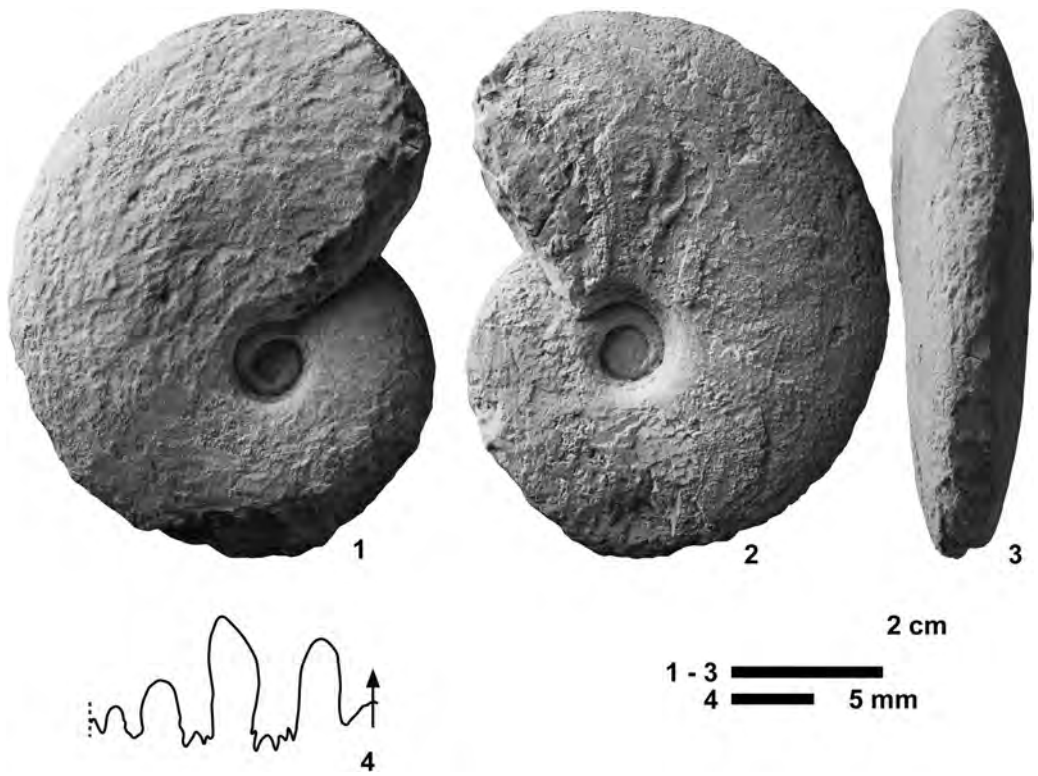


Fig. 54. 1–4, *Pseudaspidites muthianus* (Krafft and Diener, 1909), NMNS PM23504, from BT01-09.

11, figs. 1–4, text-fig. 31; Brühwiler *et al*., 2012c, p. 136, figs. 14M–R.

*Pseudaspidites* sp. Brühwiler *et al*., 2010, p. 413, fig. 7.11a-e.

non *Pseudaspidites* cf. *muthianus* (Krafft and Diener, 1909). Brühwiler *et al*., 2012a, p. 17, pl. 3, figs. 3–5.

*Pseudaspidites* cf. *muthianus* (Krafft and Diener, 1909). Brühwiler *et al*., 2012b, p. 53, figs. 37A–B, I.

*Lectotype*: Specimen designated by Spath (1934, p. 163), is GSI 9404, original of Krafft and Diener (1909, p. 59, pl. 6, fig. 5) from the "*Hedenstroemia*" beds at Mud, Spiti area, northwest Himalayan region.

*Material examined*: Three specimens, NMNS PM23499–23501, from BT01-03, one specimen, NMNS PM23502, from BT01-04, one specimen, NMNS PM23503, from BT01-05, one specimen, NMNS PM23504, from BT01-09, and one specimen, NMNS PM23505, from BT01-11.

*Description*: Very involute, very compressed shell with elliptical whorl section, arched venter (juveniles) or subtabulate venter (mature), indistinct ventral shoulders, and slightly convex flanks with maximum whorl width at mid-flank. Narrow umbilicus with moderately high, vertical wall and rounded shoulders. Ornamentation consists of weak radial folds. Suture ceratitic. Lateral saddle elongated, and second saddle slanted slightly toward umbilicus. First lateral lobe deep, wide with many denticulations at base, and second lateral lobe about two thirds depth of first lobe.

*Measurements (mm)*:

| Specimen no. | D | U | H | W | U/D | W/H |
|---|---|---|---|---|---|---|
| NMNS PM23500 | 61.0 | 7.8 | 31.7 | 16.5 | 0.13 | 0.52 |

→

Fig. 55. 1–4, *Pseudaspidites muthianus* (Krafft and Diener, 1909), NMNS PM23499, from BT01-03.


1
2
4
3
2 cm

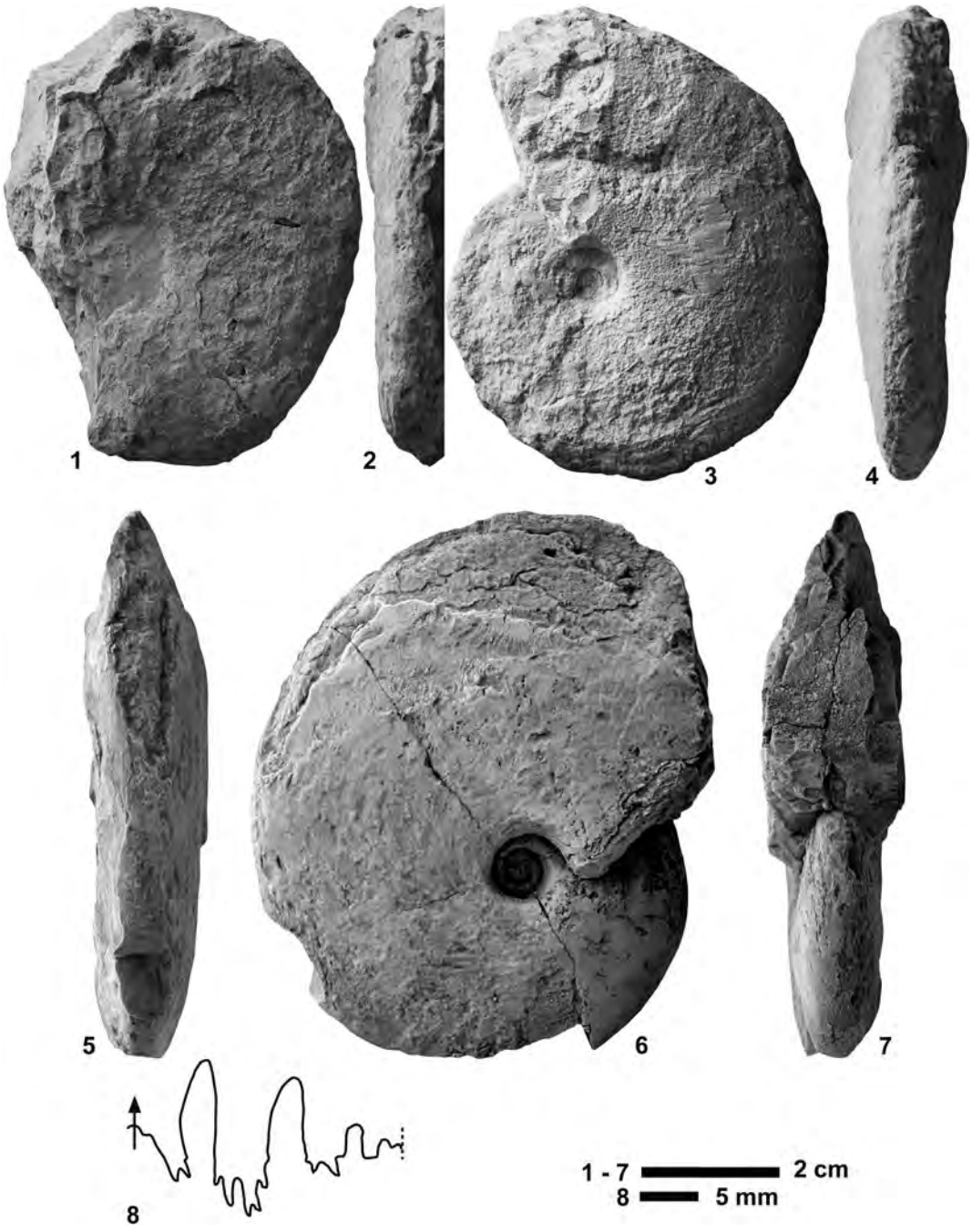


Fig. 56. *Pseudaspidites muthianus* (Krafft and Diener, 1909). 1–2, NMNS PM234502, from BT01-04. 3–4, NMNS PM23500, from BT01-03. 5–8, NMNS PM23501, from BT01-03.

| | | | | | | |
|---|---|---|---|---|---|---|
| NMNS PM23504 | 73.0 | 10.1 | 40.0 | 19.2 | 0.14 | 0.48 |
| NMNS PM23501 | 78.0 | 8.5 | — | — | 0.11 | — |
| NMNS PM23499 | 87.0 | 12.0 | 46.5 | 20.5 | 0.14 | 0.44 |
| NMNS PM23505 | 105.5 | 17.0 | 52.0 | 28.0 | 0.16 | 0.54 |
| NMNS PM23503 | — | — | 64.0 | 33.0 | — | 0.52 |

*Discussion*: Brayard and Bucher (2008) discussed and illustrated the intraspecific variation of *Pseudaspidites muthianus* from South China and synonymized many species described by Chao (1959). we agree with their analysis. According to this demonstrated range of intraspecific variation, a specimen described as *Pseudaspidites* sp. by Brühwiler *et al*. (2010) from South Tibet should be included within the intraspecific variation of *P. muthianus*. A specimen from the Salt Range described as *P.* cf. *muthianus* by Brühwiler *et al*. (2012b) is more evolute than specimens of *P. muthianus* of comparative size from South China and Spiti. This particular specimen may represent an evolute variant as stated by Brühwiler *et al*. (2012b, p. 53), because it otherwise is very similar. In contrast, specimens described as *P.* cf. *muthianus* by Brühwiler *et al*. (2012a) from exotic blocks in Oman have a subammonitic suture that is very similar to that of Ussuritid ammonoids. These specimens probably should be assigned to Ussuritids.

Smith (1932) described three specimens from Idaho as *Clypeoceras muthianum*, and Kummel and Steele (1962) later erected *Pseudaspidites wheeleri* based on these three specimens (Smith, 1932, pl. 27, figs. 1, 2). This species differs from *P. muthianus* by its much more involute coiling.

*Occurrence*: Described specimens from BT01-03, BT01-04, BT01-05, BT01-09 and BT01-11 within the portion of the *Novispathodus* ex gr. *waageni* Zone that includes the *Flemingites rursiradiatus* beds (lowest Middle Smithian = middle Lower Olenekian) and *Urdyceras tulongensis* beds (lower Middle Smithian = middle Lower Olenekian) in the Bac Thuy Formation, northeastern Vietnam. This species also occurs in the Middle Smithian in South China (*Flemingites rursiradiatus* beds and *Owenites koeneni* beds, Brayard and Bucher, 2008), South Tibet (*Brayardites compressus* beds, Brühwiler *et al*., 2010), Spiti (*Brayardites compressus* beds and *Escarguelites spitiensis* horizon, Brühwiler *et al*., 2012c), and the Salt Range (*Radioceras evolvens* beds, Brühwiler *et al*., 2012b).

## Genus ***Leyeceras*** Brayard and Bucher, 2008

*Type species*: *Leyeceras rothi* Brayard and Bucher, 2008.

### ***Leyeceras rothi*** Brayard and Bucher, 2008

Figs. 57–62

*Leyeceras rothi* Brayard and Bucher, 2008, p. 39, pl. 14, figs. 1–3.

? *Leyeceras* cf. *rothi* Brayard and Bucher, 2008. Brühwiler *et al*., 2012a, p. 18, pl. 5, figs. 1–5, pl. 6, figs. 1–3.

*Holotype*: PIMUZ 25964, figured by Brayard and Bucher (2008, p. 39, pl. 14, fig. 3), from the *Owenites koeneni* beds in Jinya, northwestern Guangxi, South China.

*Material examined*: Two specimens, NMNS PM23518–23519, from BT02-03, one specimen, NMNS PM23520, from a float limestone block at PK01, one specimen, NMNS PM23521, from KC01-11, two specimens, NMNS PM23514, 23522, from KC01-13, and one specimen, NMNS PM23523, from a float limestone block at BT02.

*Description*: Moderately evolute, very compressed shell with elliptical whorl section, arched or subtabulate venter, indistinct ventral shoulders, and slightly convex flanks with maximum whorl width near mid-flank. Fairly narrow umbilicus with moderately high, vertical wall and rounded shoulders. Ornamentation consists only of radial lirae. Suture ceratitic. Lateral saddle elongated, and second saddle slanted slightly toward umbilicus. First lateral lobe deep, wide with many denticulations at base, and second lateral lobe about two thirds depth of first lobe.

*Measurements (mm)*:

| Specimen no. | D | U | H | W | U/D | W/H |
|---|---|---|---|---|---|---|

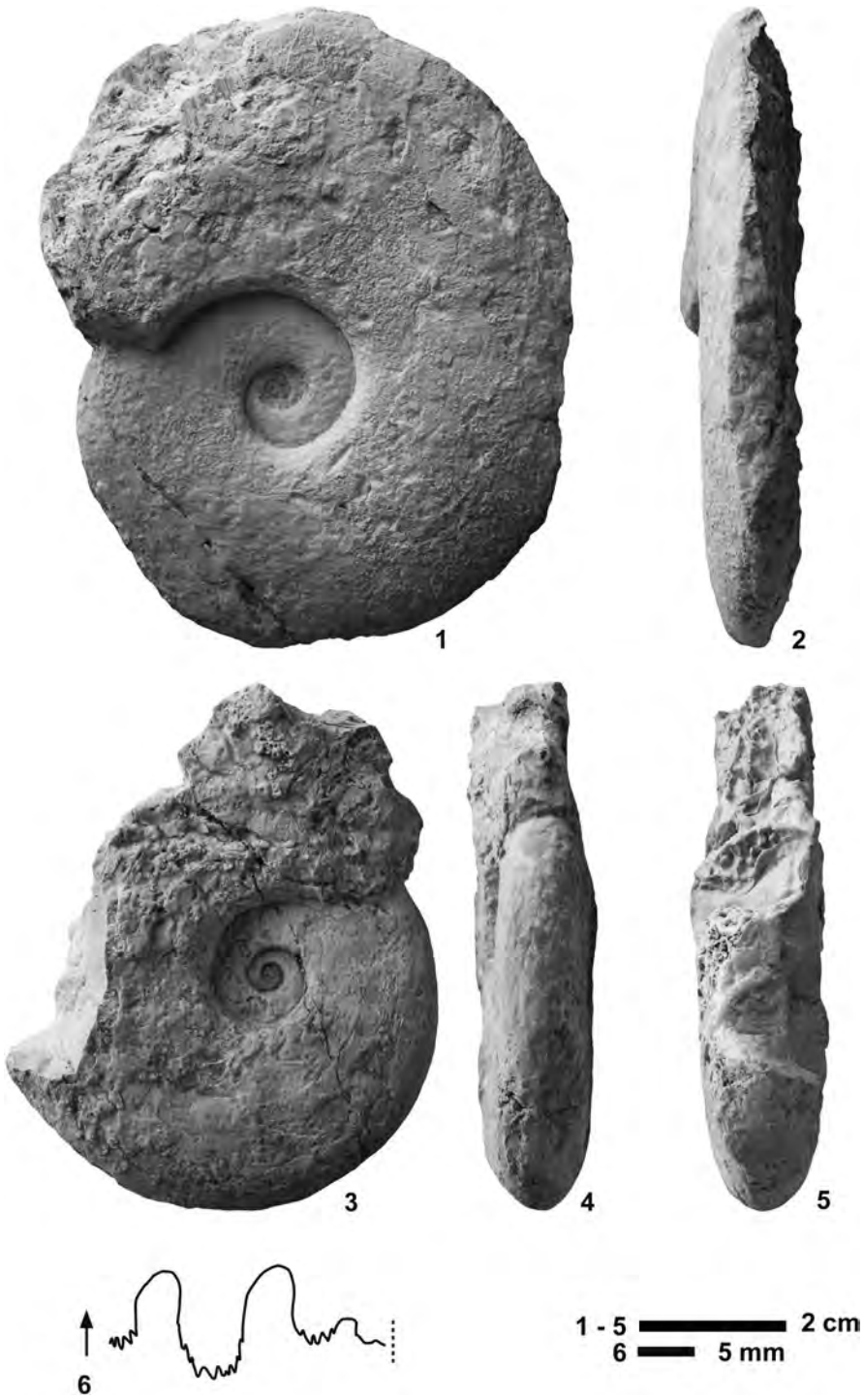


Fig. 57. *Leyeceras rothi* Brayard and Bucher, 2008, from BT02-03. 1–2, NMNS PM23518. 3–6, NMNS PM23519.


Fig. 58. *Leyeceras rothi* Brayard and Bucher, 2008, NMNS PM23523, from a float limestone block at BT02.


Fig. 59. *Leyeceras rothi* Brayard and Bucher, 2008, NMNS PM23523, from a float limestone block at BT02.


Fig. 60. *Leyeceras rothi* Brayard and Bucher, 2008, NMNS PM23523, from a float limestone block at BT02.


Fig. 61. *Leyeceras rothi* Brayard and Bucher, 2008, from KC01-13. 1–2, NMNS PM23522. 3–5, NMNS PM23514.


Fig. 62. *Leyeceras rothi* Brayard and Bucher, 2008. 1–2, NMNS PM23520, from a float limestone block at PK01. 3–4, NMNS PM23521, from KC01-11.

| | | | | | | |
|---|---|---|---|---|---|---|
| NMNS PM23519 | 61.0 | 12.8 | 31.0 | 17.0 | 0.21 | 0.55 |
| NMNS PM23518 | 89.0 | 20.2 | 40.0 | — | 0.23 | — |
| NMNS PM23520 | 94.0 | 21.7 | 43.0 | 10.5 | 0.23 | 0.48 |
| NMNS PM23521 | 100.2 | 23.0 | 46.0 | — | 0.23 | — |
| NMNS PM23522 | 138.5 | 28.8 | 68.4 | 29.0 | 0.21 | 0.42 |
| NMNS PM23523 | 163.0 | 39.5 | 75.0 | 31.0 | 0.24 | 0.41 |

*Discussion*: Specimens described as *Leyeceras* cf. *rothi* by Brühwiler *et al*. (2012a) from Oman have more convex flanks than the type specimens of *L. rothi* from South China, but otherwise are very similar. They may be conspecific with *L. rothi*.

*Occurrence*: Described specimens from BT02-03, KC01-11 and KC01-13 within the portion of the *Novispathodus* ex gr. *waageni* Zone that includes the *Leyeceras* horizon of the *Owenites koeneni* beds (middle Middle Smithian = middle Lower Olenekian) in the Bac Thuy Formation, northeastern Vietnam. This species also occurs in the Middle Smithian in South China (*Owenites koeneni* beds, Brayard and Bucher, 2008).

Genus ***Guodunites*** Brayard and Bucher, 2008

*Type species*: *Guodunites monneti* Brayard and Bucher, 2008.

### *Guodunites monneti*
Brayard and Bucher, 2008
Fig. 63

*Guodunites monneti* Brayard and Bucher, 2008, p. 83, pl. 44, figs. 1–2; Brayard *et al*., 2009, p. 473, pl. 1, figs. 1–14, text-fig. 3A–C; Brühwiler *et al*., 2012a, p. 19, pl. 7, figs. 1–5.

? *Guodunites* cf. *monneti* Brayard and Bucher, 2008. Jenks *et al*., 2010, p. 10, figs. 6A–D, 7.

*Guodunites* cf. *monneti* Brayard and Bucher, 2008. Jenks *et al*., 2010, p. 10, fig. 6E–H.

*Holotype*: PIMUZ 26193, figured by Brayard and Bucher (2008, p. 83, pl. 44, fig. 1), from the *Owenites koeneni* beds in Jinya, northwestern Guangxi, South China.

*Material examined*: Three specimens, NMNS PM23515–23517, from KC02-02.

*Description*: Fairly involute, very compressed shell with narrowly rounded venter, indistinct ventral shoulders, and slightly convex flanks with maximum whorl width near mid-flank. Umbilicus fairly narrow with gently inclined wall. Ornamentation consists of distinct, fine strigation on flanks disappearing on venter as well as slightly biconcave growth lines that become strongly projected on ventral shoulders. Suture line not well preserved.

*Measurements (mm)*:

| Specimen no. | D | U | H | W | U/D | W/H |
|---|---|---|---|---|---|---|
| NMNS PM23515 | 29.2 | 7.7 | 13.4 | 7.3 | 0.26 | 0.54 |
| NMNS PM23516 | 59.1 | 11.4 | 27.3 | 12.0 | 0.19 | 0.44 |

*Discussion*: Jenks *et al*. (2010) described four medium-sized specimens as *Guodunites* cf. *monneti* from western USA. One specimen (Jenks *et al*., 2010, fig. 6E–H) is nearly identical to *G. monneti* from Oman and South China and is clearly conspecific with *G. monneti*. However, the other three specimens have a much wider umbilicus (U/D: 0.25–0.27, Jenks *et al*., 2010, table 4) than *G. monneti* (U/D: 0.18–0.20, Brayard *et al*., 2009, table 1). They may belong to a more evolute form of *G. monneti.*

A poorly preserved specimen described as *Owenites slavini* (Popov, 1962) by Kummel and Erben (1968, p. 124, pl. 21, figs. 3–4; GPIBo. 24) from Afghanistan is characterized as having a very compressed shell with a narrowly rounded venter and slightly convex flanks ornamentated by strigation. The specimen is somewhat similar to *Guodunites monneti* as stated by Brayard *et al*. (2009, p. 476), but differs by stronger strigation covering its flanks and venter. *G. monneti* has fine strigation on its flanks, but it disappears on the venter. Kummel and Erben's (1968) specimen is not conspecific with *G. monneti.*

*Occurrence*: Described specimen from KC02-02 within the portion of the *Novispathodus* ex gr. *waageni* Zone that includes the *Guodunites* horizon of the *Owenites koeneni* beds (upper Middle Smithian = middle Lower Olenekian) in the Bac Thuy Formation, northeastern Vietnam. This species also occurs in the Middle Smithian in South China (*Owenites*

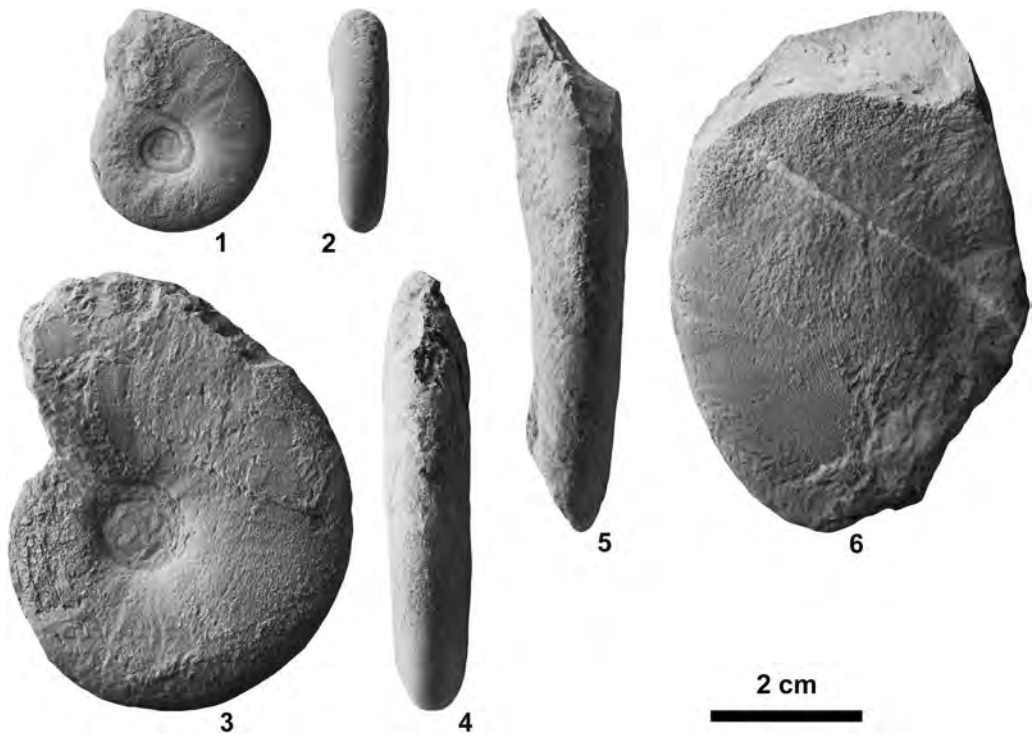


Fig. 63. *Guodunites monneti* Brayard and Bucher, 2008, from KC02-02. 1–2, NMNS PM23515. 3–4, NMNS PM23516. 5–6, NMNS PM23517.

*koeneni* beds, Brayard and Bucher, 2008), Oman (*Owenites koeneni* fauna, Brühwiler *et al*., 2012a), and western USA (*Meekoceras gracilitatis* Zone, Jenks *et al*., 2010).

Family Dieneroceratidae Spath, 1934
Genus ***Dieneroceras*** Spath, 1934

*Type species*: *Ophiceras dieneri* Hyatt and Smith, 1905.

***Dieneroceras***? ***goudemandi*** (Brayard and Bucher, 2008)

Figs. 64–66

?*Dieneroceras tientungense* Chao, 1959, p. 192, pl. 2, figs. 5–6, 8–10, 29.

?*Dieneroceras*? *vermiforme* Chao, 1959, p. 192, pl. 2, figs. 14–16, 28, text-fig. 7b.

?*Dieneroceras ovale* Chao, 1959, p. 192, pl. 2, figs. 11–13, text-fig. 7a.

*Pseudoflemingites goudemandi* Brayard and Bucher, 2008, p. 49, pl. 22, figs. 1–5, text-fig. 44.

*Pseudoflemingites goudemandi* Brayard and Bucher, 2008. Brühwiler *et al*., 2012a, p. 24, pl. 14, figs. 4–5.

*Holotype*: PIMUZ 26004, figured by Brayard and Bucher (2008, p. 49, pl. 22, fig. 2), from the *Owenites koeneni* beds in Jinya, northwestern Guangxi, South China.

*Material examined*: one specimen, NMNS PM23546, from KC01-01, one specimen, NMNS PM23547, from KC01-10, one specimen, NMNS PM23548, from KC01-11, six specimens, NMNS PM23549–23554, from KC01-13, one specimen, NMNS PM23555, from KC02-02, three specimens, NMNS PM23556–23558, from BT02-03, and two specimens, NMNS PM23559–23560, from BT01-14.

*Description*: Very evolute, fairly compressed shell with elliptical whorl section, subtabulate venter, slightly rounded shoulders,

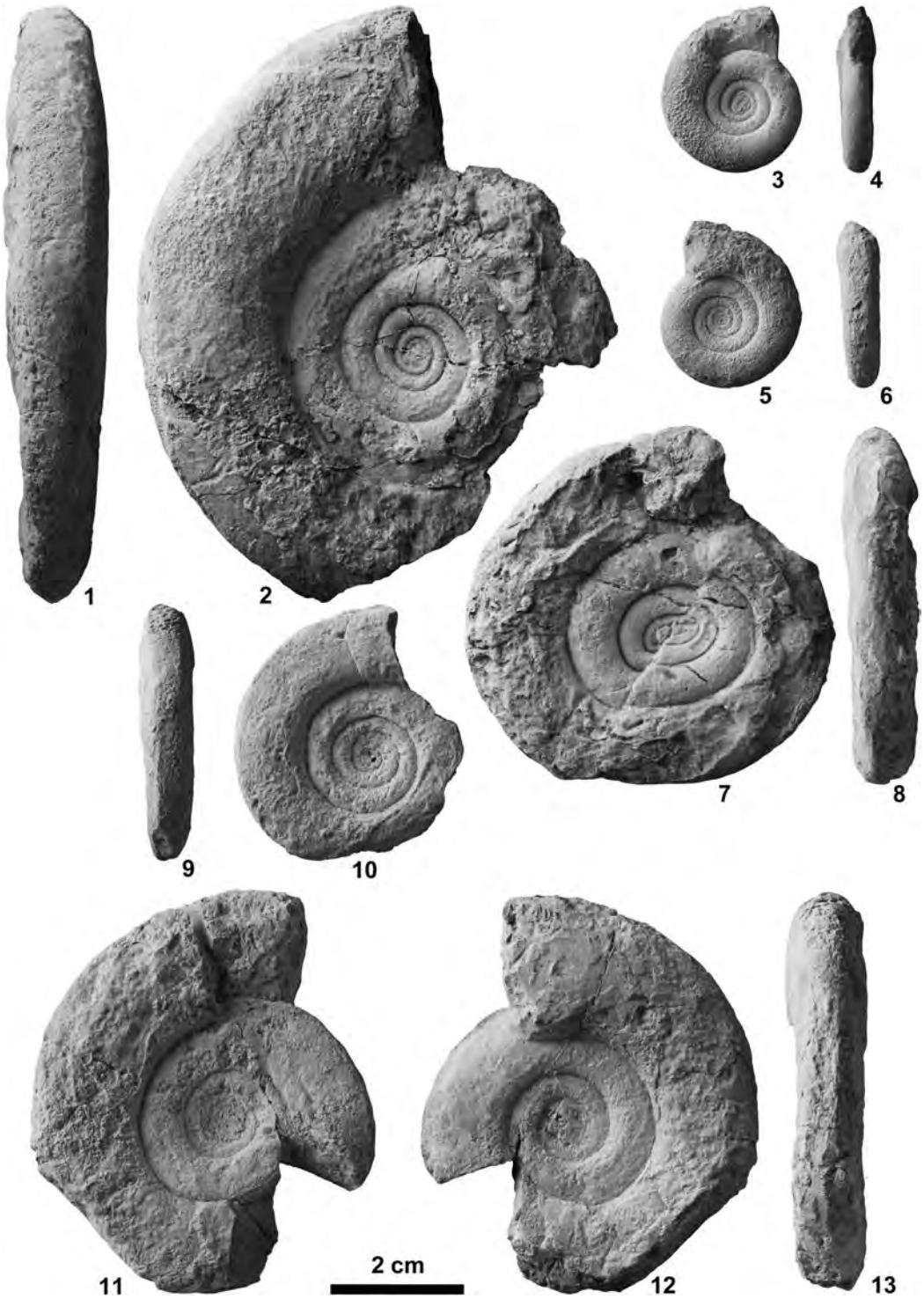


Fig. 64. *Dieneroceras*? *goudemandi* (Brayard and Bucher, 2008). 1–2, NMNS PM23556, from BT02-03. 3–6, NMNS PM23557, from BT02-03. 7–8, NMNS PM23558, from BT02-03. 9–10, NMNS PM23559, from BT01-14. 11–13, NMNS PM23560, from BT01-14.

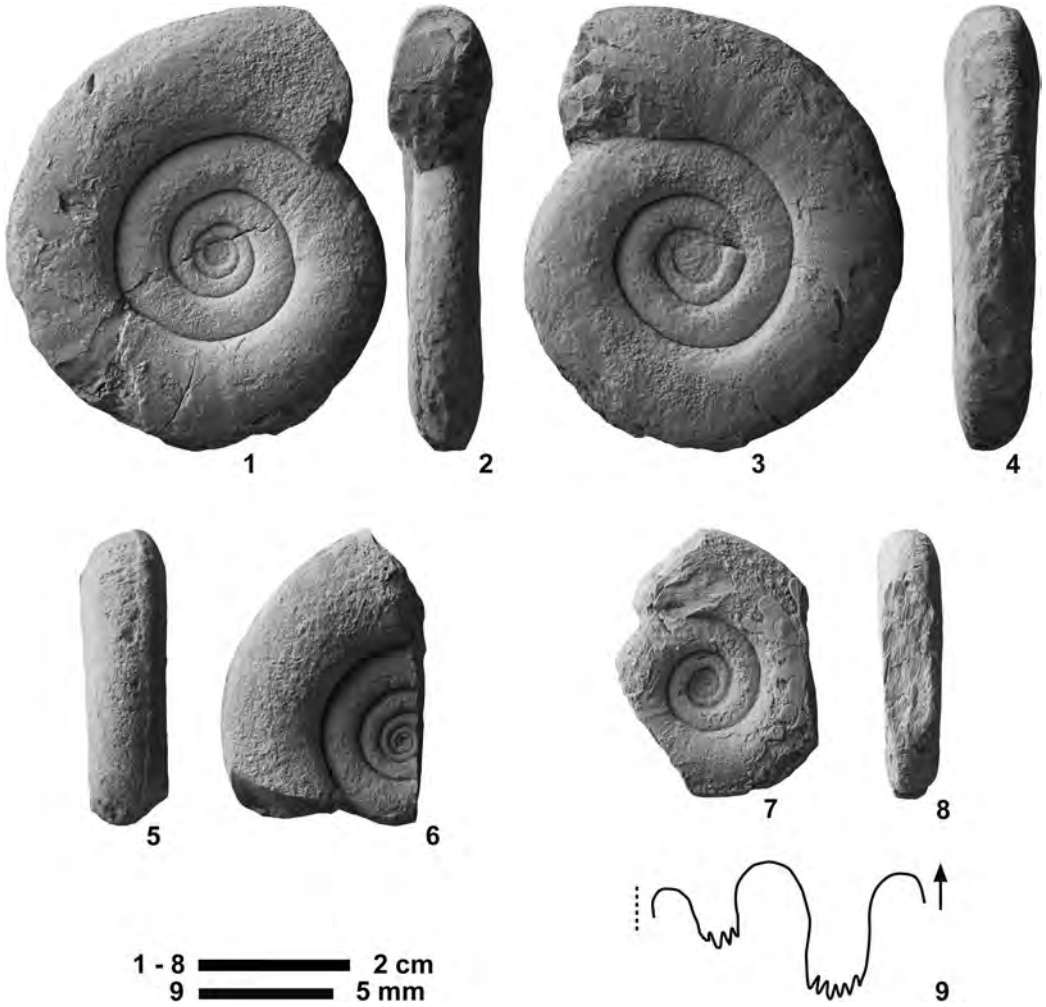


Fig. 65. *Dieneroceras*? *goudemandi* (Brayard and Bucher, 2008), from KC01-13. 1–4, NMNS PM23552. 5–6, NMNS PM23553. 7–9, NMNS PM23554.

and slightly convex flanks with maximum whorl width at mid-flank. Umbilicus fairly wide with low, nearly vertical wall and rounded shoulders. Surface smooth or ornamented with weak radial folds. Suture ceratitic. First lateral saddle nearly equal to second saddle, and third saddle lower than second saddle. First lateral lobe deep, wide with many denticulations at base, and second lateral lobe half depth of first lobe.

*Measurements (mm)*:

| Specimen no. | D | U | H | W | U/D | W/H |
|---|---|---|---|---|---|---|
| NMNS PM23557 | 23.0 | 10.7 | 7.1 | 6.0 | 0.47 | 0.85 |
| NMNS PM23549 | 25.0 | 11.4 | 6.8 | 4.4 | 0.46 | 0.65 |
| NMNS PM23553 | 25.8 | 12.3 | 8.3 | 7.4 | 0.48 | 0.89 |
| NMNS PM23555 | 26.9 | 13.7 | 7.3 | 6.6 | 0.51 | 0.90 |
| NMNS PM23550 | 30.2 | 13.8 | 9.5 | 6.7 | 0.46 | 0.72 |
| NMNS PM23546 | 32.6 | 14.0 | 11.0 | — | 0.43 | — |
| NMNS PM23554 | 35.3 | 15.1 | 11.1 | 8.3 | 0.43 | 0.75 |
| NMNS PM23559 | 39.0 | 19.2 | 11.1 | 8.0 | 0.49 | 0.72 |
| NMNS PM23547 | 52.5 | 25.6 | 16.0 | — | 0.49 | — |
| NMNS PM23558 | 54.0 | 25.9 | 15.3 | 11.0 | 0.48 | 0.72 |
| NMNS PM23560 | 55.6 | 23.8 | 18.0 | 11.2 | 0.43 | 0.62 |
| NMNS PM23552 | 60.1 | 28.0 | 17.7 | 12.8 | 0.47 | 0.72 |
| NMNS PM23551 | 73.8 | 34.3 | 21.2 | 14.0 | 0.46 | 0.66 |


Fig. 66. *Dieneroceras*? *goudemandi* (Brayard and Bucher, 2008). 1, NMNS PM23546, from KC01-01. 2–3, NMNS PM23547, from KC01-10. 4–5, NMNS PM23548, from KC01-11. 6–7, NMNS PM23549, from KC01-13. 8–9, NMNS PM23550, from KC01-13. 10–11, NMNS PM23551, from KC01-13. 12–13, NMNS PM23555, from KC02-02.

| | | | | | | |
|---|---|---|---|---|---|---|
| NMNS PM23556 | 91.0 | 43.1 | 28.0 | 15.3 | 0.47 | 0.55 |

*Discussion*: Brayard and Bucher (2008) attributed this species to *Pseudoflemingites* Spath, 1930, but their specimens' elliptical whorl section, subtabulate venter and slightly rounded ventral shoulders do not agree well with the diagnostic characters of *Pseudoflemingites*, which has a narrowly rounded venter and indistinct shoulders. Even though the overall shell morphology of this species is similar to that of *Dieneroceras*, the smooth shell surface differs from *Dieneroceras*, which is characterized by fine strigation. Therefore, the assignment to this genus is questionable.

Chao (1959) described three new species, *Dieneroceras tientungense*, *D.*? *vermiforme*, and *D. ovale*, from the middle Smithian (Owenitan) of South China. Their shells, which are less than 4 cm in diameter, are very similar to the inner whorls of the type specimens of *Pseudoflemingites goudemandi* Brayard and Bucher, 2008. Ultimately, they may be shown to be conspecific with this taxon, but further taxonomic studies are necessary to confirm this attribution.

*Occurrence*: Described specimen from KC01-01, KC01-010, KC01-11, KC01-13, KC02-02, BT02-03 and BT01-14 within the portion of the *Novispathodus* ex gr. *waageni* Zone that includes the *Owenites koeneni* beds (middle to upper Middle Smithian = middle Lower Olenekian) in the Bac Thuy Formation, northeastern Vietnam. This species also occurs in the Middle Smithian in South China (*Owenites koeneni* beds, Brayard and Bucher, 2008) and Oman (*Owenites koeneni* fauna, Brühwiler *et al*., 2012a).

Family Flemingitidae Hyatt, 1900

Genus ***Flemingites*** Waagen, 1895

*Type species*: *Ceratites flemingianus* de Koninck, 1863.

### ***Flemingites rursiradiatus*** Chao, 1959

Figs. 67, 68.1

?*Flemingites evolutus* Chao, 1959, p. 204, pl. 7, figs. 13–14, pl. 8, figs. 5–6, text-fig. 12c.

?*Flemingites nalilingensis* Chao, 1959, p. 205, pl. 6, figs. 6–7, text-fig. 12d.

*Flemingites rursiradiatus* Chao, 1959, p. 205, pl. 6, figs. 1–5, 8–10, text-fig. 13; Brayard and Bucher, 2008, p. 44, pl. 18, figs. 1–7, pl. 9, figs. 1–3, text-fig. 39; Brühwiler *et al*., 2012a, p. 20, pl. 12, figs. 1–5.

*Flemingites ellipticus* Chao, 1959, p. 206, pl. 4, figs. 5–7, 10–12, text-fig. 12a.

?*Flemingites ellipticus* var. *kaohwaiensis* Chao, 1959, p. 207, pl. 4, figs. 8–9.

*Flemingites kwangsiensis* Chao, 1959, p. 208, pl. 8, fig. 8.

*Flemingites* cf. *rursiradiatus* Chao, 1959. Vu Khuc, 1984, p. 34, pl. 1, figs. 4–5; Vu Khuc, 1991, p. 122, pl. 46, figs. 2–3.

*Flemingites* aff. *flemingianus* (de Koninck, 1863). Vu Khuc, 1984, p. 34, pl. 3, fig. 2; Vu Khuc, 1991, p. 122, pl. 46, fig. 1.

*Flemingites flemingianus* (de Koninck, 1863). Brayard and Bucher, 2008, p. 44, pl. 17, figs. 1–5, text-fig. 38.

*Holotype*: NIGP 12174, figured by Chao (1959, p. 205, pl. 6, figs. 8–10), from the Flemingitan (lower Smithian) in the Linglo district (Lolou), western Guangxi, South China.

*Material examined*: Five specimens, NMNS PM23506–23509, 23513 from BT01-03, one specimen, NMNS PM23510, from BT01-05 and one specimen, NMNS PM23511, from BT02-01.

*Description*: Very evolute, fairly compressed shell with elliptical to subquadratic whorl section, subtabulate venter, rounded ventral shoulders, and slightly convex flanks with maximum whorl width at mid-flank. Umbilicus fairly wide with moderately high, nearly vertical wall and rounded shoulders. Ornamentation consists of conspicuous, dense strigation covering entire shell and variable strength, radial to conspicuous rursiradiate ribs arising on umbilical shoulder and fading away on ventral shoulder. Suture not preserved.

*Measurements (mm)*:

| Specimen no. | D | U | H | W | U/D | W/H |
|---|---|---|---|---|---|---|
| NMNS PM23513 | 21.0 | 10.1 | 13.0 | 10.0 | 0.41 | 0.77 |

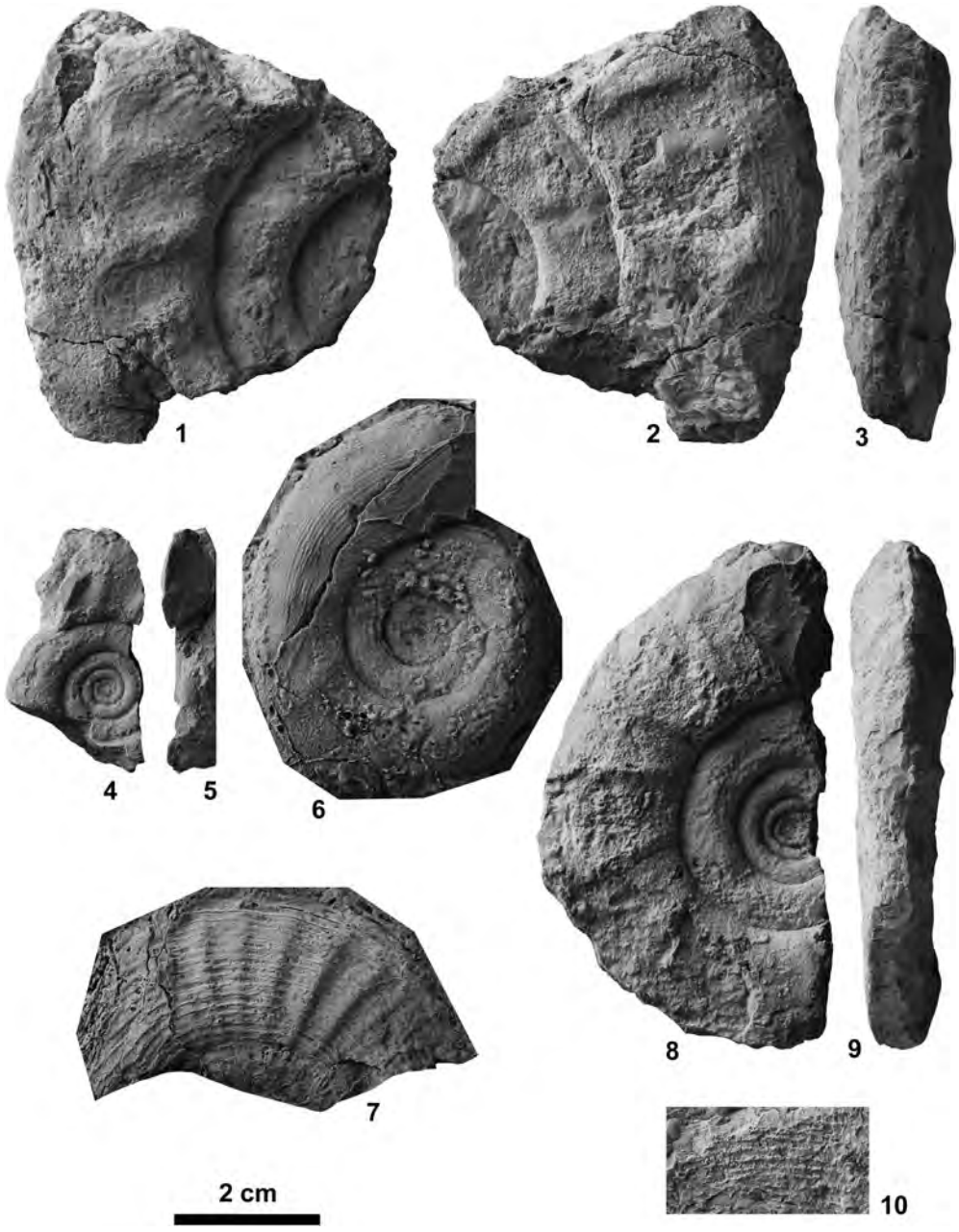


Fig. 67. *Flemingites rursiradiatus* Chao, 1959. 1–3, NMNS PM23511, from BT02-01. 4–5, NMNS PM23513, from BT01-03. 6, NMNS PM23506 (rubber cast of outer mold), from BT01-03. 7, NMNS PM23509 (rubber cast of outer mold), from BT01-03. 8–9, NMNS PM23508, from BT01-03. 10, NMNS PM23510, from BT01-05.


Fig. 68. 1, *Flemingites rursiradiatus* Chao, 1959, NMNS PM23507, from BT01-03. 2, *Euflemingites* sp. indet., NMNS PM23512 (rubber cast of outer mold), from a float limestone block at BT02.

| | | | | | | |
|---|---|---|---|---|---|---|
| NMNS PM23506 | 47.0 | 19.5 | 7.3 | 6.1 | 0.48 | 0.84 |
| NMNS PM23508 | 69.5 | 31.0 | 20.5 | 14.5 | 0.45 | 0.71 |
| NMNS PM23507 | 85.0 | 39.0 | — | — | 0.46 | — |
| NMNS PM23511 | — | — | 31.0 | 17.0 | — | 0.55 |

*Discussion*: Brayard and Bucher (2008) collected many specimens assignable to *Flemingites* from a 3 m thick limestone bed in the Luolou Formation, South China and identified them as *Flemingites rursiradiatus*, *F. flemingianus* and *F. radiates*. Brühwiler *et al.* (2012b, p. 68) later pointed out that specimens described as *F. flemingianus* by Brayard and Bucher (2008) differ from that taxon by their more evolute coiling and lower whorl height at comparable size, and stated that they may represent a weakly ribbed variant of *F. rursiradiatus*. Specimens assigned to *F. rursiradiatus* by Brayard and Bucher (2008) exhibit a wide range of intraspecific variation and they include forms very similar to the types of *F. ellipticus* and *F. kwangsiensis* erected by Chao (1959). This evidence suggests that these two species of Chao are conspecific. Chao's other species, *F. evolutus*, *F. nalilingensis* and *F. ellipticus* var. *kaohwaiensis* are also very similar to juveniles of *F. rursiradiatus*, but it is questionable whether they are conspecific because their ornamentation is poorly preserved.

*Occurrence*: Described specimens from BT01-03, BT01-05 and BT02-01 within the portion of the *Novispathodus* ex gr. *waageni* Zone that includes the *Flemingites rursiradiatus* beds (lowest Middle Smithian = middle Lower Olenekian) in the Bac Thuy Formation, northeastern Vietnam. This species also occurs in the lowest Middle Smithian in South China (*Flemingites rursiradiatus* beds, Brayard and Bucher, 2008) and Oman (*Flemingites rursiradiatus* fauna, Brühwiler *et al.*, 2012a).

### Genus ***Euflemingites*** Spath, 1934

*Type species*: *Flemingites guyerdetiformis* Welter, 1922.

### ***Euflemingites*** sp. indet.

Fig. 68.2

*Material examined*: One specimen, NMNS PM23512, from a float limestone block at BT02.

*Description*: Moderately evolute, very compressed shell with rounded venter, indistinct ventral shoulders, and gently convex flanks forming an elliptical whorl section with maximum whorl width at mid-flank. Umbilicus fairly narrow with moderately high, vertical wall and rounded shoulders. Ornamentation consists of conspicuous, dense strigation covering entire shell. Spiral ridges number about 25 between umbilical shoulders and mid-line of venter. Suture not preserved.

*Discussion*: The described specimen is very similar to *Euflemingites tsotengensis* Chao, 1959 from South China, *E. guyerdetiformis* (Welter, 1922) from Timor, *E. prynadai* (Kiparisova, 1947) from South Primorye and *E. cirratus* (White, 1879) from western USA, but the fragmental nature of the specimen precludes a definitive species assignment.

*Occurrence*: Described specimen was found in a float limestone block at BT02. Although the exact horizon from which the block originated is uncertain, judging from the locality where it was found, it certainly came from a limestone bed (Middle Smithian) in the Bac Thuy Formation, northeastern Vietnam.

## Genus ***Anaflemingites*** Kummel and Steele, 1962

*Type species*: *Anaflemingites silberlingi* Kummel and Steele, 1962.

### ***Anaflemingites hochulii*** Brayard and Bucher, 2008

Figs. 69–72

*Anaflemingites hochulii* Brayard and Bucher, 2008, p. 51, pl. 23, figs. 3–6, text-fig. 45.

*Subflemingites involutus* (Welter, 1922). Brühwiler *et al*., 2012a, p. 23, pl. 13, figs. 1–3.

*Holotype*: PIMUZ 26020, figured by Brayard and Bucher (2008, p. 51, pl. 24, fig. 5), from the *Owenites koeneni* beds in Jinya, northwestern Guangxi, South China.

*Material examined*: Three specimens, NMNS PM23773–23775, from float limestone blocks at BT02 and five specimens, NMNS PM23776–23780, from KC01-13.

*Description*: Moderate to fairly evolute, very compressed shell with elliptical whorl section, rounded venter, indistinct ventral shoulders, and slightly convex flanks with maximum whorl width at mid-flank. Umbilicus moderately wide with low, gently sloped wall and rounded shoulders. Ornamentation on juvenile whorls consists of sinuous growth lines and weak strigation near venter. Suture ceratitic. First lateral saddle lower than second saddle. First and second lateral lobes deep, wide with many denticulations at base.

*Measurements (mm)*:

| Specimen no. | D | U | H | W | U/D | W/H |
|---|---|---|---|---|---|---|
| NMNS PM23774 | 33.8 | 11.2 | 13.5 | 8.7 | 0.33 | 0.64 |
| NMNS PM23773 | 43.0 | 14.8 | 16.2 | 10.9 | 0.34 | 0.67 |
| NMNS PM23775 | 60.2 | 18.8 | 28.2 | 13.2 | 0.31 | 0.47 |
| NMNS PM23776 | 82.2 | 25.6 | 34.0 | 14.0 | 0.31 | 0.41 |
| NMNS PM23780 | 151.3 | 51.9 | 58.3 | 21.7 | 0.34 | 0.37 |

*Discussion*: Specimens described as *Subflemingites involutus* (Welter, 1922) by Brühwiler *et al*. (2012a) from Oman are very similar to *Anaflemingites hochulii*, and are clearly conspecific. *A. silberlingi* Kummel and Steele, 1962 from western USA is also very close to *A. hochulii*, but differs by the fine strigation that covers its entire shell (Jenks *et al*., 2010).

*Occurrence*: Described specimens from KC01-13 within the portion of the *Novispathodus* ex gr. *waageni* Zone that includes the *Leyeceras* horizon of the *Owenites koeneni* beds (middle Middle Smithian = middle Lower Olenekian) in the Bac Thuy Formation, northeastern Vietnam. This species also occurs in the Middle Smithian in South China (*Owenites koeneni* beds, Brayard and Bucher, 2008) and Oman (*Owenites koeneni* fauna, Brühwiler *et al*., 2012a).

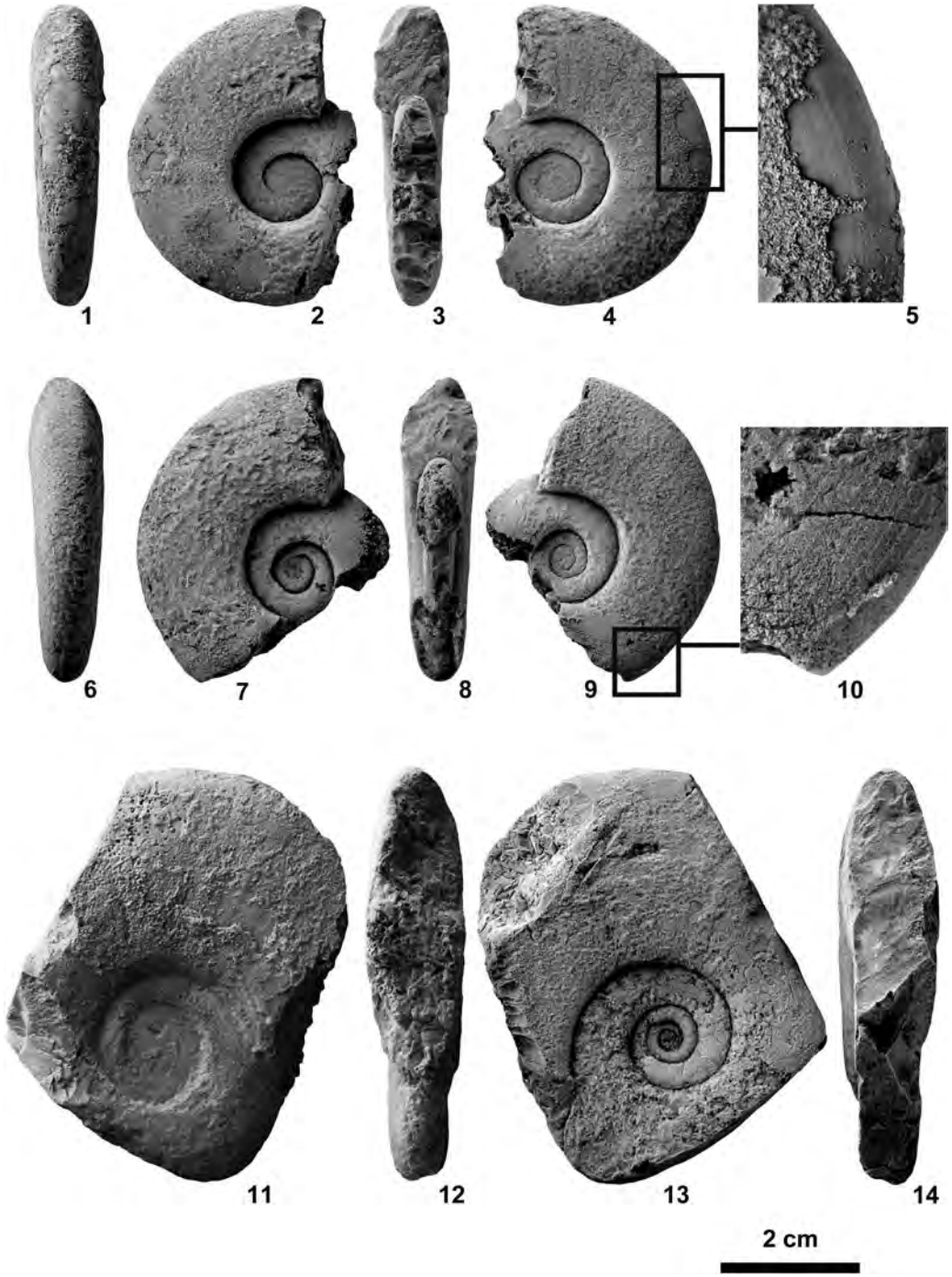


Fig. 69. *Anaflemingites hochulii* Brayard and Bucher, 2008, from float limestone blocks at BT02. 1–5, NMNS PM23773. 6–10, NMNS PM23774. 11–14, NMNS PM23775.

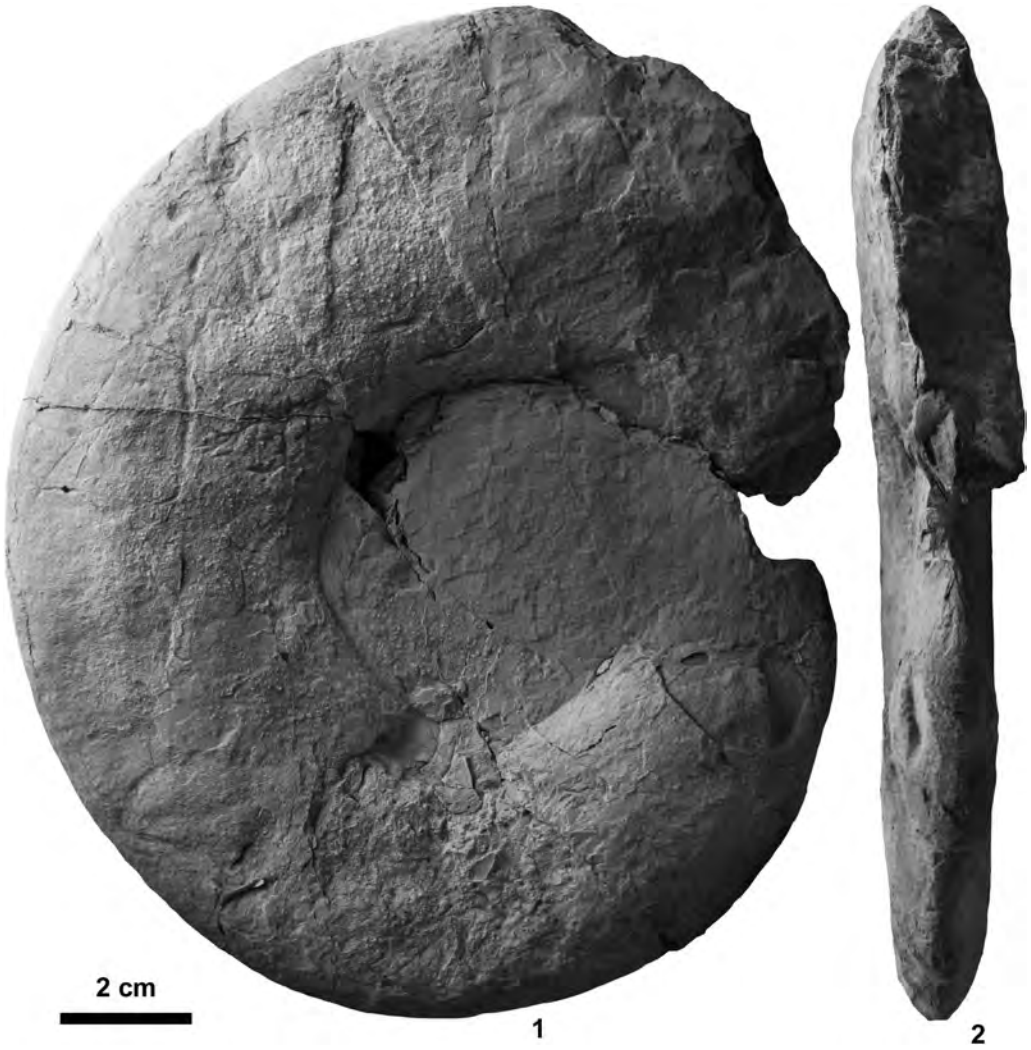


Fig. 70. *Anaflemingites hochulii* Brayard and Bucher, 2008. NMNS PM23780, from KC01-13.